Design of an Advanced VTOL Dropship

A Project Report

Presented to

The Faculty of the Department of Mechanical and Aerospace Engineering

San José State University

In Partial Fulfillment

of the Requirements for the Degree

Master of Science

by

Dwayne Eddie Hickman Jr.

December 2009

SAN JOSÉ STATE UNIVERSITY

The Undersigned Project Committee Approves the Thesis Titled

DESIGN OF AN ADVANCED VTOL DROPSHIP

by
Dwayne Eddie Hickman Jr.

APPROVED FOR THE DEPARTMENT OF MECHANICAL AND AEROSPACE ENGINEERING

Dr. Nikos Mourtos, Department of Mechanical & Aerospace Engineering Date

Dr. Periklis Papadopoulos, Department of Mechanical & Aerospace Engineering Date

Dr. Sean Swei, Department of Mechanical & Aerospace Engineering Date

Abstract

Design of an Advanced VTOL Dropship

By Dwayne Eddie Hickman Jr.

This report discusses the preliminary design of a next generation Special Forces-optimized transport vehicle. On April 6, 2009 Secretary of Defense Robert M Gates gave a briefing outlining recommend changes for the Department of Defense. Part of his recommendation was "To grow our special operations capabilities, we will increase personnel by more than 2,800 or five percent and will buy more special forces-optimized lift, mobility, and refueling aircraft." This report follows mission requirements development and preliminary system design for a Special Forces-optimized lift and mobility aircraft. Key requirements for a Special Forces optimized transport vehicle include rapid deployment, stealth, and independence from airstrips. The analysis performed for this report was done using a combination of text references and computer tools, primarily the Advanced Aircraft Analysis (AAA) program.

The developed aircraft is the Advanced Vertical Takeoff and Landing Dropship (AVD). The AVD uses vertical takeoff and landing (VTOL), low observables, and light weight materials to meet or exceed mission requirements. Although the aircraft is "advanced," it is not intended require any new technologies to be developed. It will leverage the state of the art materials and methods currently available to fill a critical hole in the current capabilities of the US Special Forces units.

TABLE OF CONTENTS

Nomenclature

AAA - Advanced Aircraft Analysis

AR - Wing Aspect Ratio

AVD - Advanced VTOL Dropship

b - Wing Span [ft]

c.g. - Center of Gravity [ft]

CR - Cruise

C_D - Drag Coefficient

$C_{D,L}$ - Drag Coefficient due to lift

C_{D0} - Zero Lift Drag Coefficient

C_L - Lift Coefficient

d_m - Diameter of Main Landing Gear

d_n - Diameter of Nose Landing Gear

f - Equivalent Parasite Drag [ft^2]

FOD - Foreign Object Damage

Γ - Wing Dihedral Angle [deg]

h_{cr} - Cruise Height (altitude) [ft]

i - Wing Incidence Angle [deg]

Λ - Wing Sweep Angle [deg]

L/D - Lift to Drag Ratio

LE - Leading Edge

nm - Nautical Mile

M - Mach Number

mff - Mass Fuel Fraction

PL - Payload

P_m - Load on Main Landing Gear [lb]

P_n - Load on Nose Landing Gear [lb]

R - Range [NM]

R_{CR} - Combat Radius [NM]

R_f - Ferry Range [NM]

RCS - Radar Cross-Section

RoC - Rate of Climb [ft/sec]

S - Wing Area [ft^2]

S_s - Strut Stroke Length [ft]

sfc - Specific Fuel Consumption (c_j) [lb/sec]

SL - Standard Landing

STO - Standard Take Off

T - Thrust [lb]

t/c = Wing Thickness to Chord Length Ratio

TO - Take Off

TE - Trailing Edge

t/c - Airfoil thickness to chord ratio

T/W - Thrust to Weight Ratio

V_{cr} - Cruise Velocity [knots, ft/sec]

VL - Vertical Landing

V_a - Approach Speed

V_{max} - Max Velocity

V_s - Stall Speed

VTO - Vertical Take Off

VTOL - Vertical Take Off and Landing

WE - Empty Weight [lb]

WF - Fuel Weight [lb]

WPL - Payload Weight [lb]

W/S - Wing Loading

WTO - Take Off Weight [lb]

LIST OF FIGURES

LIST OF TABLES

1 INTRODUCTION

On April 6, 2009 Secretary of Defense Robert M Gates gave a briefing outlining recommend changes for the Department of Defense. Part of his recommendation was "To grow our special operations capabilities, we will increase personnel by more than 2,800 or five percent and will buy more special forces-optimized lift, mobility, and refueling aircraft." This report discusses the preliminary design of a next generation Special Forces-optimized transport vehicle to meet this need. It follows the development of mission requirements through preliminary system design. Key requirements for a Special Forces optimized transport vehicle include rapid deployment, stealth, and independence from airstrips. The analysis performed for this report was done using a combination of text references and computer tools, primarily the Advanced Aircraft Analysis (AAA) program.

The developed aircraft is the Advanced Vertical Takeoff and Landing Dropship (AVD). The AVD uses vertical takeoff and landing (VTOL), low observables, and light weight materials to meet or exceed mission requirements. Although the aircraft is "advanced," it is not intended require any new technologies to be developed. It will leverage the state of the art materials and methods currently available to fill a critical hole in the current capabilities of the US Special Forces units.

1.1 BACKGROUND

There are several vehicles that would meet the minimum requirement of transporting Special Forces units. Some seafaring vessels, such as the HSV-2 Swift (Figure 1-1 below), are used in the transport of Special Forces units. The Swift has a top speed of approximately 40 knots, and an impressive cargo capacity of over 300 passengers or 600 short tons. This allows the Swift to rapidly deploy soldiers and vehicles. The Swift has obvious short comings in low speed and dependence on a shoreline for deployment (1).

Figure 1-1 - HSV 2 Spirit (1)

There are also several rotorcraft options for Special Forces transports, including the MH-47D Chinook (Figure 1-2). The Chinook can transport up to 33 soldiers with equipment at speeds up to 170 knots. With several possible configurations of crew, personnel, and internal/external cargo, the Chinook is a very adaptable vehicle. Helicopters offer the benefit of vertical takeoff and landing (VTOL) and provide a stable platform for rapid troop deployment. Helicopters suffer from slow speeds a large radar signature, and relatively short range (2).

Figure 1-2 - MH-47D Chinook (2)

One of the most versatile options currently available is the CV-22 Osprey (Figure 1-3). The Osprey is the latest vehicle to be outfitted for Special Forces missions. As such it is considered the baseline for comparison. It utilizes a tilt-rotor propulsion system that allows for VTOL and hover functions of a helicopter with the fuel efficiency and speed of a turboprop. With a maximum speed of 275 knots and a range of 879 nm, the Osprey is relatively slow, with a short range, and no stealth capability (3).

Figure 1-3 - CV-22 Osprey (3)

There is already speculation on what the mission requirements for the next generation special operations aircraft would be. The Federation of American Scientist (FAS) has stated what they believe to be the mission requirements for the next generation special operations aircraft. They envision the new aircraft replacing both the CV-22 and the MC-130. The system would have a mission range of 2400nm, combat radius of 1000nm, STOL with max fuel and 4000lbs at standard sea level conditions (1500ft over 50ft obstacle), vertical takeoff and landing (VTOL) with 4000lbs at mid-mission point (4000ft/85°F), High Speed of 250-400ktas), low to moderate signature, system reliability of 92% with an 85% fix rate (4hrs), capable of performing clandestine missions, carrier operations, and with a survivable ground environment under hovering aircraft (4).

2 Mission Specification and Comparative Study

This section identifies key mission characteristics and requirements for the AVD, and provides a brief comparison with current aircraft (5).

2.1 Mission Specification

This section lists key AVD mission specifications. The specifications were derived from reference (4) and best engineering judgment.

- Payload Capacity
  - Crew - 2 (220lb each)
  - Troops - 14 (220lb each)
  - Equipment - 14 (100lb each)
- Range
  - Max - 2400nm
  - Combat radius - 1000nm
- Speed
  - Cruise - 470 knots (@30,000, M=0.80)
  - Supercruise - 782 knots(@50,000ft, M=1.36)
  - Max speed - 956 knots (@50,000, M=1.67)
- Take-off
  - STO 1500 ft over 50 ft obstacle (w/max fuel and 5000 lbs on standard day @sea level, used for max range)
  - VTO (w/max fuel and 5000 lbs on standard day @sea level)
  - VTO (w/5000lbs @ mid-mission point 4000ft/86 degrees F)
  - Compatible with C-11 type ship based catapult

- Landing
    - SL 1500ft over 50 ft obstacle (w/50% fuel and 5000 lbs on standard day @sea level)
    - VL (w/max fuel and 5000 lbs on standard day @sea level)
    - VL (w/5000lbs @ mid-mission point 4000ft/86 degrees F)
    - Compatible with ship based arrested landing device
- Approach speed
    - 72 knots
- Noise requirements
    - Effort should be made to minimize sonic boom while over land.

2.2 Mission Profile

Figure 2-1 illustrates the reference design mission used to achieve the 1000nm combat radius. It uses a short takeoff and landing (STOL), subsonic cruise, and a VTOL deployment mid mission.

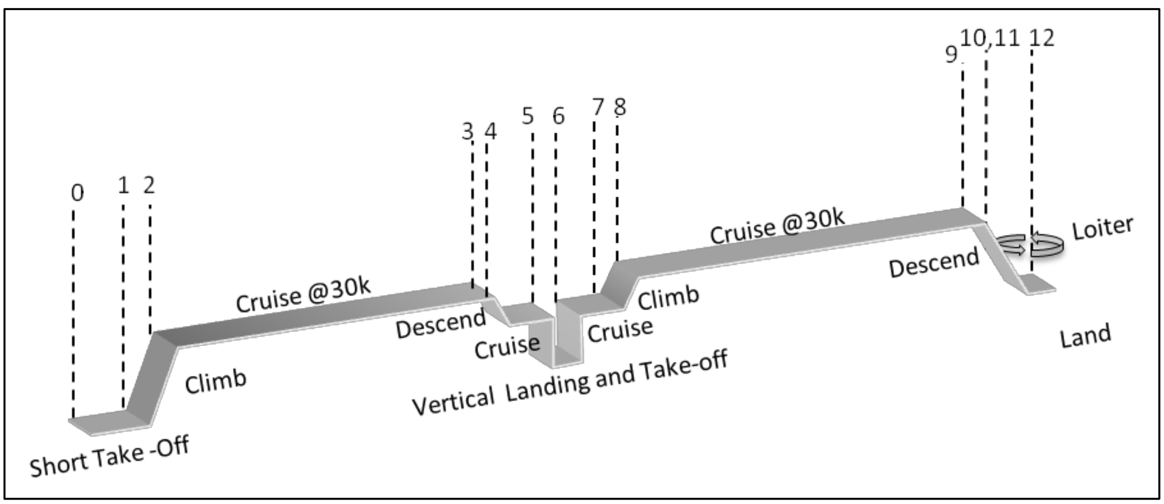

Figure 2-1 - Design Mission (Rc = 1000nm)

Figure 2-2 shows the profile used to achieve the max range mission. It uses STOVL and subsonic cruise. Warfighters are deployed via aerial deployment mid-mission.

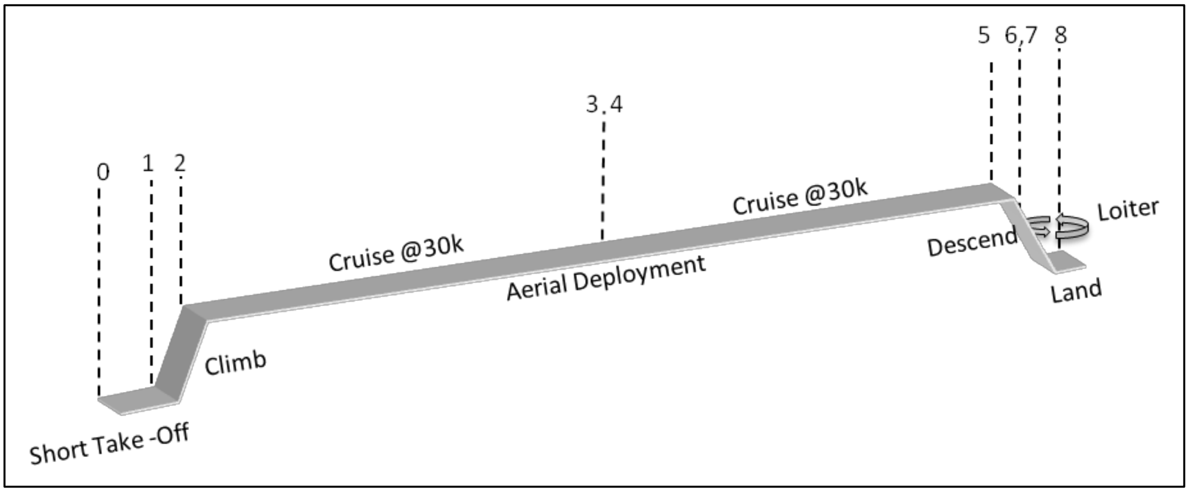

Figure 2-2 - Max Range Mission (2400nm)

Figure 2-3 shows a quick deployment short range mission utilizing supersonic cruise and VTOL at beginning, mid, and end mission points.

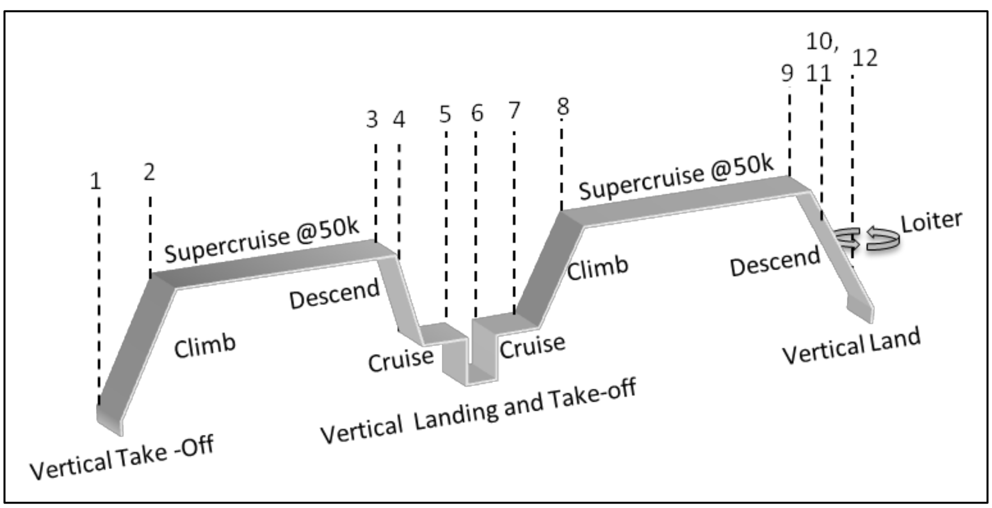

Figure 2-3 - Short Range w/ Supercruise

2.3 Critical Mission Requirements

Key mission requirements are listed in Table 2-1. Radar Cross-Section (RCS) requirements are dependent upon classified information about anticipated missions. They are noted as to be determined (TBD) at this stage in design.

Table 2-1 - Mission Requirements

Req ID	Requirement
MIS 1.0	The AVD program shall have a maximum range equal to or greater than 2,400nm.
MIS 1.1	The AVD shall have a combat radius equal to or greater than 1000nm.
MIS 2.0	The AVD shall be capable of vertical take-off and landing at full take-off weight.
MIS 2.1	The AVD shall be compatible with a ship based catapult and reset systems.
MIS 2.2	The AVD shall be capable of short takeoff and landing (1500 ft over 50 ft obstacle).
MIS 3.0	The AVD shall have a time to target of no more than 3hrs.
MIS 4.0	The AVD shall be capable of transporting 14 troops (220lb each) and equipment (100lb each).
MIS 4.1	The AVD shall adhere to troop transport standards including but not limited to (cabin temperature, pressure, air quality, physical restraint during take-off/landing)
MIS 4.2	The AVD shall have a survivable ground environment under aircraft during hover.
MIS 5.0	The goal is to have a forward RCS no greater than [TBD] dB within [TBD] degrees off the nose at +/- [TBD] degrees elevation.
MIS 5.1	The rear RCS should be no greater than [TBD] db within [TBD] degrees at +/- [TBD] degrees in elevation.
MIS 5.2	The lateral RCS should be no greater than [TBD] db at +/- [TBD] degrees in elevation.

2.4 Comparative Study of Similar Aircraft

This section notes the characteristics of similar aircraft.

2.4.1 Mission capabilities

Table 2-2 highlights the capabilities and configuration of comparison aircraft. Note that the MV-22VB is the only aircraft on the list capable of being used as a Special Forces transport; it will therefore be used as the main vehicle for future comparisons.

Table 2-2 - Aircraft Characteristics

Name	Supersonic	Carrier Launch	VTO	VL	Stealth	2000mi Range	Wing Location	Tail Type
MV-22VB	-	X	X	X	-	-	High	Boom-mount
B-1B	X	-	-	-	X	X	Low	Cruciform
F-35C	X	X	-	X	X	-	Mid	Twin
F-22	X	-	-	-	X	X	Mid	Twin
Harrier GR.7	-	X	X	X	-	-	High	Conventional
B2	X	-	-	-	X	X	Mid	-
Aerion	X	-	-	-	-	X	Low	Cruciform

2.4.2 Important Design Parameters

Table 2-3 and Table 2-4 note some key parameters of the reference aircraft introduced in section 3.1.

Table 2-3 - Aircraft Parameters I

Name	Crew	PL type	W_{TO} [lb]	$W_{TO(max)}$ [lb]	W_{PL} [lb]	W_E [lb]	W_F [lb]	T [lbf]	V_{cr} [knots]	V_{max} [knots]
MV-22VB	2	24(Seated), 32 (floor loaded)	47,500	60,500	15000	33140	-	2x 6,150hp	241	305
B-1B	4	Bombs	326,000	477,000	134,000	192,000	10,000	4x 14,600 (30,780 w/ afterburner)	-	721
F-35C	1	Weapons (missiles, bombs)	44,400	70,000	18,000	34,800	20,085	25,000 (42,000 w/afterburner) +18,000 liftfan	-	1,115
F-22	1	Weapons (missiles, bombs)	64,460	83,500	20,000	43,430	18,000	2x 35,000	1,060	1,303
AV-8B+	1	Weapons (missiles, bombs)	22,950	20,755 (VTO) 31,000 (STO)	13,200 (STO)	13,968	-	23,500	-	575
B2	2	Bombs	336,500	376,000	50,000	158,000	-	4x 17,300	470	525
Aerion	2	Passengers	45,000	90,000	-	-	45,400	2x 19,600	M1.6	M1.5

(6)

Table 2-4 - Aircraft Parameters II

Name	R [nm]	R_f [nm]	R_c [nm]	h_{cr}	Length	Height	S [ft^2]	b	AR	T/W (100% fuel)	T/W (50% fuel)	Wing Loading [lb/ft^2]	RoC [ft/min]
MV-22VB	879	2,417	370	26,000	57.3	17.9	301	45.83	6.97	0.259	-	-	2,320
B-1B	6,478	-	2,993	60,000	146	34	1,950	137 79 (swept)	9.6 3.2 (swept)	0.38	-	167	-
F-35C	1,400	-	640	60,000	51.5	14.9	668	43	2.76	0.77	0.95	91.4	-
F-22	1,600	1,738	410	65,000	62	16.7	840	44.5	2.36	1.08	1.26	77	-
AV-8B+	1,200	1,800	300	50,000	46.3	11.7	243	30.33	3.78	1.13	-	94.29	14,700
B2	6,000	-	-	50,000	69	17	5,140	172	5.76	0.205	-	67.3	
Aerion	4,000	-	-	51,000	148.3	23.3	1,200	64.2	3.43	-	-	-	-

(6)

2.5 DISCUSSION

There are several aircraft that have some characteristics of the proposed AVD. The payload capacity of the larger aircraft far exceeds that required for the AVD. The smaller fighter aircraft have a more comparable payload capacity, but have less volume. The range for the B-1B, B2, and Aerion are comparable for to that specified for the AVD. The only one that can accomplish a similar mission is the MV-22B, which has been optimized for a general transportation tasks and fails to meet many of the listed requirements. Each aircraft selected will act as a valid reference point for some stage of the AVD development.

3 CONFIGURATION SELECTION

This is the section details the AVD configuration study and selection.

3.1 DISCUSSION OF MAJOR DESIGN IMPACT ITEMS

This section covers items which have a major impact on the AVD design.

3.1.1 DISCUSSION OF MISSION REQUIREMENTS

A list of mission requirements is found in Table 2-1. Key mission requirements are listed in Table 2-1. MIS 1.0 and 2.X proved to be the most difficult to achieve. Attaining the required range will require an efficient cruise, light weight, and advanced high speed aerodynamics. The short takeoff and landing require high lift devices which are heavy and directly and indirectly increase drag during cruise. The low observable requirements in 5.X will also be difficult to achieve along with an aerodynamic profile that supports an extended range.

3.2 COMPARATIVE STUDY OF AIRPLANES WITH SIMILAR MISSION PERFORMANCE

This section provides discussion on the physical configuration of the similar aircraft identified in section 2.4.

3.2.1 MV-22 Osprey

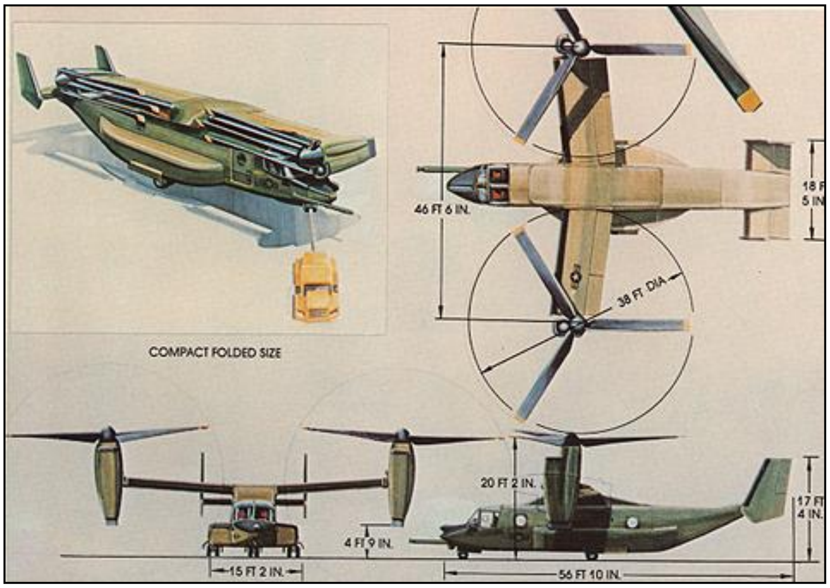

Figure 3-1- MV-22VB (Osprey) (7)

- Fuselage - The Osprey's fuselage is designed for packing efficiency. Due to its low cruising speed it does not require an advanced aerodynamic profile. The space has instead been optimized to maximize usable interior space.
- Propulsion - The aircraft was designed with the intent of having hovering efficiency similar to a helicopter, while having cruise efficiency similar to an airplane. This was accomplished using two Rolls-Royce T406s. They are placed at the tips of the wings to allow for adequate spacing of the large rotors. The rotors can move 90° from horizontal to vertical to facilitate VTOL and cruise. (3)
- Wings - Wings approximately rectangular in planform. This is acceptable for the aircraft's low top speed. It also allows for the increased structural robustness needed to support the two propulsion units on each tip. The wings are mounted high to provide adequate ground clearance for the rotors during a conventional take

off and landing (CTOL), and to allow access for troops to maneuver around the aircraft. The wings also swing back into a storage configuration which greatly reduces the effective width for storage, especially when based on an aircraft carrier.

- Tail - The tail is mounted at the end of a wedge created by the need for a ramp for ingress/egress. The H configuration allows for better lateral control without the need for a larger vertical tail.
- Cabin - The cabin is designed to transport crew, equipment, vehicles, or any other payload that will fit and meet weight requirements. The restraints for personnel and cargo are designed for subsonic speeds.

3.2.2 *B-1B Lancer*

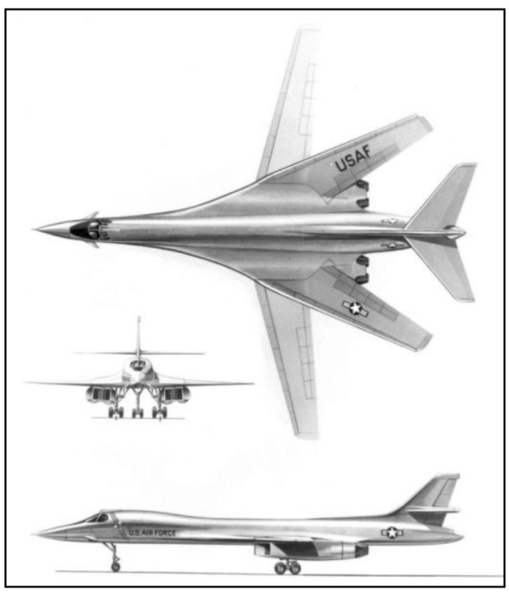

Figure 3-2 - B-1B (Lancer) (8)

- Fuselage - The Lancer has a streamlined fuselage to help lower supersonic drag and provide a low radar signature.

- Propulsion - The Lancer accomplishes the speed requirements of its mission by way of four GE F101-GE-102 jet engines. The engines can produce a total of 123,120 lbs of thrust with afterburners, propelling the aircraft up to Mach 1.25. The wings are mounted beneath the wings for ease of access. (9)
- Wings - The Lancer has a need for high speeds and long ranges. Each prefers a different wing configuration. The Lancer utilizes a swept wing that goes upswept for efficient cruise and loiter at low speeds, and sweeps back for more efficient cruising at high speeds.
- Cabin - The Lancer holds a crew of four in the forward part of the aircraft, the rest is reserved for internal payload.

3.2.3 F-35 Joint Strike Fighter (JSF)

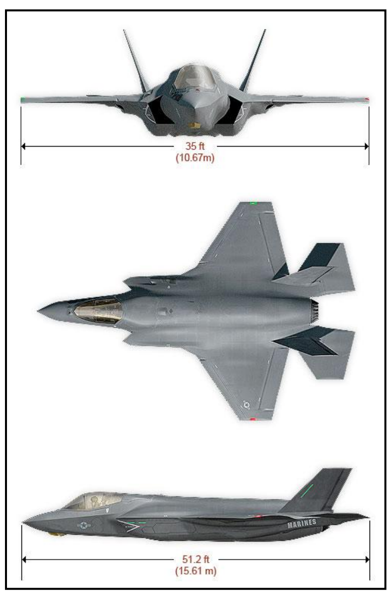

Figure 3-3 - F-35 (Joint Strike Fighter) (10)

- Fuselage - Conventional fuselage optimized for supersonic flight and low radar signature.
- Propulsion - Pratt and Whitney F135 (25,000lb, 42,000lb w/ afterburner) + Rolls-Royce Liftfan (18,000lb) The wings are mounted beneath the wings for ease of access.
- Wings - Conventional high wing. Shaped for supersonic flight, leading and trailing edges of wing and tail were also positioned to achieve desired stealth characteristics.
- Cabin - Cockpit supports one pilot

3.2.4 *F-22 Raptor*

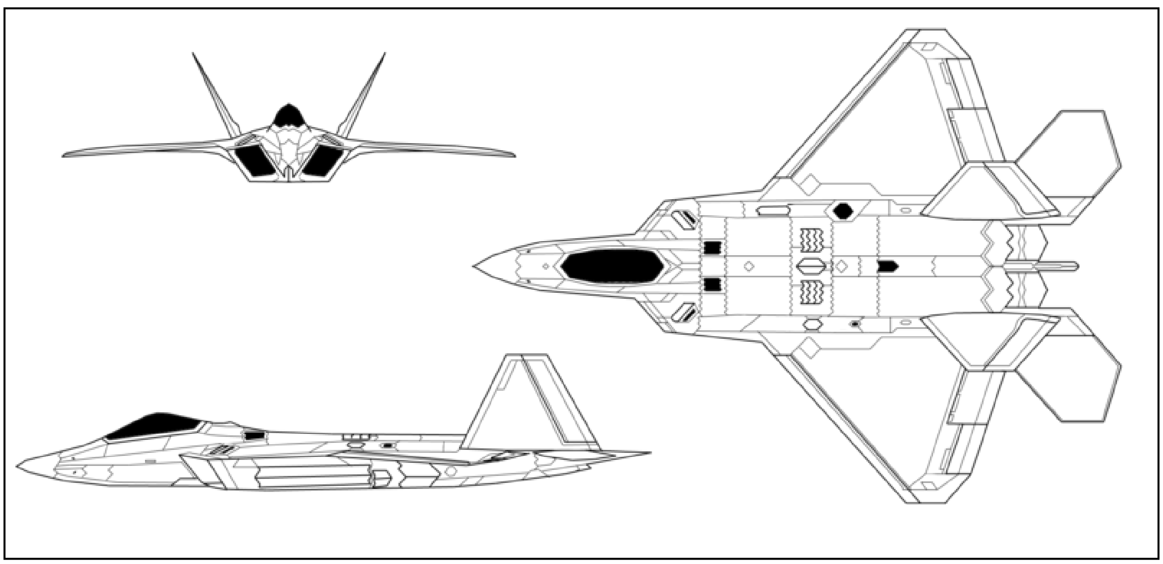

Figure 3-4 - F-22 (Raptor) (11)

- Fuselage - Conventional fuselage optimized for supersonic flight and low radar signature.

- Propulsion - 2x Pratt and Whitney F119 (35,000lb/each) The wings are mounted beneath the wings for ease of access.
- Wings - Conventional high wing. Shaped for supersonic flight, leading and trailing edges of wing and tail were also positioned to achieve desired stealth characteristics.
- Cabin - Cockpit supports one pilot

3.2.5 AV-8B+ Harrier II

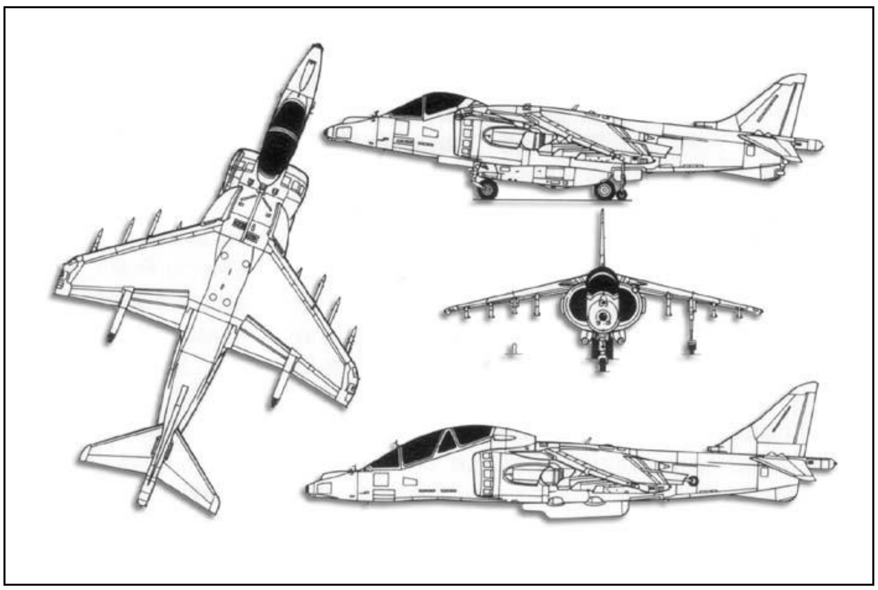

Figure 3-5 - AV-8B+ (Harrier II) (12)

- Fuselage - Conventional fuselage optimized for subsonic flight and positioning of two sets of vectored exhaust nozzles
- Propulsion - The AV-8B achieves VTOL by way of a single Rolls-Royce F402-RR-408 (23,500lb) with thrust vectoring nozzles (11)

- Wings - high mounted wings to support location of engine and swivel nozzles. Wing must be removed in order to service engine. Compromise was allowed in order to minimize weight in support of VTOL.
- Cabin - Cockpit supports one pilot

3.2.6 B-2 Spirit

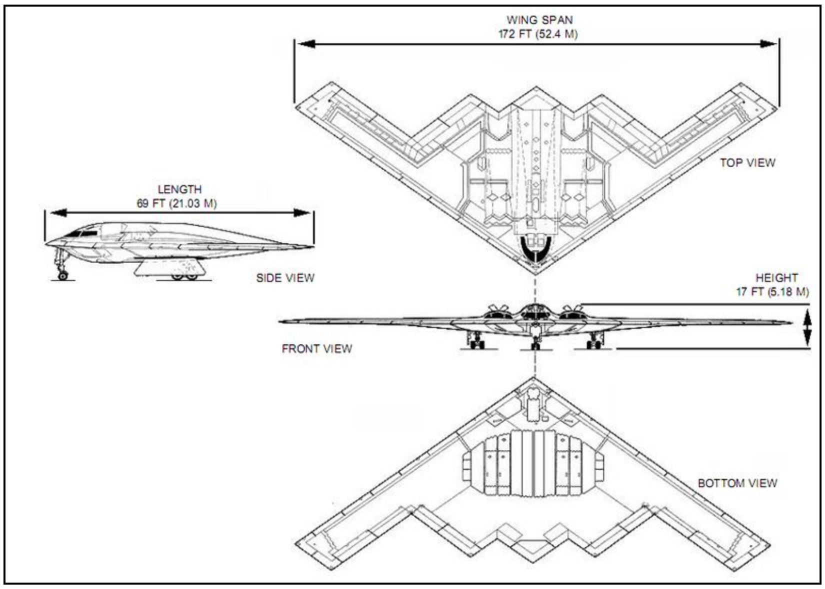

Figure 3-6 - B2 (Spirit) (12)

- Fuselage/Wing - The spirit uses a lifting body configuration to maximize L/D and minimize radar signature. The lack of a vertical or horizontal tail is also to minimize radar signature.
- Propulsion - 4x GE F118-GE-100 (17,300 lb each) (12) Engines are buried in the fuselage to minimize RCS and thermal signature.
- Cabin - Cockpit for two pilots.
- Cargo Bay - Two internal bays for 50,000lb of ordnance

3.2.7 *AERION SUPERSONIC BUSINESS JET*

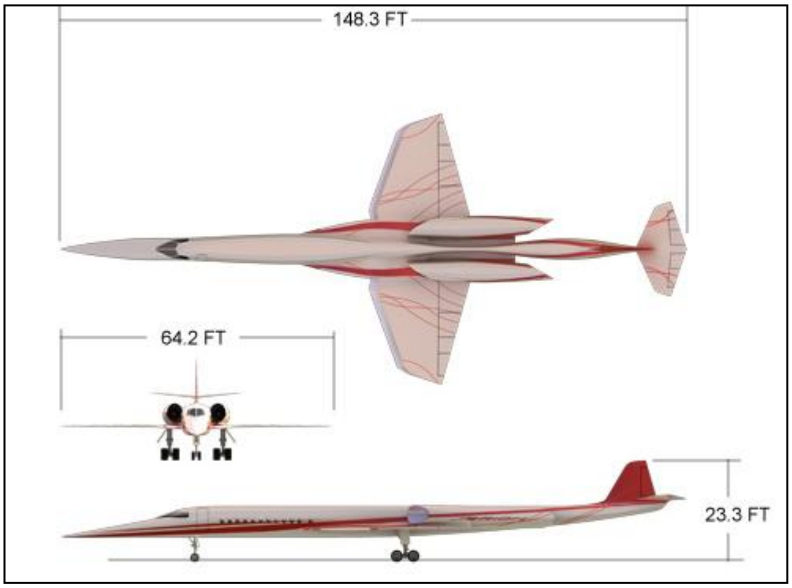

Figure 3-7 - Aerion Supersonic Business Jet (13)

- Fuselage - Designed with natural laminar flow (NLF) concept. This new wing planform reduces drag up to its cruise speed of M1.6 while minimizing sonic boom (7).
- Propulsion - 2x PW JT8D-219 (19,600 lbs)
- Wings - Designed with NLF concept. This new wing planform reduces drag up to its cruise speed of M1.6 while minimizing sonic boom (7).
- Cabin - The Aerion has a typical luxury airliner cabin. It boasts several available configurations that optimize the number of passengers, comfort, productivity, etc.

3.3 SELECTION OF PROPULSION SYSTEM

Selecting an adequate propulsion system is one of the most critical design considerations for a VTOL aircraft. Due to physics and mechanics VTOL requires substantially more thrust than cruise. This leads to an engine that either cannot do VTOL, is inefficient at cruise, or additional engines that are only utilized for VTOL.

3.3.1 SELECTION OF THE PROPULSION SYSTEM TYPE

Due to the high thrust required to achieve the speed and VTOL requirements a turbofan was selected as the primary propulsion system. Due to balancing and additional thrust requirements of VTOL a set of liftfans is also anticipated.

3.3.2 SELECTION OF THE NUMBER OF ENGINES

For VTOL there are several options: engine(s) with thrust vectoring, separate cruise engine(s) and lift engines, engine with liftfan, etc. Each option also has several sub-options. The engine with thrust vectoring option is used on the AV-8+ Harrier II and the engine with liftfan is used on the F-35 JSF. A single set of engines for VTOL and cruise is inherently inefficient. A separate engine for cruise and VTOL solves the efficiency problem, but the lift engines tend to add a considerable weight penalty. Using a liftfan (either shaft or tip driven) has been shown to be able to produce an adequate thrust augmentation for a lesser weight penalty. Based on the current weight estimate of 40,000lb, anticipated thrust requirements, reliability, cg positioning, engine volume and positioning estimates for one versus two engines a two engine/two liftfan configuration was selected for the AVD.

3.3.3 *Engine Selection*

Several characteristics were considered when selecting a propulsion system including: development cost, reliability, and thrust class. Using a rubber-engine in the design would have facilitated the overall system design process, but with such a critical system the decision was made to go with a pre-existing engine.

There are a few issues with using an existing engine. The first is that the there is limited room to customize the solution, this may yield an engine that either has too high a thrust, or too low. Given the choice between the two the high low thrust option will offer better efficiency but may not meet time to target or take-off requirements. The high thrust option may add un-needed weight and need to be run in at a suboptimal point during cruise increasing fuel consumption and decreasing range.

With hundreds of options the selection had to be narrowed early in development. The three engines selected for further investigation were the Pratt & Whitney F119, F135, and JT8D. The F135 the newest and most advanced engine currently available. The F-135 offers 25,000lb of thrust (42,000lb with afterburner) and has a proven track record with use with a liftfan. The F119 is the slightly older cuisine of the F-135. The current application of the 35,000lb thrust class engine is in a twin configuration on the F-22 Raptor. First flown in 1964, the JT8D is the more seasoned option. It currently has over a dozen variants ranging from 14,000 to 21,000lb thrust that support civilian and military, subsonic and supersonic aircraft. The JT8D powers one-sixth of the world's airline aircraft and has accumulated more than half a billion hours (15).

JT8D's proven history, availability, user knowledge base, and wide range of thrust options made it the preferred engine for AVD. The primary requirements for the propulsion system are the ability for VTOL at take-off weight, and the ability to supercruise at M 1.36+. The JT8D has experience in the supercruise category

3.4 Configuration Selection

3.4.1 Overall Configuration

The AVD will function as a land and aircraft carrier based transport vehicle. The fuselage will be a conventional single shell sized for 14 troops with equipment. It will have a pilot/co-pilot cockpit. The exterior will be designed to minimize observable signatures and drag. The aircraft's requirements in order of importance are: safely carry troops, achieve desired range, achieve desired stealth characteristics, and achieve desired cruise speeds.

3.4.2 Wing Configuration

Thing wing will be an aft swept high wing. Leading edge (LE) sweep angle will be sized minimize drag for the supersonic cruise condition. Wing geometry may need adjustments to account for low observable considerations. The table below details initial wing geometry estimates based on comparison aircraft. A more detailed wing analysis is covered in section 7.

Table 3-1 - Wing Geometry

Airfoil	Dihedral Angle	Incidence Angle	Aspect Ratio	Sweep Angle	Taper Ratio	Wing Area	Wing Type
NACA 64,1-412	0	0	2.87	39	0.5	840	ctl/high

3.4.3 *Empennage Configuration*

The AVD will utilize a dual V-tail and inverted V-tail, effectively making an X-tail. This dual tail system will limit the horizontal and vertical span of the tail improving packaging. It will also inherently help reduce right angles for which will aid in maintaining a low RCS.

3.4.4 *Integration of the Propulsion System*

A two-engine/single liftfan and two-engine/dual-liftfan configurations were considered for the AVD. Both configurations utilize air bled from the compressor to power roll stabilizing jets positioned at the aircrafts extremities.

The two-engine/single liftfan configuration has an engine buried in the fuselage beneath each wing and a tip driven liftfan in the aft boom structure of the tail. This configuration provides clean uninterrupted flow to the inlets while being able to support stealth requirements. Having the engines directly adjacent to the troop cabin causes increased heating and noise which would be unfavorable.

The two-engine/dual-liftfan configuration finds the twin engines buried in the aft portion of the fuselage and the two shaft driven liftfans nested beneath the wings. This configuration offers lower noise and temperatures to the troop cabin and provides a center of gravity more in line with the geometric center while still providing a general configuration that will support stealth requirements. The low interior noise and heat and better weight distribution were the main drivers for choosing this configuration.

As with any VTOL aircraft, hot gas ingestion, needs to be analyzed to ensure engine performance during hover. The inlets for the AVD have been placed on top of the fuselage.

This has the potential for flow problems at high angles of attach, but will minimize exhaust ingestion during hover. Since the AVD is not intended for high maneuvering scenarios like that of a fighter, this is seen as an acceptable trade. Inlets, fan, and engine components will need to be analyzed and tested against expected foreign object damage (FOD) conditions during the detailed design phase.

4 WEIGHT SIZING & SENSITIVITIES

This section details the weight sizing analysis for the AVD.

4.1 MISSION WEIGHT ESTIMATES

This section covers items which have a major impact on the AVD design.

4.1.1 DATA BASE FOR TAKEOFF WEIGHTS AND EMPTY WEIGHTS OF SIMILAR AIRPLANES

Below is a list of aircraft empty and takeoff weights used for functionalization.

Table 4-1 - Weight Database

#	Airplane Name	W_{TO} [lb]	W_E [lb]	Class	Source
1	Eurofighter 2000	46297.0	22044.0	Fighter	AAA
2	Dassault Rafael	47399.0	21319.0	Fighter	AAA
3	MD Mirage F-1	35715.0	16314.0	Fighter	AAA
4	Grumman F14A	74348.0	39762.0	Fighter	AAA
5	LM F-22 Raptor	64460.0	43430.0	Fighter	Wikipedia
6	LM F-35 JSF	44400.0	34800	Fighter	Wikipedia
7	V-22 Osprey	47500.0	33140.0	Transport	Wikipedia
8	B1 Lancer	326000.0	192000.0	Bomber	Wikipedia
9	AV-8B Harrier II	22950.0	13968.0	Fighter	Wikipedia

4.1.2 *DETERMINATION OF REGRESSION COEFFICIENTS A AND B*

Figure 4-1 is a plot generated using the AAA program showing the regression curve and A and B coefficients for the selected comparison aircraft.

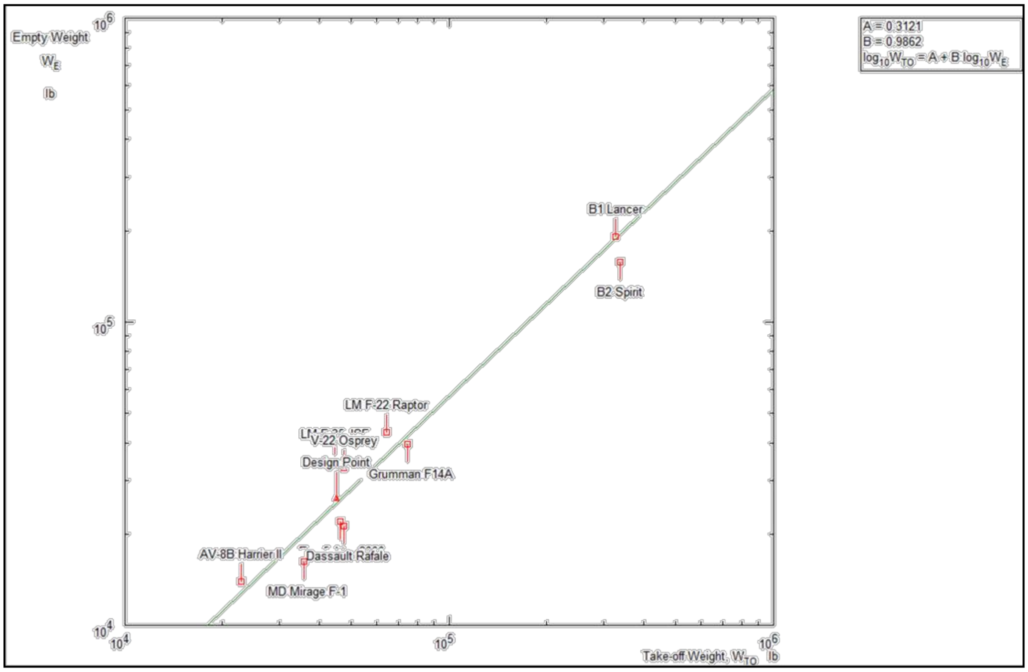

Figure 4-1 - Regression Curve

4.1.3 *DETERMINATION OF MISSION WEIGHTS*

The weight profiles below were calculated using the AAA program. The three major design missions laid out in section 2.2 were analyzed. The 1000 nm design mission is considered the baseline mission. It was used as the starting point and a reference for the long and short range missions. Weight sizing was based on calculated mass fuel fractions (mff). The main elements in generating the mff, and in turn the weight, were L/D and sfc. They along with the mission range and speed were used to calculate the cruise mff (mff_c). The takeoff and landing mff ($mff_{TO/L}$) was also used for capturing the difference between short and vertical takeoff scenarios.

4.1.3.1 Design Mission

The design mission used the parameters below. The L/D was based on typical ratios for transports and fighters. The sfc is the cruise value from the manufacture. The mff_c was calculated. The $mff_{TO/L}$ value used is standard for takeoff/landing. These values lead to the mission parameters and weights in Table 4-2 and Table 4-3. The design takeoff weight was calculated to be 37,934 lb.

Table 4-2 - Design Mission Weight Parameters

Parameter	Value
L/D	12.0
sfc_c (c_j)	0.737
mff_C *(per segment)*	0.8896
$mff_{TO/L}$	0.9950
TakeoffWeightRegCoeffA	0.312135
TakeoffWeightRegCoeffB	0.986194
EstimatedTakeoffWeight	45500
PassengerWeight	220
NumberPax	14
BagWeight	100
PilotWeight	220
NumberPilots	2
CrewOtherWeight	0
NumberOtherCrew	0
CargoWeight	0
TrappedFuelOilFraction	0.5
FuelReserveFraction	10

Parameter	Value
PlotWeightTakeoffMin	10000
PlotWeightTakeoffMax	80000
MissionFuelFraction	0.721764
ExpendedPayloadWeight	0
FuelWeight	10554.53
MissionFuelWeight	11609.98
MaxFuelWeight	11609.98
ReserveFuelWeight	1055.453
TrappedFuelWeight	189.6684
CrewWeight	440
NumberCrew	2
PayloadWeight	4480
UsefulWeight	16529.98
EmptyWeight	21214.03
TakeoffWeight	37933.68

Table 4-3 - Design Mission Profile Weights

	Mission Profile	Segment BeginWeight	Segment FuelUsedWeight	Segment BeginFuelWeight
1	Warmup	37933.7	189.7	11610.0
2	Taxi	37744.0	188.7	11420.3
3	Take-off	37555.3	187.8	11231.6
4	Climb	37367.5	183.1	11043.8
5	Cruise	37184.4	4105.2	10860.7
6	Descent	33079.2	165.4	6755.5
7	Cruise	32913.8	164.6	6590.1
8	Loiter	32749.2	57.4	6425.5
9	Land/Taxi	32691.8	653.8	6368.1
10	Payload Exp	32037.9	0.0	5714.2
11	Take-off	32037.9	640.8	5714.2
12	Climb	31397.2	51.4	5073.5
13	Cruise	31345.8	156.8	5022.1
14	Climb	31189.0	102.0	4865.3
15	Cruise	31087.0	3432.0	4763.3
16	Descent	27655.0	138.3	1331.3
17	Land/Taxi	27516.7	137.6	1193.0

4.1.3.2 Long Range Mission

The long range mission used the parameters below. The L/D was based on typical ratios for transports and fighters. The sfc is the cruise value from the manufacture. The mff_c was calculated to achieve the maximum range. An iterative approach yielded a max range of 3275 nm. Note that this is approximately 800 nm further than the mission requirement. The $mff_{TO/L}$ value used is standard for takeoff/landing. These values lead to the mission parameters and weights in Table 4-4 and Table 4-5. The design takeoff weight of 37,934 lb was maintained.

Table 4-4- Long Range Mission Weight Parameters

Parameter	Value
L/D	12.0
sfc_c (c_j)	0.737
mff_C *(only one segment)*	0.6817
$mff_{TO/L}$	0.9950
TakeoffWeightRegCoeffA	0.312135
TakeoffWeightRegCoeffB	0.986194
EstimatedTakeoffWeight	45500
PassengerWeight	220
NumberPax	14
BagWeight	100
PilotWeight	220
NumberPilots	2
CrewOtherWeight	0
NumberOtherCrew	0
CargoWeight	0
TrappedFuelOilFraction	0.5

Parameter	Value
FuelReserveFraction	10
PlotWeightTakeoffMin	10000
PlotWeightTakeoffMax	80000
MissionFuelFraction	0.721764
ExpendedPayloadWeight	0
FuelWeight	10554.53
MissionFuelWeight	11609.98
MaxFuelWeight	11609.98
ReserveFuelWeight	1055.453
TrappedFuelWeight	189.6684
CrewWeight	440
NumberCrew	2
PayloadWeight	4480
UsefulWeight	16529.98
EmptyWeight	21214.03
TakeoffWeight	37933.68

Table 4-5 - Long Range Mission Profile Weights

	Mission Profile	Segment BeginWeight	Segment FuelUsedWeight	Segment BeginFuelWeight
1	Warmup	37933.7	189.7	11610.0
2	Taxi	37744.0	188.7	11420.3
3	Take-off	37555.3	187.8	11231.6
4	Climb	37367.5	183.1	11043.8
5	Cruise	37184.4	4105.2	10860.7
6	Descent	33079.2	165.4	6755.5
7	Cruise	32913.8	164.6	6590.1
8	Loiter	32749.2	57.4	6425.5
9	Land/Taxi	32691.8	653.8	6368.1
10	Payload	32037.9	0.0	5714.2
11	Take-off	32037.9	640.8	5714.2
12	Climb	31397.2	51.4	5073.5
13	Cruise	31345.8	156.8	5022.1
14	Climb	31189.0	102.0	4865.3
15	Cruise	31087.0	3432.0	4763.3
16	Descent	27655.0	138.3	1331.3
17	Land/Taxi	27516.7	137.6	1193.0

4.1.3.3 SHORT RANGE VTOL MISSION

The short range VTOL mission used the parameters below. The L/D was based on a supersonic cruise vehicle. The sfc during cruise was based on the value from reference (9). Detailed engine data on the JT8D-7 can be found in Appendix 1. The mff_c was calculated to maintain supercruise velocity and weight. The $mff_{TO/L}$ value was calculated by doubling the fuel spent during a conventional takeoff. These values lead to the mission parameters and weights in Table 4-6 and Table 4-7. The design takeoff weight of 37,934 lb was maintained. An iterative approach was used to calculate a short range combat radius of 650 nm.

Table 4-6 - Short Range Mission Weight Parameters

Parameter	Value
L/D	6.0
sfc_c (c_j)	0.800
mff_C	0.8882
$mff_{TO/L}$	0.9900
TakeoffWeightRegCoeffA	0.312135
TakeoffWeightRegCoeffB	0.986194
EstimatedTakeoffWeight	45500
PassengerWeight	220
NumberPax	14
BagWeight	100
PilotWeight	220
NumberPilots	2
CrewOtherWeight	0
NumberOtherCrew	0
CargoWeight	0
TrappedFuelOilFraction	0.5
FuelReserveFraction	10

Parameter	Value
PlotWeightTakeoffMin	10000
PlotWeightTakeoffMax	80000
MissionFuelFraction	0.724401
ExpendedPayloadWeight	0
FuelWeight	10211.62
MissionFuelWeight	11232.78
MaxFuelWeight	11232.78
ReserveFuelWeight	1021.162
TrappedFuelWeight	185.262
CrewWeight	440
NumberCrew	2
PayloadWeight	4480
UsefulWeight	16152.78
EmptyWeight	20714.36
TakeoffWeight	37052.4

Table 4-7 - Short Range Mission Profile Weights

	Mission Profile	Segment BeginWeight	Segment FuelUsedWeight	Segment BeginFuelWeight
1	Warmup	37052.4	185.3	11232.8
2	Taxi	36867.1	184.3	11047.5
3	Take-off	36682.8	366.8	10863.2
4	Climb	36316.0	178.0	10496.4
5	Cruise	36138.0	3768.3	10318.4
6	Descent	32369.7	161.8	6550.0
7	Cruise	32207.8	161.1	6388.2
8	Loiter	32046.7	56.2	6227.1
9	Land/Taxi	31990.6	639.8	6170.9
10	Payload Exp	31350.7	0.0	5531.1
11	Take-off	31350.7	627.0	5531.1
12	Climb	30723.7	50.3	4904.1
13	Cruise	30673.5	153.4	4853.8
14	Climb	30520.1	99.8	4700.4
15	Cruise	30420.2	3172.1	4600.6
16	Descent	27248.1	136.2	1428.5
17	Land/Taxi	27111.9	271.1	1292.3

4.2 Takeoff Weight Sensitivities

This section goes over weight sensitivities and trade studies performed for AVD. The results of this work will be used to tune the design parameters.

4.2.1 Calculation of Takeoff Weight Sensitivities

Below is weight sensitivity information calculated using AAA.

Table 4-8 Weight Sensitivity Parameters

Parameter	Value
TakeoffWeightRegCoeffB	0.986
MissionFuelFraction	0.72
PayloadWeight	4480
CrewWeight	440
TrappedFuelOilFraction	0.5
FuelReserveFraction	10
TakeoffWeight	37933.68
EmptyWeight	21214.03
SensitivPayloadWeight	8.21
SensitivCrewWeight	8.21
SensitivEmptyWeight	1.76

Table 4-9 - Mission Sensitivity Table (Design Mission)

	Mission Profile	Sensitiv Expended Payload	Sensitiv Refuel Weight	Sensitiv JetSFC [lb-hr]	Sensitiv Range [lb/nm]	Sensitiv LiftToDrag [lb]	Sensitiv Endur [lb/hr]
1	Warmup	-	-	-	-	-	-
2	Taxi	-	-	-	-	-	-
3	Take-off	-	-	-	-	-	-
4	Climb	-	-	1647.5		-80.9	12141.9
5	Cruise	-	-	39225.7	28.9	-2409.1	-
6	Descent	-	-	-	-	-	-
7	Cruise	-	-	1681.1	24.8	-88.5	-
8	Loiter	-	-	588.4	-	-31.0	13009.2
9	Land/Taxi	-	-	-	-	-	-
10	Payload Exp	6.89	-	-	-	-	-
11	Take-off	-	-	-	-	-	-
12	Climb	-	-	549.2	-	-27.0	12141.9
13	Cruise	-	-	1681.1	24.8	-88.5	-
14	Climb	-	-	1098.3	-	-54.0	12141.9
15	Cruise	-	-	39225.7	28.9	-2409.1	
16	Descent	-	-	-	-	-	-
17	Land/Taxi	-	-	-	-	-	-

4.2.2 *TRADE STUDIES*

Four trade studies were performed to show the effect of critical vehicle parameters on the mission performance. The range versus payload trade study data is found in Table 4-10 and Figure 4-2. This graph clearly shows how range could be gained or lost by modifying the payload. The min load case has a payload weight of 0, indicating two pilots and no troops or equipment. The higher weight missions would require changing the configuration of the cabin and trading troops for heavy equipment/vehicles.

Table 4-10 - $Range_{CR}$ vs W_{PL} Data

W_{PL} [lb]	$Range_{CR}$ [nm]
0	1688
1000	1520
2000	1365
3000	1210
4000	1065
4480	1000
5000	925
6000	790
7000	655

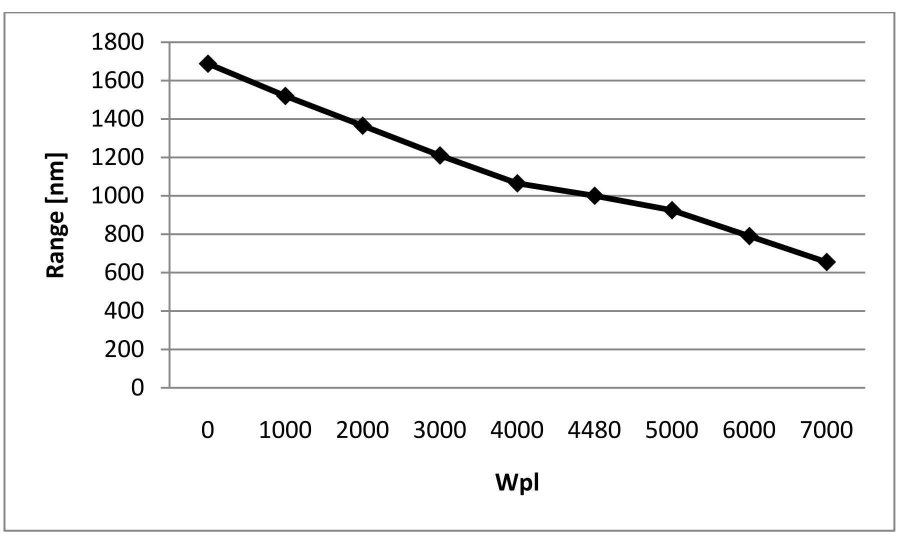

Figure 4-2 - $Range_{CR}$ vs W_{PL} (WTO 37,934 lb)

The range versus L/D trade study data is found in Table 4-11 and Figure 4-3. The range versus L/D trade shows the importance of the L/D estimate. Being off by 1 can result in a shortage of 100nm.

Table 4-11 - $Range_{CR}$ vs L/D Data

L/D	$Range_{CR}$ [nm]
7	580
8	665
9	750
10	830
11	915
12	1000
13	1080
14	1165
15	1250

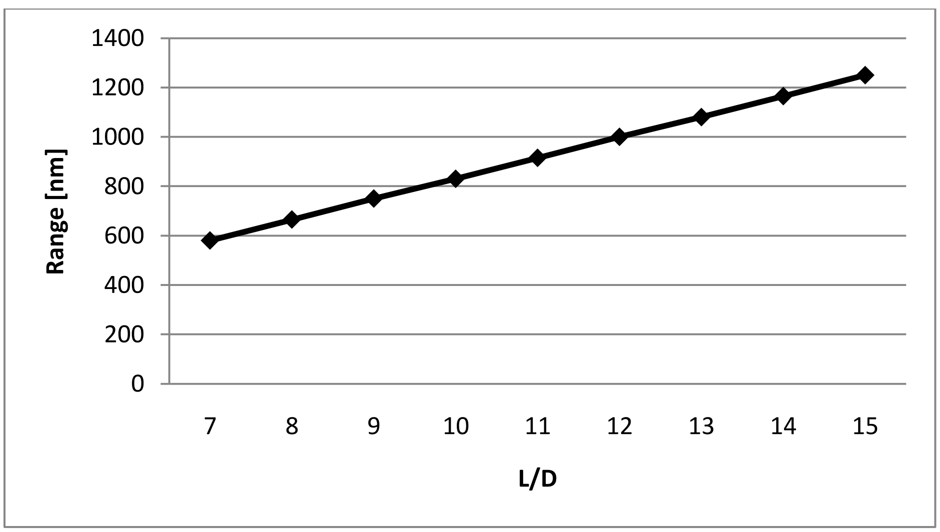

Figure 4-3 - $Range_{CR}$ vs. L/D (WTO 37,934 lb)

The W_{TO} versus L/D trade study data is found in Table 4-12 and Figure 4-4. The W_{TO} versus L/D trade highlights the amount of weight that would need to be added to maintain range if the initial L/D estimate was too high. Over 5,000 lb would need to be added if the L/D estimate was 1 too high. This would result in a situation where there could be negative margin in thrust for VTOL (i.e. VTOL would not be possible for that configuration). The data also shows that being able to increase L/D could lower takeoff weight, allowing for a smaller engine. The slope of the curve starts to taper off around 11, and goes flat around

Table 4-12 - W_{TO} vs L/D Data

L/D	W_{TO} [lb]
9	76091
10	54311
11	43996
12	37934
13	33933
14	31092
15	28968

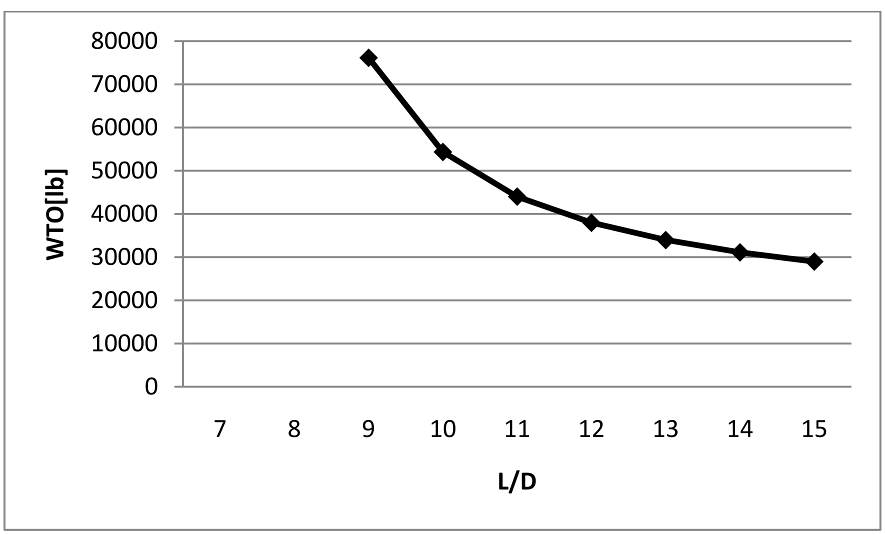

Figure 4-4 - W_{TO} vs L/D (Range 1000 nm)

The range versus specific fuel consumption (sfc) trade study data is found in Table 4-13 and Figure 4-5. The range versus sfc trade shows how range would be lost or gained with changes in sfc. The curve is fairly linear with a modest slope. If sfc estimates were off they would have marginal effects on overall range. The sfc will change with speed and altitude. Inlet and exit nozzle geometry could be used to help modify the sfc for different cruise conditions if needed.

Table 4-13 - $Range_{CR}$ vs sfc Data

sfc	$Range_{CR}$ [nm]
0.50	1475
0.55	1340
0.60	1225
0.65	1130
0.70	1050
0.737	1000
0.80	920
0.85	865
0.90	815

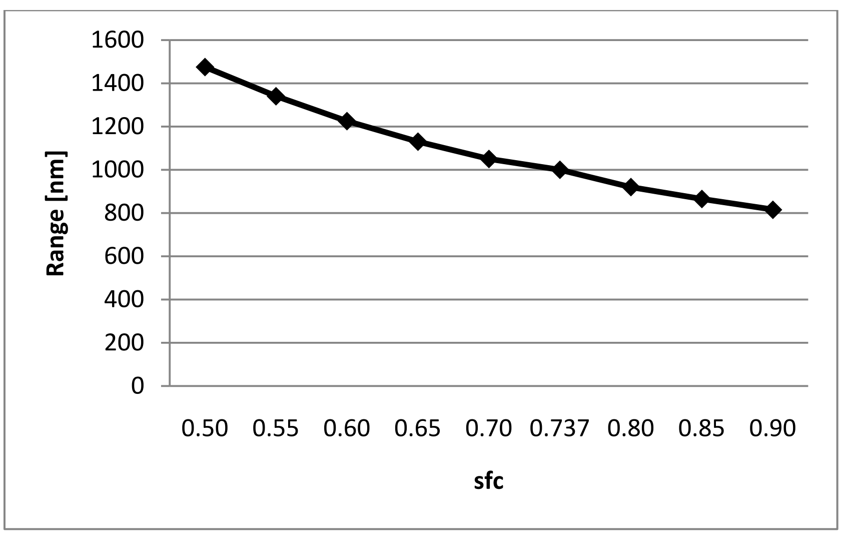

Figure 4-5 - $Range_{CR}$ vs sfc (WTO 37,934 lb)

4.3 DISCUSSION

The sensitivity and trade studies in section 4.2 show the importance of initial estimates. For some values such as L/D setting an unreasonable value may result in an unrealistic design. The payload and takeoff weight versus range plots can be used by mission planners to set load conditions based on a given mission profile. Based on standard values an aggressive yet attainable goal has been set for the AVD. Advances in composite fuselage structures may result in a fuselage weight lighter than that estimated from the reference aircraft. HondaJet for instance, has developed a technique of co-curing integral structure and honeycomb sandwich structures which lessons manufacturing complexity and weight.(9)

5 Performance Constraint Analysis

This section details the performance analysis and configuration selection for the AVD.

5.1 Calculation of Performance Constraints

The performance constraints considered are:

- Stall Speed
- Takeoff Distance
- Landing Distance
- Drag Polar Estimates
- Climb Constraints
- Maneuvering Constraints
- Speed Constraints

5.1.1 Stall Speed

Since the AVD is an advanced military VTOL aircraft no stall speed, V_s, requirement was identified. For reference stall speed was estimated versus wing loading, W/S, for various C_{Lmax} using Equation 5.1. The results are plotted below in Figure 5-1. It can be seen that the higher C_{Lmax} yields the lower stall speed, which is desirable. Raymer notes that for short takeoff aircraft a C_{Lmax} of 3 is attainable (10). Figure 5-1 can be used to determine the stall speed at various flight conditions (i.e. different C_L and W/S values).

Since stall speed is independent of T/W, the values would show up as vertical lines for a given W/S on a T/W vs W/S plot.

Equation 5.1 - Stall Speed (V_s)

$$V_s = \sqrt{\frac{2\frac{W}{S}}{\rho C_{Lmax}}}$$

Table 5-1 - Calculated Stall Speed (V_s)

CL	(W/S)	Vs	S
3	50	70.014	758.674
	100	99.01475	379.337
	150	121.2678	252.8913
	200	140.028	189.6685
2.2	50	81.75874	758.674
	100	115.6243	379.337
	150	141.6103	252.8913
	200	163.5175	189.6685
2	50	85.74929	758.674
	100	121.2678	379.337
	150	148.5221	252.8913
	200	171.4986	189.6685
1.8	50	90.38769	758.674
	100	127.8275	379.337
	150	156.5561	252.8913
	200	180.7754	189.6685

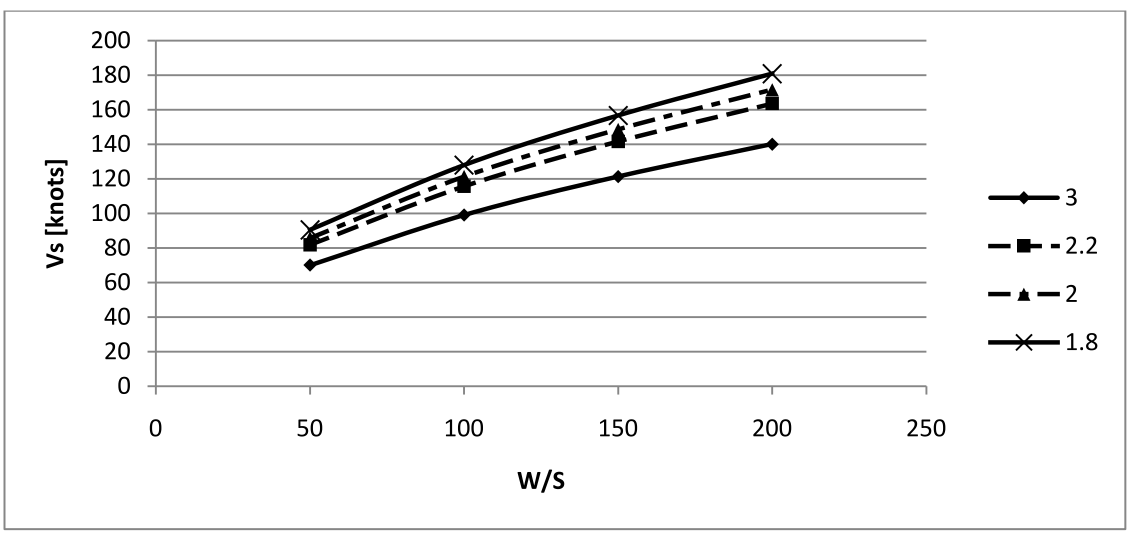

Figure 5-1 - Stall Speed (V_s) vs. Wing Loading (W/S)

5.1.2 Takeoff Distance

T/W values were calculated versus W/S for various C_L values. The values can be seen in Table 5-2 and Figure 5-2. Using the takeoff weight calculated section 4 the corresponding wing area and Thrust were also calculated.

The JT8D was selected as the power plant of choice in 3.3. A list of JT8D models and their thrust ratings can be found in Table 5-3. Those thrust values are also plotted on the thrust versus wing area curves in Figure 5-3. Figure 5-3 can be used to simultaneously select an engine and wing area.

Table 5-2- Calculated Thrust to Weight Ratio

CL	(W/S)	S	T	(T/W)
2.2	50	758.674	17770	0.468449
	100	379.337	30240	0.79718
	150	252.8913	42970	1.132766
	200	189.6685	55700	1.468351
2	50	758.674	18980	0.500347
	100	379.337	32780	0.864139
	150	252.8913	46800	1.233731
	200	189.6685	60780	1.602269
1.8	50	758.674	20480	0.539889
	100	379.337	35900	0.946388
	150	252.8913	51460	1.356577
	200	189.6685	67000	1.76624

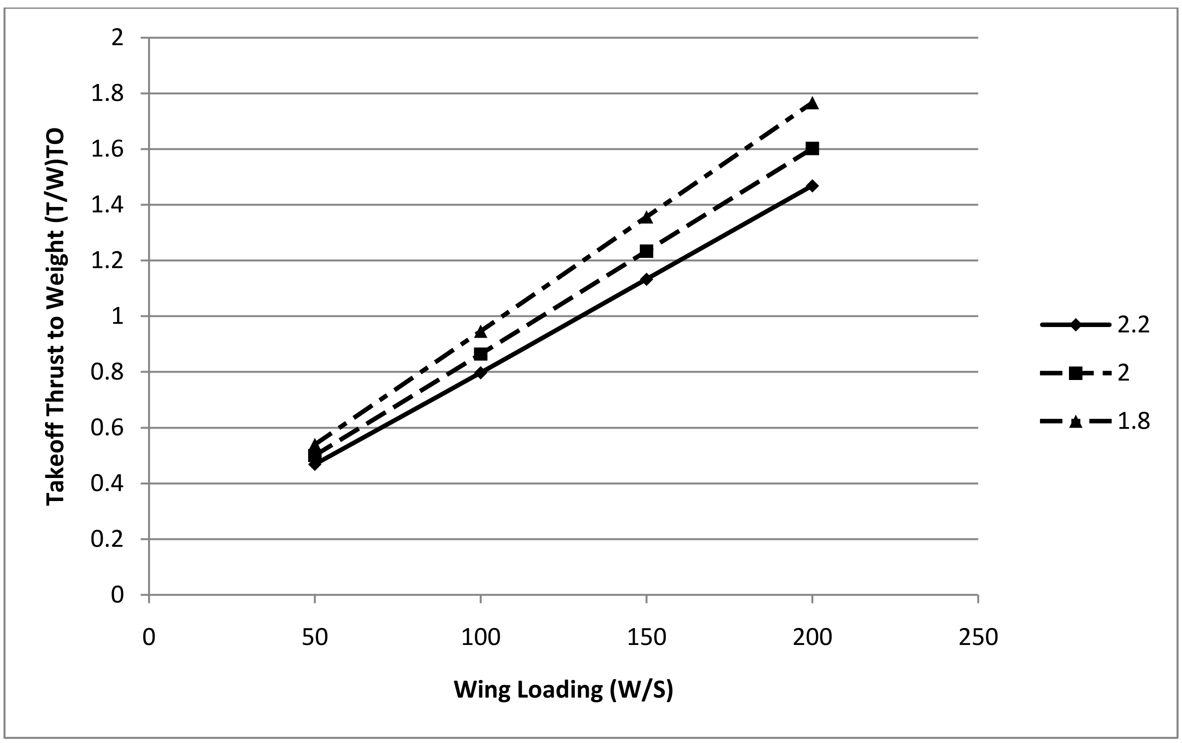

Figure 5-2 - Effect of $C_{L,TO}$, W/S and T/W

Table 5-3- JT8D Thrust Offerings (11)

Model	1x	2x	(T/W)
JT8D-5	12,250	24500	0.645864
JT89-7	14,000	28000	0.73813
JT8D-9	14,500	29000	0.764492
JT8D-11	15,000	30000	0.790854
JT8D-15	15,500	31000	0.817215
JT8D-17	16,000	32000	0.843577
JT8D-17AR	16,400	32800	0.864667
JT8D-17R	17,400	34800	0.91739
JT8D-209	18,500	37000	0.975386
JT8D-217	20,000	40000	1.054471
JT8D-219	21,000	42000	1.107195

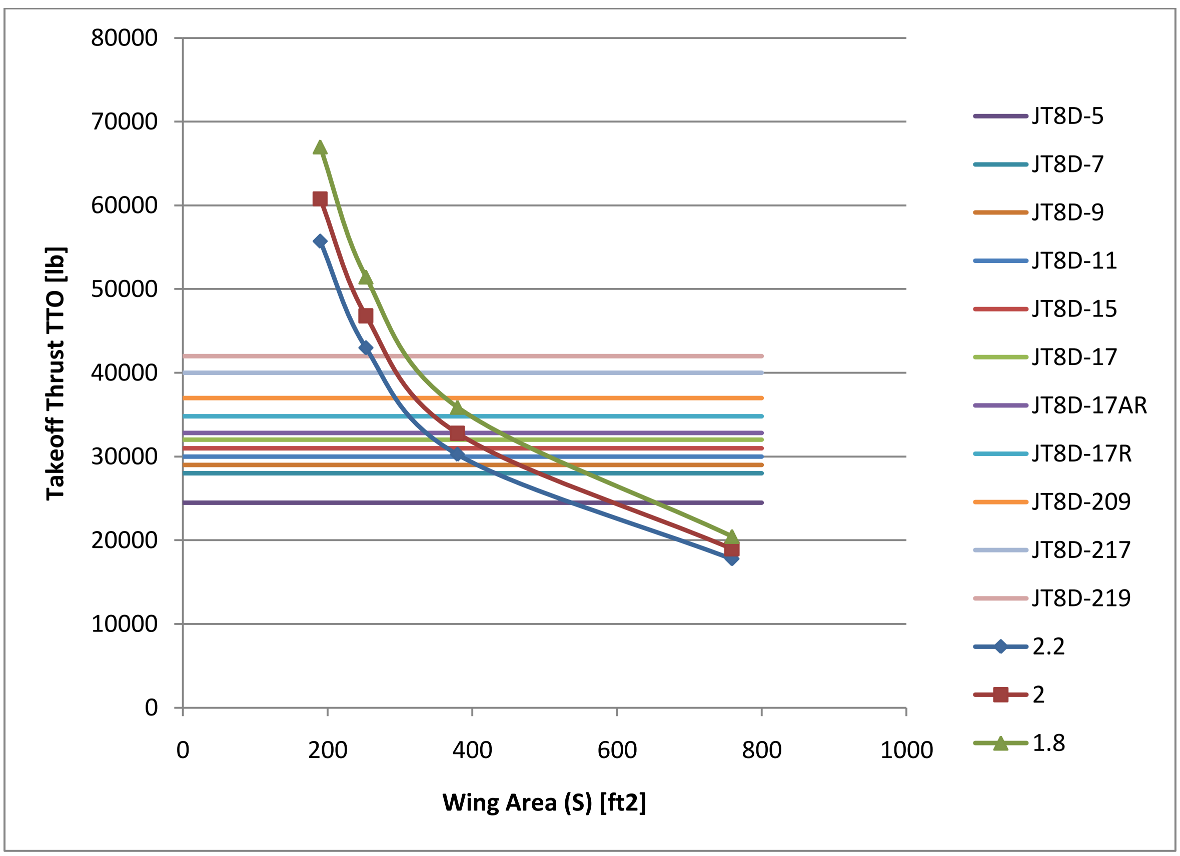

Figure 5-3 - Thrust versus Wing Area for various C_L

5.1.3 Landing Distance

The AVD has an aggressive landing requirement of 1500ft over a 50ft obstacle. The approach speed and corresponding stall speed were calculated per FAR25 methods. W/S values were found for various C_{LmaxL}s using AAA. The W/S and corresponding S values for a 30,247 lb (0.8*W_{TO}) landing weight are located in Table 5-5 and Figure 5-4.

Table 5-4 - Approach/Stall Speed

Parameter	Value
SFL	1500
V_a	70.71
V_S	58.93

Table 5-5 - W/S versus C_{Lmax} for Landing

CLmaxL	(W/S)L	S
3	52.37	579.5
2.2	38.4	790.3
2	34.9	869.5
1.8	31.42	965.8

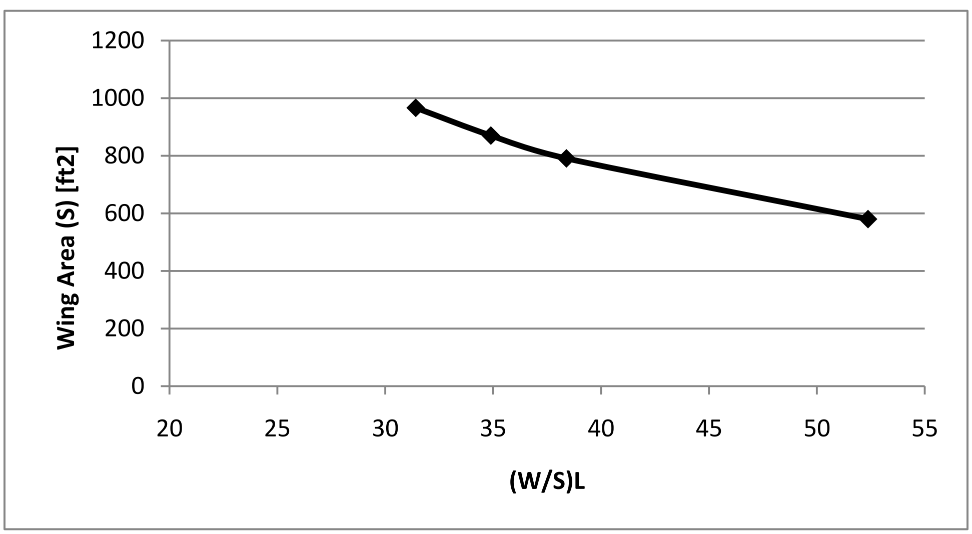

Figure 5-4 - Wing Area (S) vs $(W/S)_L$ ($WL=0.8W_{TO}$)

5.1.4 *Drag Polar Estimation*

The design mission used the parameters below. The L/D was based on typical ratios for

5.1.5 *Climb Constraints*

The long range mission used the parameters below. The L/D was based on typical ratios

Table 5-6 - Climb Parameters

Parameter	Value
S [ft^2]	750
f	9
Cd0	0.012
L/D	12.26
AR	2.87
e	0.8
rho[sls]	0.002224
Climb Engine, out gear up	
RC_{-1eng} [fps]	15.63
Climb Clean	
RC [fps]	149.31
Pdl	0.993

Table 5-7 - Climb Calculations

$(W/S)_{TO}$	V	RC/V	1/(L/D)	$(T/W)_{TO}$ one eng. 95deg F	$(T/W)_{TO}$ two eng. 95deg F	$(T/W)_{TO}$ two eng. sls
50	390.937	0.040	0.082	0.122	0.243	0.286
100	552.869	0.028	0.082	0.110	0.220	0.258
150	677.123	0.023	0.082	0.105	0.209	0.246
200	781.874	0.020	0.082	0.102	0.203	0.239

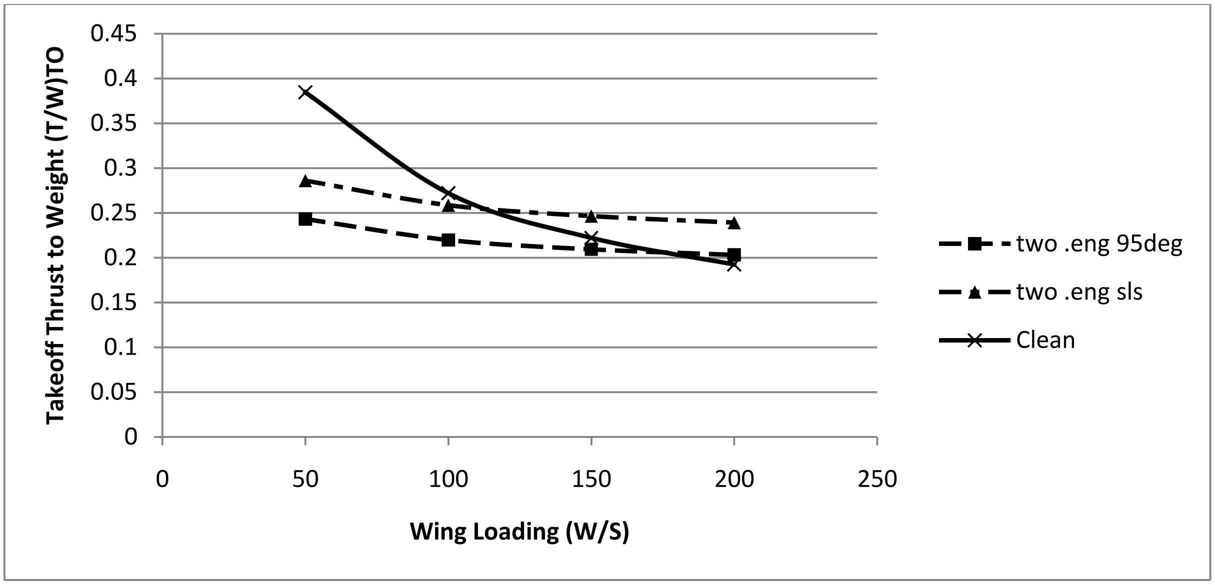

Figure 5-5 - Climb T/W vs W/S

5.1.6 *MANEUVERING CONSTRAINTS*

No maneuvering constraints were levied against the AVD.

5.1.7 *SPEED CONSTRAINTS*

T/W was calculated for the design speeds conditions: M=0.8 at 30,000ft, M=1.36 at 50,000ft, and M=1.67 at 50,000ft. The values are tabulated in the tables below, and plotted in Figure 5-6.

Table 5-8 - W/S and T/W at M=0.8 @ 30k ft

Parameter	Value
M	0.8
h	30000
V	796.4
q	282
Cd0	0.014
A	3
e	0.8

W/S	Profile Drag Term	Induced Drag Term	T/W	T [lb]	(T/W)TO
50	0.079	0.024	0.102	3810	0.409903
100	0.039	0.047	0.087	3217	0.346046
150	0.026	0.071	0.097	3602	0.38747
200	0.020	0.094	0.114	4232	0.455213

Table 5-9 - W/S and T/W at M=1.36 @ 50k ft

Parameter	Value
M	1.36
h	50000
V	1319.8
q	315
Cd0	0.04
A	3
e	0.8

W/S	Profile Drag Term	Induced Drag Term	T/W	T [lb]	(T/W)TO
50	0.252	0.021	0.273	10153	1.092209
100	0.126	0.042	0.168	6251	0.672418
150	0.084	0.063	0.147	5472	0.588627
200	0.063	0.084	0.147	5474	0.588836

Table 5-10 - W/S and T/W at M=1.68 @ 50k ft

Parameter	Value
M	1.67
h	50000
V	1319.8
q	471
Cd0	0.04
A	3
e	0.8

W/S	Profile Drag Term	Induced Drag Term	T/W	T [lb]	(T/W)TO
50	0.377	0.014	0.391	14534	1.563518
100	0.188	0.028	0.217	8053	0.866236
150	0.126	0.042	0.168	6241	0.671354
200	0.094	0.056	0.151	5597	0.602072

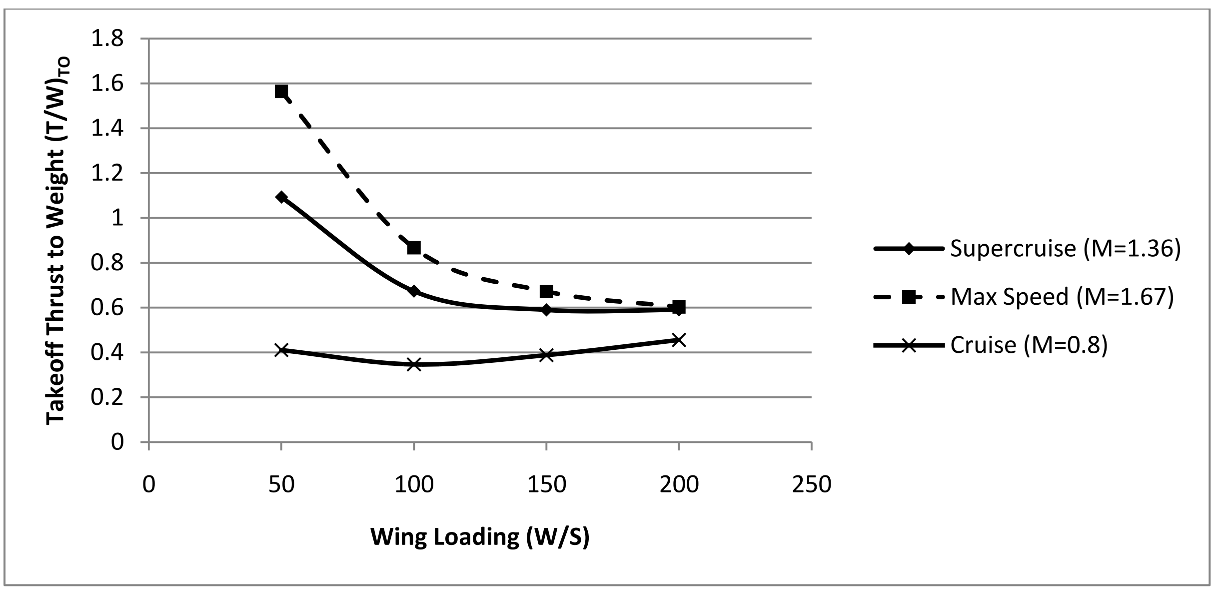

Figure 5-6 - T/W vs. W/S for various flight conditions

5.1.8 Summary of Performance Constraints

The aircraft performance constraints have been consolidated in the matching plot in Figure 5-7.

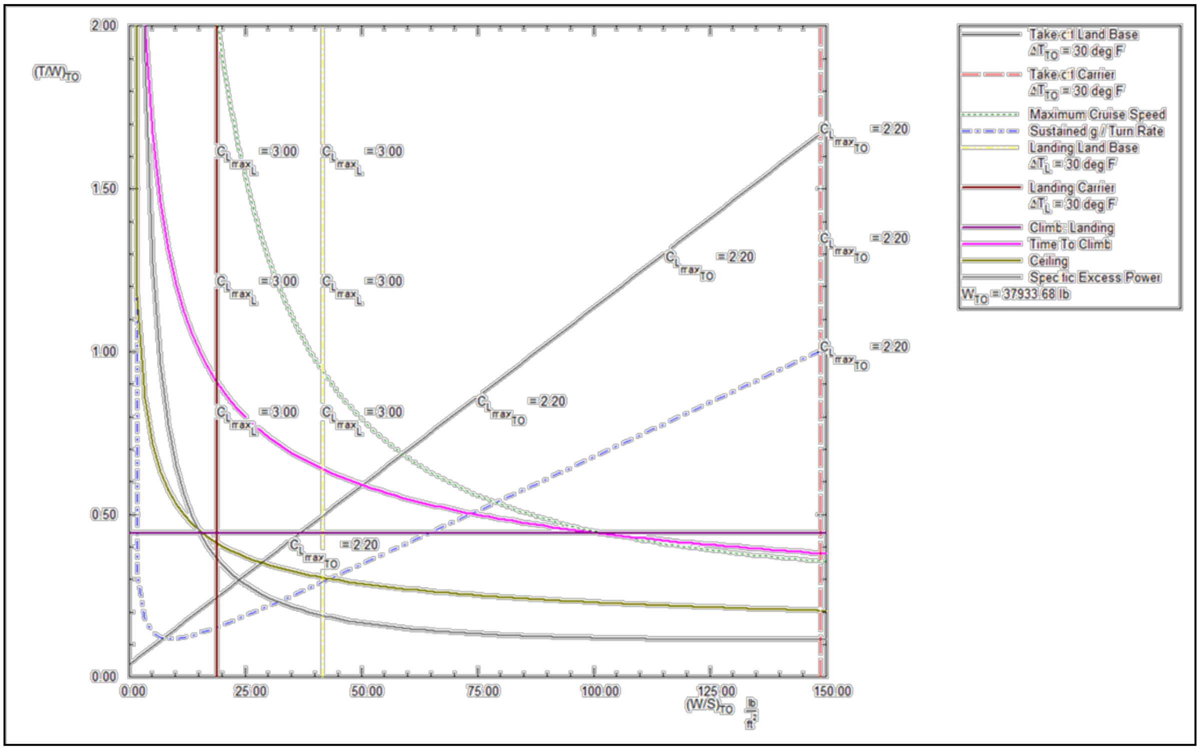

Figure 5-7 - Matching Plot

5.2 Discussion

The performance values identified can be used to select a thrust and wing area based on figures of system requirements and figures of merit assigned to conflicting requirements (e.g. range and weight).

Based on the matching plot in Figure 5-7, the W/S should be greater than 56 and the T/W at takeoff should be greater than 0.6. A W/S of 56 corresponds to a wing area of 677ft^2 for the design take-off weight. A wing area of 680ft^2 was chosen. The thrust requirement is driven by VTOL which is not on the matching plot. The F135 has a dry thrust of 25,000lb and runs a Liftfan with a thrust rating of 18,000lb. Using this as a reference it is estimated that the AVD will use two liftfans will have a maximum thrust of 15,000lb. Screenshots of the performance constraints used in this section can be found in Appendix 2.

6 Fuselage Design

This section details the fuselage design for the AVD. The fuselage is divided into two sections for design purposes, the cockpit and cabin.

6.1 Cockpit Layout Design

The cockpit houses the primary controls and avionics displays for the aircraft. The AVD utilizes a two person cockpit as seen in Figure 6-1. The red circles aft of the cockpit are the aircrafts two liftfans used for VTOL.

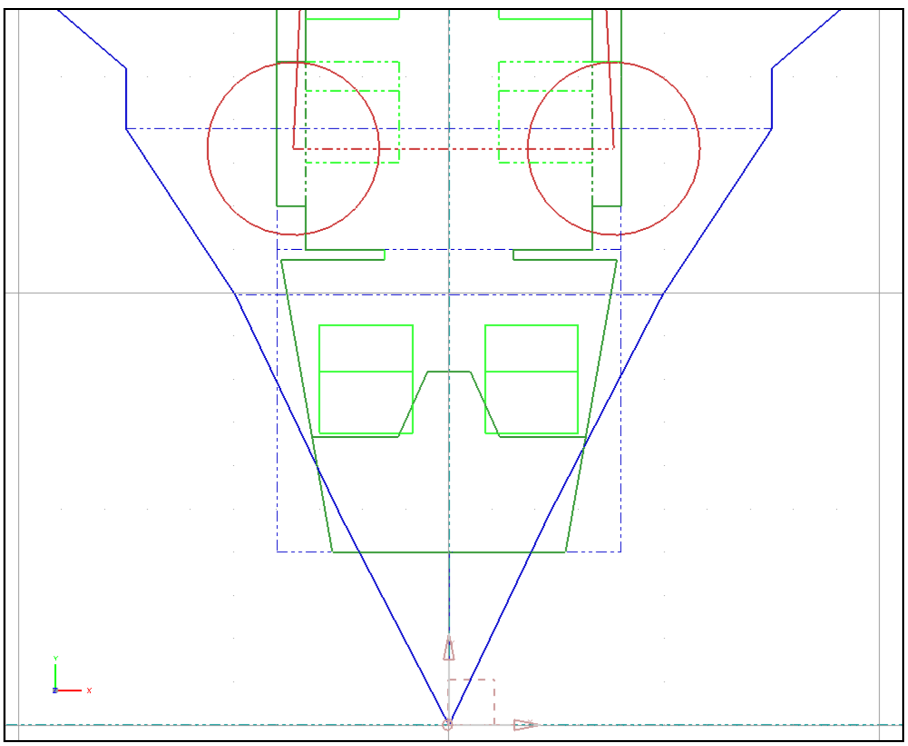

Figure 6-1 - Cockpit Top

Figure 6-2 shows the AVD cockpit dimensions. The cockpit layout is based on the cargo and bomber dimensions identified in Airplane Design Part III (12) Figure 2.11.

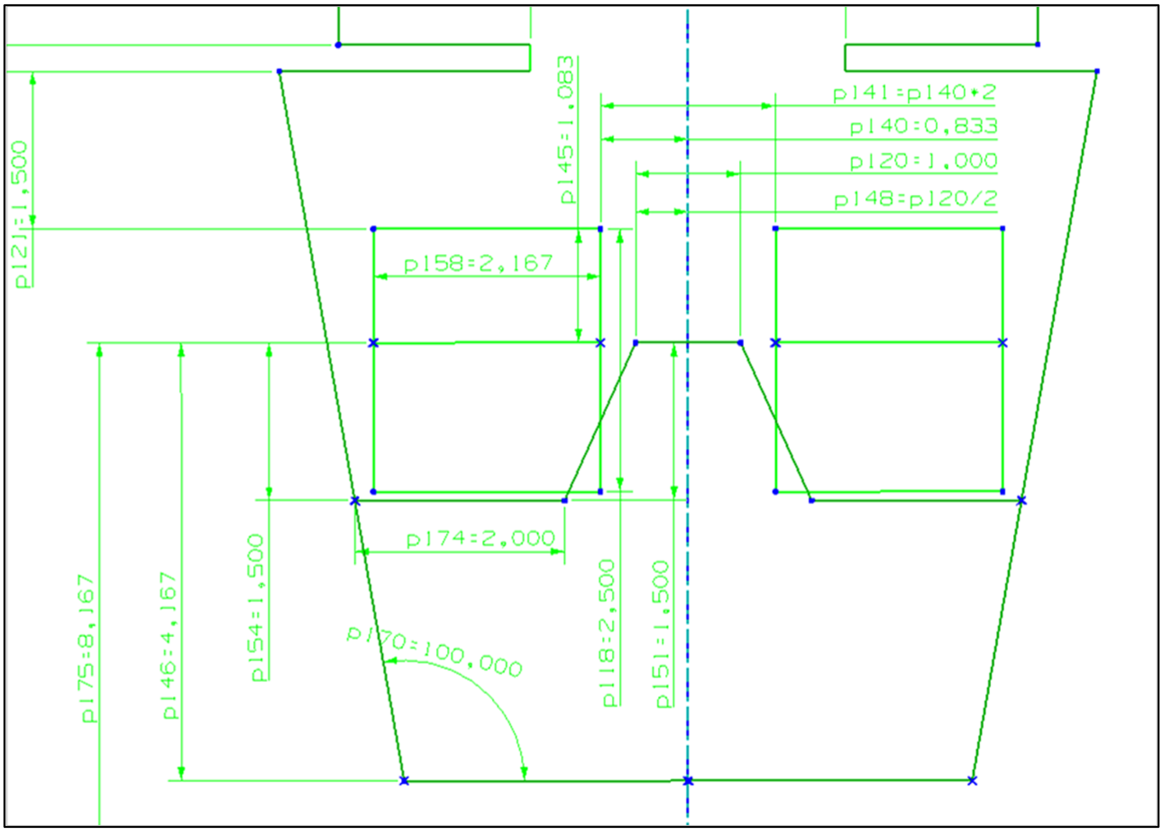

Figure 6-2 - Cockpit Top Dimensions

Figure 6-3 shows a view of the cockpit from the front (forward to aft). The pilots have dual controls on the main control panel and a center control panel. The windscreen of the AVD will incorporate a multifunction heads-up display (HUD) capable of displaying critical data to the pilots.

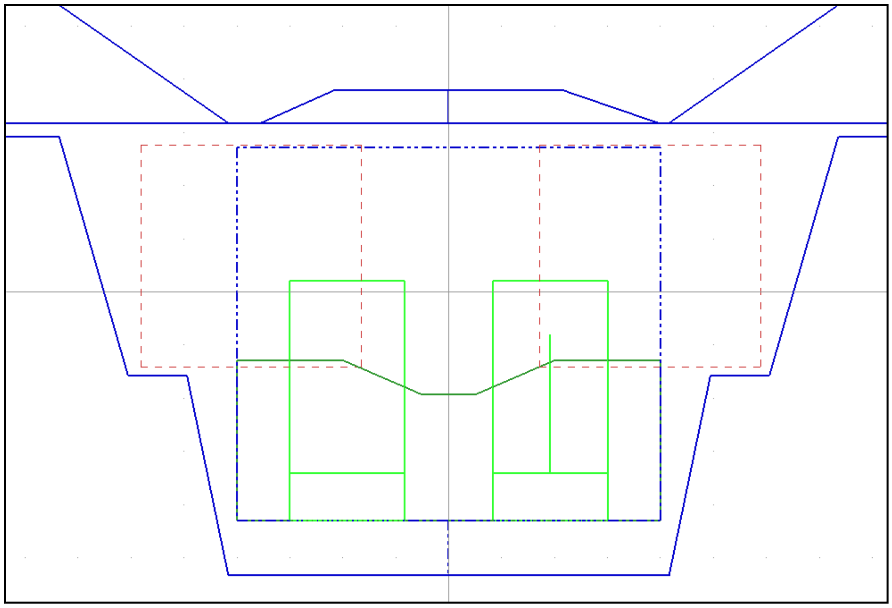

Figure 6-3 - Cockpit Front

Figure 6-4 shows the additional cockpit dimensions, including the approximate eye level of the pilot.

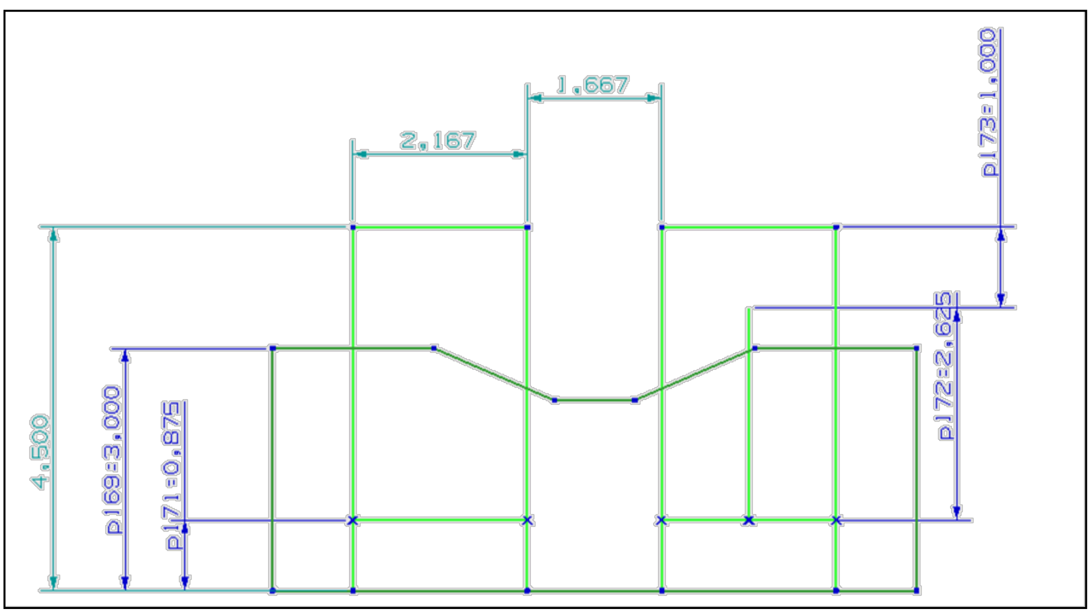

Figure 6-4 - Cockpit Front Dimensions

Figure 6-5 shows a side view of the AVD cockpit. The cockpit was designed to provide proper visibility to both pilots.

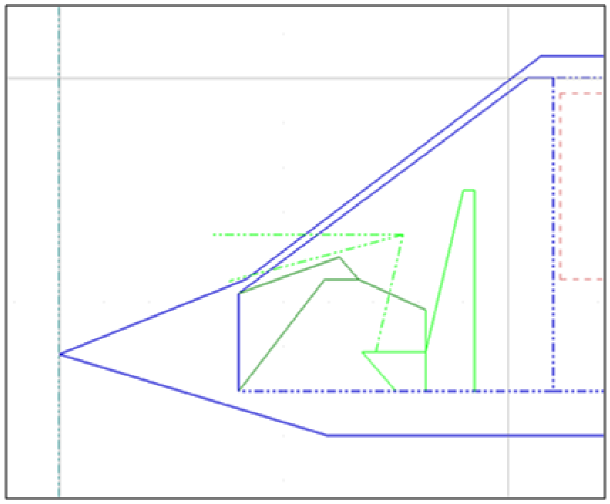

Figure 6-5 - Cockpit Side

Figure 6-6 shows additional cockpit dimensions. A reference line highlights the pilots 15 deg visibility requirement. It is anticipated the cockpit windscreen will incorporate relatively large single panes of glass to minimize the need for supports that would hinder pilot vision.

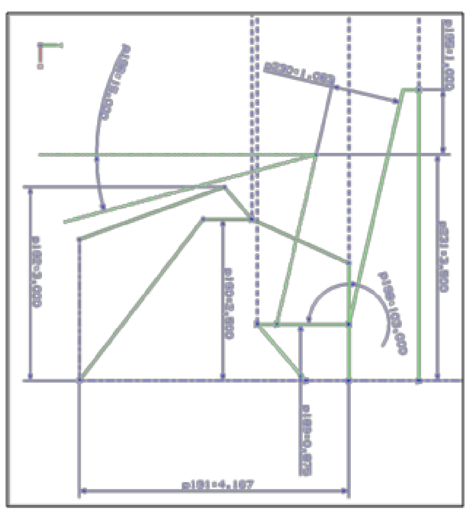

Figure 6-6 - Cockpit Side Dimensions

6.2 Cabin Layout Design

The primary purpose of the AVD is to transport Special Forces units. The bulk of the aircraft's internal volume goes towards housing 14 troops and equipment. The seats are all forward facing for safety do to the potential for high-g maneuvers and takeoff/landing. The cabin utilizes a single isle layout to help expedite egress and ingress of troops through the rear hatch.

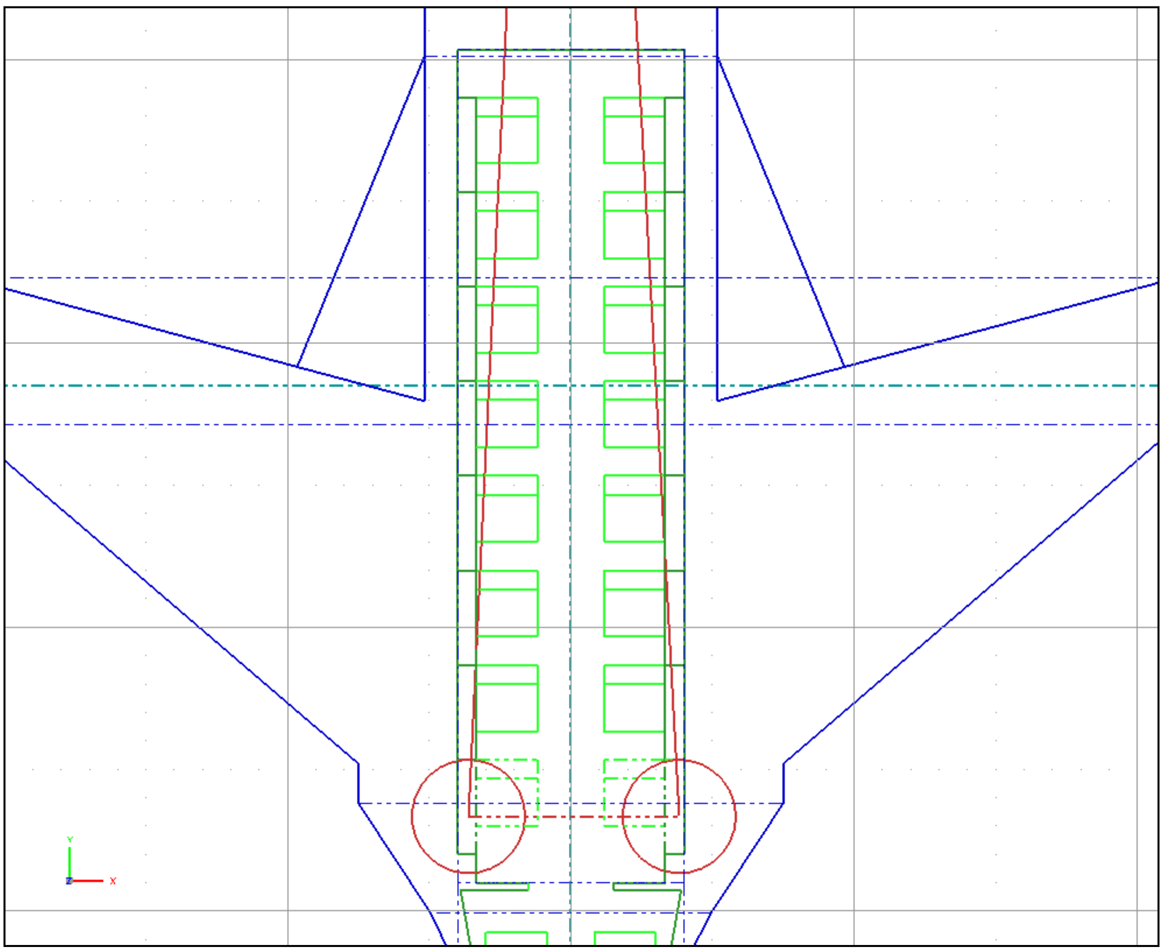

Figure 6-7 - Cabin Top

Figure 6-8 shows dimensions of the cabin. The cabin was laid out using typical passenger jet dimensions as identified in Raymer and Roskam (10)(12). Next to each seat is a large (6ft x 3ft x 1ft) storage closet for storing equipment.

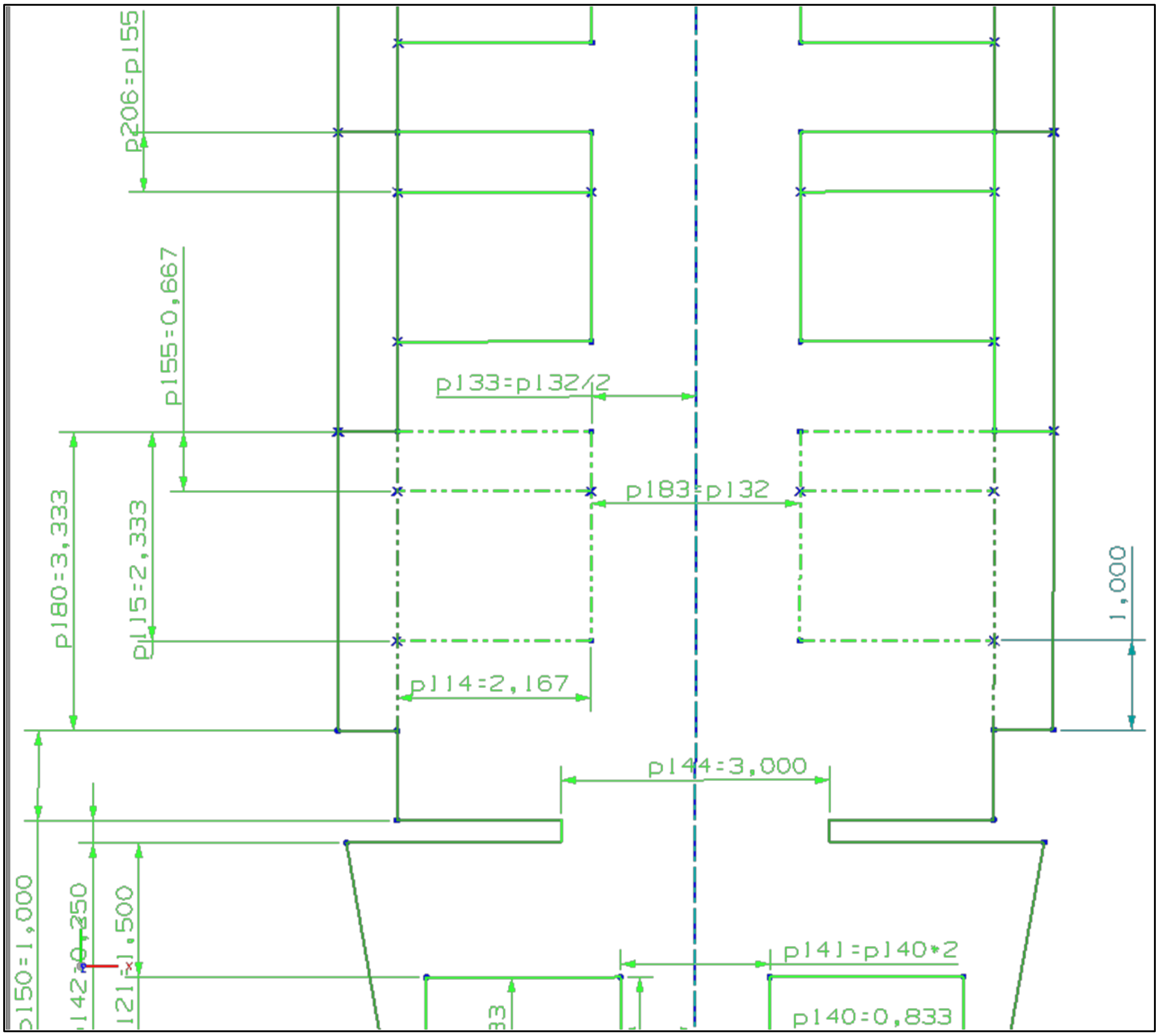

Figure 6-8 - Cabin Top Dimensions

Figure 6-9 shows a view of the cabin from the front. The side and overhead storage areas are clearly visible.

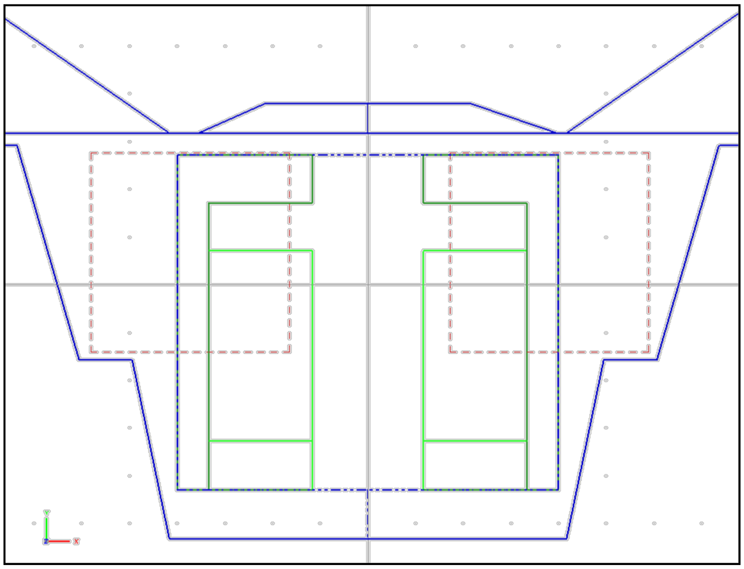

Figure 6-9 - Cabin Front

Figure 6-10 shows additional cabin dimensions.

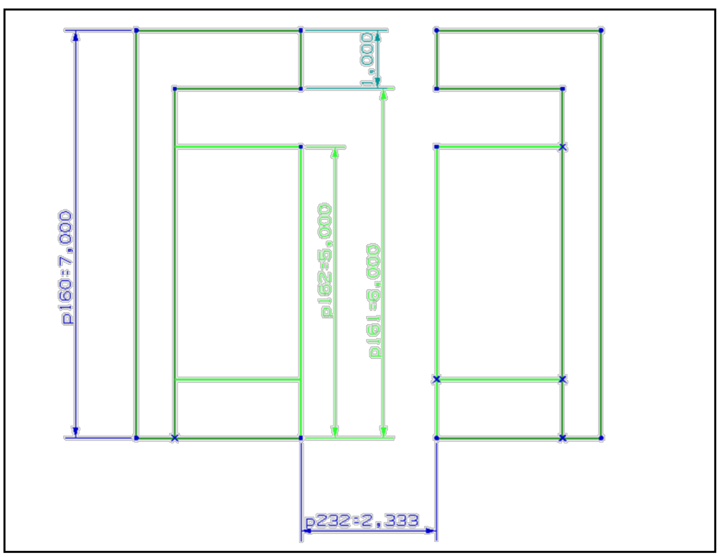

Figure 6-10 - Cabin Front Dimensions

Figure 6-11 shows a side view of the cabin. The AVD sits 14 troops in seven rows on either side of a single aisle.

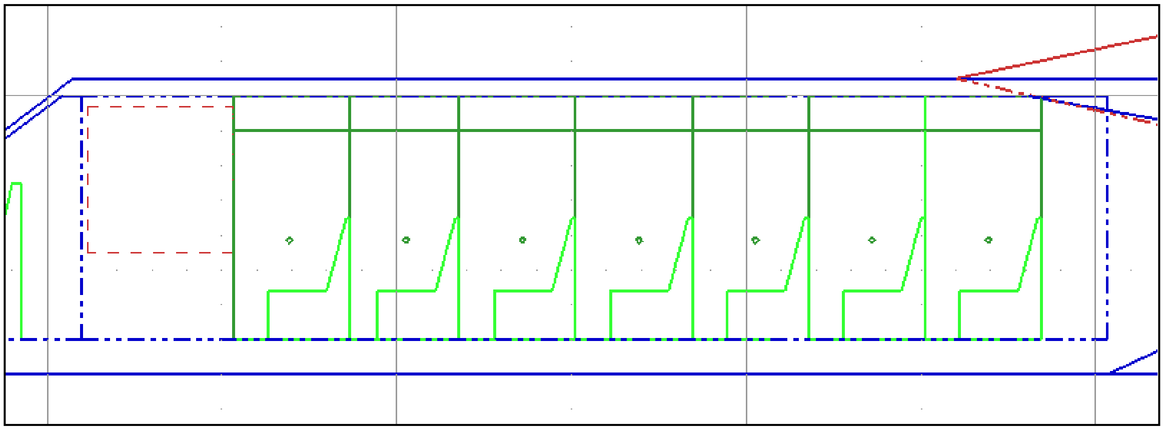

Figure 6-11 - Cabin Side

Figure 6-12 shows additional cabin dimensions. The AVD is effectively a new class of aircraft. The seats recommended for troop transports are inadequate for high-speed STOL aircraft. Dimensions for a passenger transport seat were for this preliminary design.

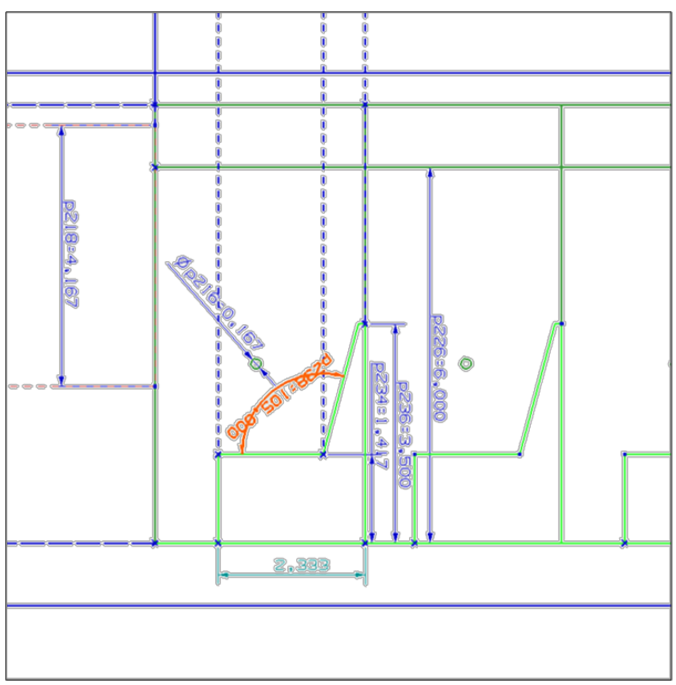

Figure 6-12 - Cabin Side Dimensions

6.3 DISCUSSION

The cockpit and cabin layouts are based upon the mission requirement to quickly transport and deploy a small number of armed troops. Standard dimensions for a transport cockpit were used. Passenger jet guidelines were used instead of troop guidelines for the cabin due to safety concerns.

7 WING, HIGH-LIFT SYSTEM AND LATERAL CONTROL DESIGN

This section details the design and analysis of the high lift and lateral control surfaces for the AVD.

7.1 WING PLANFORM DESIGN

As discussed previously in section 5, the wing area for the AVD is 680 ft^2. Equation 7.1 was used to select an initial AR of 3.1. Based on Roskam Part II Table 6.12, Raymer Fig 4.24 an initial taper ratio of 0.25 was chosen (12). Due to the supersonic cruise requirement of the AVD, dihedral angle Γ is set to 0 deg.

Equation 7.1 - Aspect Ratio from Mach Number (Raymer Table 4.1)

$$A = aM^c$$

$$3.1 = 5.570(1.74^{-1.075})$$

7.1.1 SWEEP ANGLE - THICKNESS RATIO COMBINATION

Equation 7.2 below was used to select an initial L_{LE} estimate of 54.9 deg. This corresponds to an $L_{c/4}$ of 50.9 deg based on Equation 7.3.

Equation 7.2 - Leading Edge Sweep Angle Versus M_{CR} (Raymer Fig. 4.20)

$$\Lambda_{LE} = 90 - \tan^{-1}\left(\frac{1}{M_{cr}}\right)$$

$$54.9 = 90 - \sin^{-1}\left(\frac{1}{1.74}\right)$$

Equation 7.3 - Leading Edge Versus C/4 Sweep Angle (Raymer Fig. 4.16)

$$\tan \Lambda_{LE} = \tan \Lambda_{\frac{c}{4}} + \left[\frac{(1-\lambda)}{A(1+\lambda)}\right]$$

$$50.9 = \tan^{-1}\left(\tan(54.9) - \left[\frac{(1-0.25)}{3.1(1+0.25)}\right]\right)$$

From Raymer Figure 4.21 it can be seen that the $L_{c/4}$ of 50.9 deg and aspect ratio of 3.1 would yield an increased risk of pitchup at high angles of attach in the transonic regime(10). The following values were selected based on Figure 4.21 to increase stability, AR=3.5 and $L_{c/4}$ = 30 deg. Equation 7.3 this yields corresponds to a L_{LE} = 37.8 deg. These values seem reasonable based on comparison aircraft.

CL was calculated using Equation 7.4. Equation 7.5 shows a relationship between Mcc, t/c, C_L, and Λ.Using CL and the values above and Equation 7.5 yielded a t/c of 13%. Based on the historical trend line in Raymer Figure 4.14 and the AVD's design Mach number of 1.74, a more appropriate t/c of 6% was selected (10).

Equation 7.4 - Required $C_{L,CR}$

$$C_{L_{CR}} = (W_{TO} - 0.4W_F)/qS$$

$$q_{50k_{scr}} = 513\frac{lb}{ft^2}$$

$$q_{30k_{cr}} = 812.8\ \frac{lb}{ft^2}$$

$$W_{TO} = 37934\ lb$$

$$W_F = 11610\ lb$$

$$C_{L_{50k,scr}} = 0.095$$

$$C_{L_{30k,cr}} = 0.060$$

Equation 7.5 - Relationship Between M_{cc}, t/c, C_L, and Λ

$$Mcc\text{^}2 * cos(\Lambda)\text{^}2 * (2.64 * ((\Gamma\ + 1) * 1/2) * tc/cos(\Lambda) + ((\Gamma\ + 1) * 1/2) * (2.64 * tc * .34) * Cl/cos(\Lambda)\text{^}3)/sqrt(1 - Mcc\text{^}2 * cos(\Lambda)\text{^}2) + Mcc\text{^}2 * cos(\Lambda)\text{^}2 * ((\Gamma\ + 1) * 1/2) * (1.32 * tc/cos(\Lambda))\text{^}2/(1 - Mcc\text{^}2 * cos(\Lambda)\text{^}2) + Mcc\text{^}2 * cos(\Lambda)\text{^}2 * (1 + .68 * ((\Gamma\ + 1) * 1/2) * Cl/cos(\Lambda)\text{^}2 + .34 * ((\Gamma + 1) * 1/2) * Cl/cos(\Lambda)\text{^}2) - 1 = 0$$

$$Mcc = 1.02M_{CR}$$

7.2 Airfoil Selection

A NACA 6-series airfoil was selected based on their low drag properties and availability of reference material. Due to the t/c and $C_{L,CR}$ calculated earlier a 64-006 airfoil was selected for preliminary calculations. A more advanced supercritical airfoil may offer better performance and should also be investigated prior to the detailed design phase.

Due to the supersonic cruise condition the wing incidence angel, *i*, will be 0 deg. This is supported by Table 6.12 in Roskam Part II(12).

7.3 Wing Design Evaluation

Based on calculations using NACA 64-006 the $C_{L,max}$ previously identified is not attainable. For S_w = 680 ft^2 the max C_L clean will be 0.8. This is sufficient for cruise. LE slats and double slotted flaps will be used to help bring $C_{L,max,TO}$ and $C_{L,max,L}$ to 1.5 and 1.8 respectively. In order to minimize weight and drag during cruise a larger wing area will not be used to further compensate. The additional lift required for STOVL will be accomplished by use of thrust vectoring (including thrust reversal for landing).

7.4 DESIGN OF THE HIGH-LIFT DEVICES

A LE slat and double slotted trailing edge (TE) flaps are utilized on the AVD. Triple slotted TE flaps would increase the available CL further, but were not used due to packaging constraints. The parameters below were attained using AAA to attain a $C_{L,max,TO}$ and $C_{L,max,L}$ of 1.5 and 1.8 respectively.

Equation 7.6 -High Lifting Device Parameters

$$\eta_{i,f} = 20\%$$
$$\eta_{o,f} = 97\%$$
$$c_f/c_w = 30\%$$
$$c_1/c_w = 20\%$$
$$c_2/c_w = 15\%$$
$$c_f/c_w = 30\%$$
$$c'_w/c_w = 122\%$$
$$\delta_{TO} = 40°$$
$$\delta_L = 60°$$

7.5 DESIGN OF THE LATERAL CONTROL SURFACES

Initial sizing of the AVD lateral control surfaces were based on values from Table 8.12a,b, and c in Roskam Part II(12). Ailerons for supersonic cruise vehicles tended to be outboard only. Aileron spans on average were from 0.7 to 0.97 fr.b/2, with chords from 0.2 to 0.4 fr.c_w (in/out). Outboard spoilers were also typically used. Spoiler spans were on average from 0.3 to 0.75 fr.cw, with chords from 0.08 to 0.11 (in/out).

Due to the high approach speed and aggressive STOVL requirement of the AVD, larger lateral control surfaces were chosen. The values chosen are within the referenced historical values. The table below details the chosen parameters.

Table 7-1 - AVD Aileron and Spoiler Data

Type	Ail. Span Loc. in/out fr.b/2	Ail. Chord in/out fr.cw	Inb'd Ail. Span Loc. in/out fr.b/2	Inb'd Ail. Chord in/out fr.cw	Inb'd Spoiler Span Loc. in/out fr.b/2	Inb'd Spoiler Chord in/out fr.cw	Outb'd Spoiler Span Loc. in/out fr.b/2	Outb'd Spoiler Chord in/out fr.cw	Outb'd Spoiler Hing Loc. In/out fr.cw
AVD	.6/.95	.2/.27	none	none	none	none	.3/.8	.04/.08	.85/.78

7.6 DRAWINGS

Equation 7.7 details the parameters and equations used to calculate the AVD wing geometry. Figure 7-1 and Figure 7-2 show the wing geometry and configuration.

Equation 7.7 - Calculation of Wing Geometry

$$A_w = 3.5$$

$$\lambda_w = 0.25$$

$$\Lambda_{c/4,w} = 30\ deg$$

$$\Lambda_{LE,w} = 37.6\ deg$$

$$b_w = \sqrt{AS_w} = 48.8\ ft$$

$$c_{r,w} = \frac{2S_v}{b * (1+\lambda)} = 22.3\ ft$$

$$c_{t,w} = \lambda c_r = 5.6\ ft$$

$$\bar{c} = \frac{2}{3}\frac{c_{r,w}\left(1+\lambda_w+{\lambda_w}^2\right)}{1+\lambda_w} = 15.6\ ft$$

$$\bar{Y} = \frac{b_w}{6}\left(\frac{1+2\lambda_w}{1+\lambda_w}\right) = 9.8\ ft$$

$$V_{WF} = 0.54\frac{S_w}{b_w}{}^{t}/_{c}\left[\frac{\left(1+\lambda_w\sqrt{\tau_w}+{\lambda_w}^2\tau_w\right)}{1+{\lambda_w}^2}\right] = 258\ ft^3$$

$$V_F = \frac{W_F}{\rho_F} = 231\ ft^{3*}$$

*assuming JP-8 (6.7 *lb/gal*)

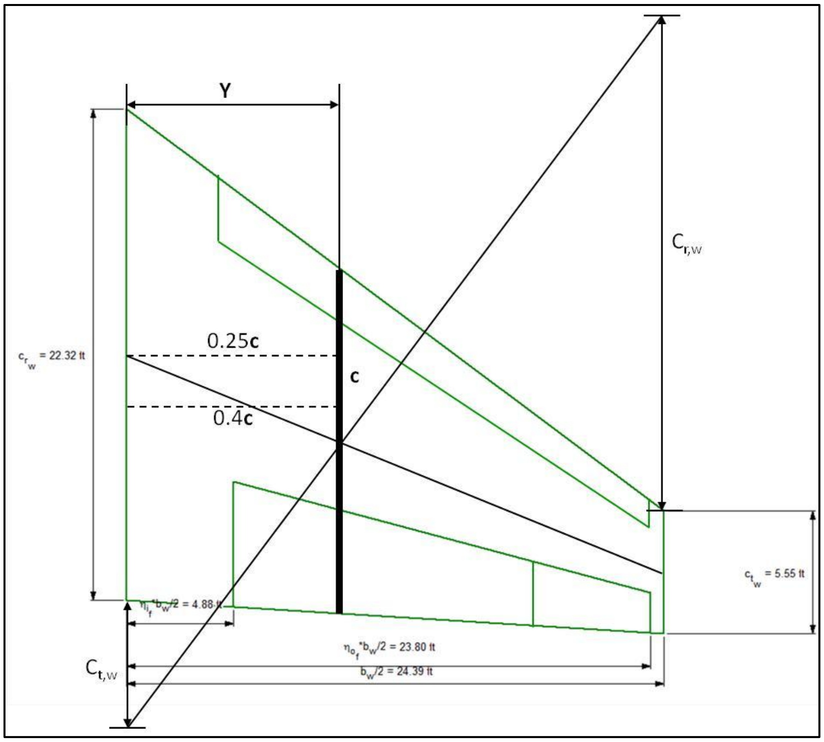

Figure 7-1 - Wing Geometry

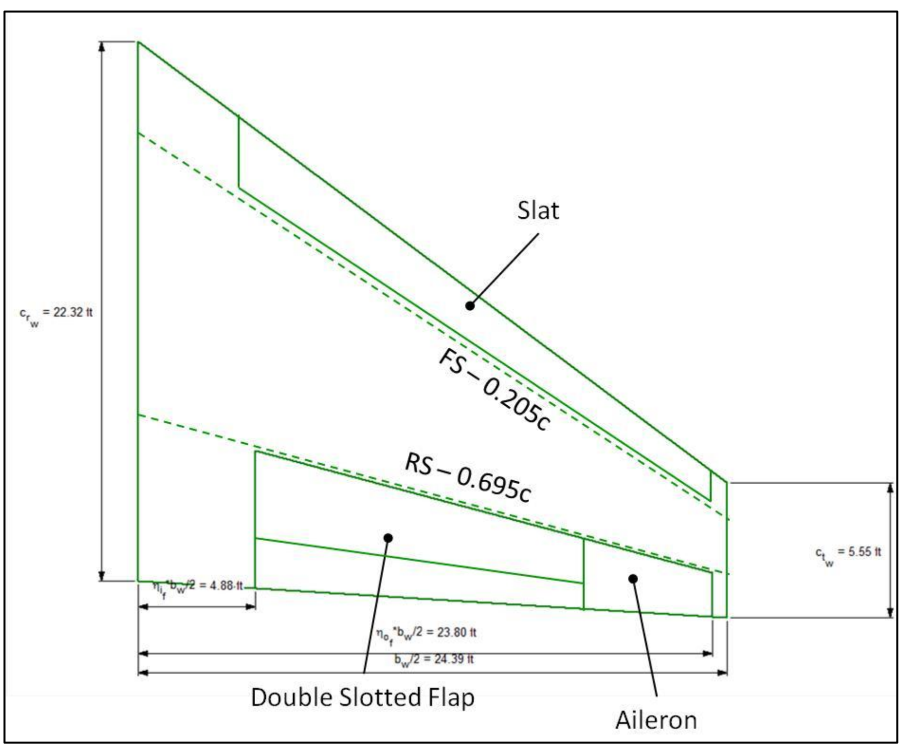

Figure 7-2 - Wing Configuration

7.7 Discussion

The supersonic cruise speed and short take-off and landing (STOVL) requirement were conflicting requirements for much of the design. Since cruise is seen as the more critical design parameter the wings were sized more for cruise conditions. High lifting devices were then used to increase the STOVL performance. Additional requirements will be levied on the propulsion system to ensure the STOVL requirements are met.

The current fuel volume fits in the wings alone. Additional fuel may be stored in large V-Tail and engine support structures. More fuel may be needed due to the increased short take-off thrust required. A higher lift wing can also be traded off with increased drag and subsequent fuel consumption.

8 DESIGN OF EMPENNAGE & LONGITUDINAL AND DIRECTIONAL CONTROLS

This section covers the design of empennage devices for the AVD.

8.1 OVERALL EMPENNAGE DESIGN

The AVD incorporates an X-Tail (double V-Tail). Analysis was done assuming a single V-Tail. The required geometry will later be divided into two V-Tails based on ground clearance requirements at takeoff. The tail was pushed as far back as possible in order to maximize its effectiveness. This methodology yields an x_v of 25 ft.

Equation 8.1 and Equation 8.2 below were used to calculate SH and SV for the AVD. Values from Table 8.12a,b, and c in Roskam Part II were used as a comparison for lateral control surface(12). The coefficients used in the equations were calculated by matching data in Table 8.12a and b in Roskam Part II(12).

Equation 8.1 - Vertical Tail Area

$$S_{VT} = c_{VT} b_w S_w / L_{VT}$$

$$S_{VT} = 0.07 * 55.3 * \frac{680}{25} = 105.3\ ft^2$$

Equation 8.2 - Horizontal Tail Area

$$S_{HT} = c_{HT} \bar{c}_w S_w / L_{HT}$$

$$S_{HT} = 0.4 * 12.28 * \frac{680}{25} = 133.6\ ft^2$$

The method used in Raymer was used to transform the calculated control surface areas into a V-Tail area (10). The area for the V-Tail was assumed to be the same as the combine area of the horizontal and vertical tails calculated above. A Dihedral angle was then calculated based on the ratio of the horizontal and vertical tails. Lastly a projected area was used to determine the remaining V-Tail parameters.

Equation 8.3 - V-Tail Area

$$S_V = S_{VT} + S_{HT}$$

$$S_V = 105.3 + 133.6 = 238.9\ ft^2$$

Equation 8.4 - V-Tail Dihedral Angle

$$\Gamma_V = \tan^{-1}\frac{S_{VT}}{S_{HT}}$$

$$\Gamma_V = \tan^{-1}\frac{75.2}{95.5} = 38.2\ deg$$

Equation 8.5 - Projected Horizontal Tail Area

$$S_{HT}^{'} = S_V \cos\Gamma_V$$

$$S_{HT}^{'} = 238.9\cos 38.2 = 187.6\ ft^2$$

8.2 Design of V-Tail

As a starting point the wing design parameters were chosen for the V-Tail. Equation 8.6 shows how these values combined with those in Section 8.1 were used to calculate the V-Tail geometry.

Equation 8.6 - Calculation of V-Tail Geometry

$$A_V = 3.5$$

$$\lambda_V = 0.25$$

$$\Lambda_{c/4,V} = 30\ deg$$

$$b_V = \sqrt{AS_v} = 25.6\ ft$$

$$c_{r,V} = \frac{2S_v}{b*(1+\lambda)} = 11.7\ ft$$

$$c_{t,V} = \lambda c_r = 2.9\ ft$$

8.3 Empennage Design Evaluation

Equation 8.7 shows the need for a static margin of -5% of the mean chord length. The mean chord length was previously calculated to be 15.6, ft allowing for an x_{cg} x_{ac} mismatch of 0.78 ft. Current estimates have x_{cg} at 28.21 ft and x_{ac} at 27.37 ft at take-off, yielding a mismatch of 0.84 ft. This corresponds to a static margin of -5.4%, which meets the goal. The AAA program will not calculate supersonic x_{ac}, but at M=0.98 x_{ac} is 27.73 ft. The fuel usage scheme will be designed to maintain static margin throughout the mission. This will be investigated further in section 9.

Equation 8.7 - Required Static Margin (Roskam Part II Eq. 11.4)

$$dc_m / dc_L = \bar{x}_{cg} - \bar{x}_{ac} = -0.05$$

8.4 Design of the Longitudinal and Directional Controls

The V-Tail will utilize a ruddervator to provide the required control functionality. Based on typical values from Table 8.12a and b in Roskam Part II the ruddervator chord ratio of 0.39/0.5 (root/tip) was selected (12). This is in the higher end of the reference values. It is anticipated that the additional control surface area will be desirable for this V-Tail configuration.

8.5 CAD DRAWINGS

Figure 7-1 is an illustration of the AVD V-Tail geometry. The mean aerodynamic chord highlighted in red.

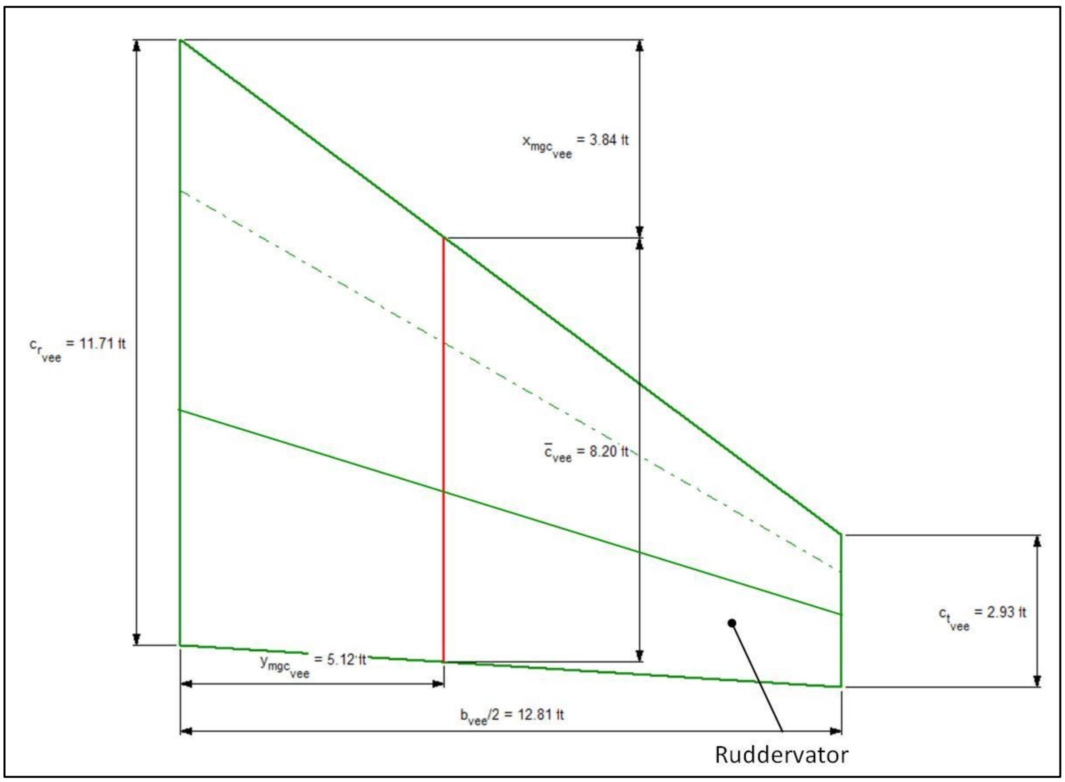

Figure 8-1 - V-Tail Geometry

8.6 DISCUSSION

The static margin calculated is based on current weight and c.g. estimates, if these estimates change the V-Tail sizing will need to be reinvestigated.

9 Weight and Balance Analysis

9.1 Introduction

This section summarizes the weight and balance analysis done on the AVD.

9.2 Weight and Balance

Weight and placement estimates were initially based on the weight fractions calculated from comparable aircraft and the layout developed in section 3. Weights and placement were then adjusted based on best engineering judgment and mission requirements.

9.2.1 Component Weights

The weights of the AVD components were calculated using the Class II methods in the AAA tool. The component weights are shown in Table 9-1. The propulsion system weight was based on manufacturer data for the selection engine (JT8D-7) plus 1,500 lbs for liftfans. The calculated tailboom weight was increased by 50% to account for the additional load due to its secondary engine support function. Note that the newly calculated take-off weight is slightly higher than the original estimate.

Table 9-1 - Component Weights

Parameter	Value	Parameter	Value
FixedEquipWeight	6273.768	FuelReserveFraction	10
StructureWeight	7716.225	TrappedFuelOilFraction	0.5
PowerplantWeight	8437.489	UserWeight	0
PayloadWeight	4480	FuelWeightClassII	11044.6
CrewWeight	440	MissionFuelWeightClassII	12149.06
ExpendedPayloadWeight	0	TrappedFuelWeightClassII	198.4751
RefuelFuelWeight	0	EmptyWeightClassII	22427.48
MissionFuelFraction	0.721764	TakeoffWeightClassII	39695.01

Table 9-2 shows the component c.g. locations based on estimated positions and weights. The data is plotted in Figure 9-1. The same plot is overlaid on an image of the AVD in Figure 9-2.

Table 9-2 - Component Center of Gravity

ID	Component	Xcg	Zcg
1	Wing	32.95	10.00
2	V-Tail	51.76	13.78
3	Fuselage	18.00	5.00
4	Tailbooms	46.65	10.00
5	Nacelles	35.20	5.25
6	Nose Landing Gear	9.00	-1.00
7	Main Landing Gear	27.00	-1.00
8	Engines	45.60	8.00
9	Fuel System	30.00	5.00
10	Air Induction System	40.00	0.00
11	Propulsion System	45.60	8.00
12	Flight Control System	5.00	1.00
13	Hydraulic and Pneumatic System	15.00	0.00
14	Instruments/Avionics/Electronics	3.00	1.00
15	Electrical System	10.00	1.00
16	Air Cond./Press./Icing System	10.00	1.00
17	Oxygen System	4.00	4.00
18	Auxiliary Power Unit	40.00	8.00
19	Furnishings	25.00	4.00
20	Cargo Handling Equipment	40.00	2.00
21	Weapon Provisions	40.00	7.00
22	Other Items	25.00	2.00

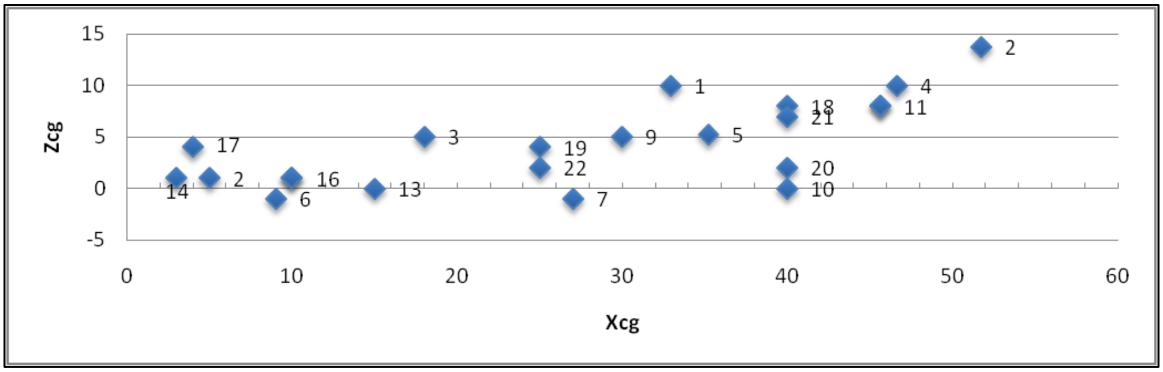

Figure 9-1 - Component Center of Gravities

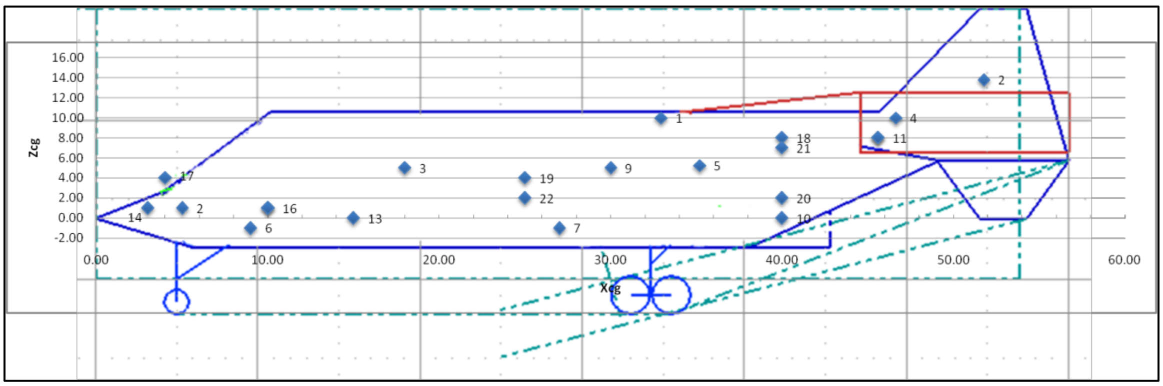

Figure 9-2 - Overlay of Component Center of Gravities

9.2.2 Center of Gravity

Table 9-3 shows the empty aircraft c.g. data based on the component c.gs in Section 9.2.1.

Table 9-3 - Empty Weight and Center of Gravity

Parameter	Value	Parameter	Value
UserWeight	0.00	XcgEmptyWeightClassII	30.10
XcgUser	20.00	YcgStructure	1.34
YcgUser	0.00	YcgPowerplant	0.00
ZcgUser	6.00	YcgFixedEquip	0.00
StructureWeight	8015.03	YcgEmptyWeightClassII	0.47
PowerplantWeight	8437.49	ZcgStructure	7.34
FixedEquipWeight	6273.77	ZcgPowerplant	7.79
EmptyWeightClassII	22726.29	ZcgFixedEquip	1.59
XcgStructure	30.88	ZcgEmptyWeightClassII	5.92
XcgPowerplant	44.60	GearWeight	1057.83
XcgFixedEquip	9.85	GearXcg	24.13

Table 9-4 shows the aircraft c.g. at take-off weight. The empty X_{cg} location is 30.10 ft; the take-off c.g. location is 29.99 ft. The wings were placed so that the subsonic aerodynamic center is located aft of the take-off c.g. at 30.13 ft. The aerodynamic center will move aft at cruise and supercruise, while the c.g. moves forward towards the empty c.g. location. This configuration will help maintain a stable platform. Note that the AVD has volume in the tailboom that could be utilized for additional fuel to extend range. This option would move the c.g. aft, and require a relocation of the wings. This configuration was not analyzed for this report.

Table 9-4 - Take-Off Weight and Center of Gravity

Parameter	Value
EmptyWeightClassII	22726.29
XcgEmptyWeightClassII	30.10
YcgEmptyWeightClassII	0.47
ZcgEmptyWeightClassII	5.92
CurrentWeight	38565.94
Xcg	29.99
Ycg	0.28
Zcg	6.60

Table 9-5 shows the minimum and maximum mission weights. This data was used to create a c.g. excursion. Figure 9-3 shows the c.g. excursion. Figure 9-4 shows the c.g. excursion zoomed in to the area of variability. The min load case was based off of the foreseen worst case operational load. This load was defined as having one pilot, no troops or equipment, and only 50lb of fuel. The maximum load was based on allowing 100lb of equipment per war-fighter and fuel tanks filled to volume capacity. Most of the offload-able weights are passengers and equipment in the fuselage and fuel in the wings. Both sections have c.g.s near the aircraft c.g. This has the effect of creating a small variability in c.g. The most forward c.g. location is located at 28.34 ft, the aft most at 29.95 ft. The c.g. at the maximum weight is at 28.34 ft.

Table 9-5 - Mission Weight Variability

Component	Component WeightMin *Input*	Component WeightMax *Input*	Component Xcg *Input*	Component Ycg *Input*	Component Zcg *Input*	Component WeightFwdCG *Output*	Component WeightAftCG *Output*
Crew	220	440	8	0	3	440	220
Trapped Fuel and Oil	50	200	26.89	0	9.29	200	50
Mission Fuel Group 1	0	12000	26.89	0	9.29	12000	0
Mission Fuel Group 2	0	0	0	0	2	0	0
Passenger Group 1	0	3000	25	0	3	3000	0
Passenger Group 2	0	0	0	0	2	0	0
Passenger Group 3	0	0	0	0	2	0	0
Passenger Group 4	0	0	0	0	2	0	0
Baggage	0	1400	25	0	1	1400	0
Cargo	0	0	0	0	2	0	0
Military Load Group 1	0	0	0	0	1	0	0
Military Load Group 2	0	0	0	0	2	0	0

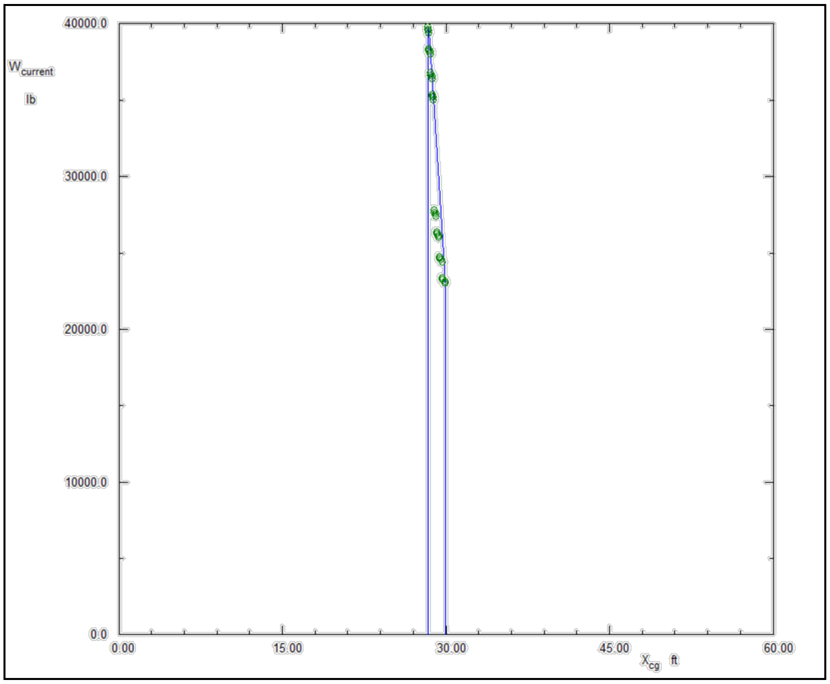

Figure 9-3 - Center of Gravity Excursion

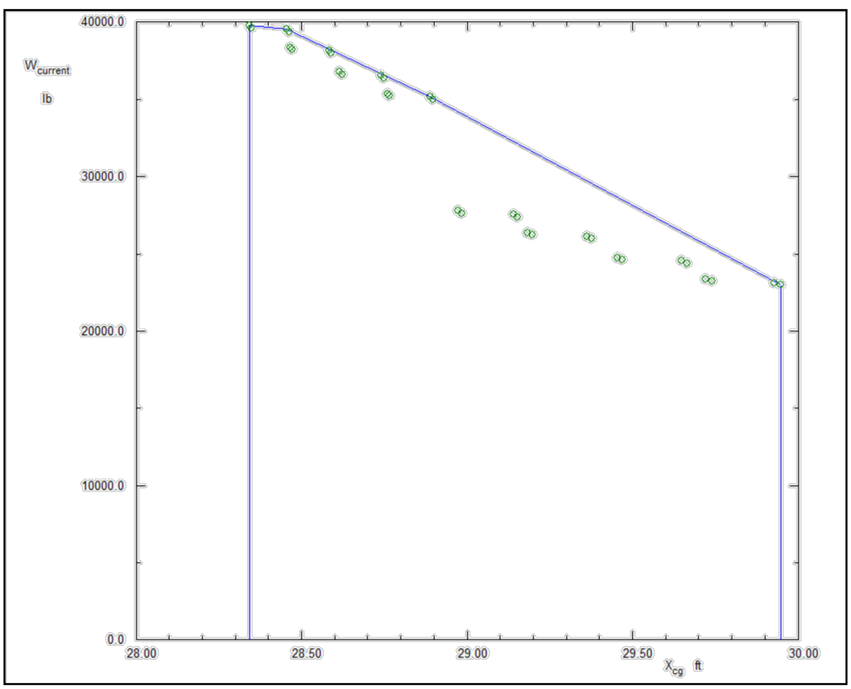

Figure 9-4 - Selection of Center of Gravity Excursion

9.3 Discussion

The weight analysis detailed in this section should be revisited if components weights or locations need to be moved further in the design process. The wings are a large portion of the empty weight and hold fuel, which is most of the expendable weight. They also have a large part in determining the aerodynamic center of the aircraft. As such, for most foreseeable changes to the weight distribution the wing location can be moved to compensate and achieve a similar balance throughout the mission.

10 LANDING GEAR DESIGN

This section covers the design of the landing gear system for the AVD. Landing gear parameters were calculated based on equations from Roskam and Raymer (12)(10). The position of the main and nose landing gear was initially done graphically based on c.g. balance and take-off ground clearance constraints.

10.1 NUMBER, TYPE AND SIZE OF TIRES

The placement of the landing gear along with the c.g. location allowed for the calculation of the strut loading. The calculated values are shown in Equation 10.1.

Equation 10.1 - Load on Landing Gear Strut (Roskam Part II Eq. 9.1,9.2)

$$P_n = \frac{W_{TO}\, l_m}{l_m + l_n} = 4{,}253\ lb$$

$$P_m = \frac{W_{TO}\, l_n}{l_m + l_n} = 17{,}721\ lb$$

$$\frac{P_n}{W_{TO}} = 0.107$$

$$\frac{2P_m}{W_{TO}} = 0.893$$

These appear to be typical loading values. Based on Roskam Part II Table 9.1, two nose wheel tires and two main gear tires per strut are acceptable (12). This yields a load of 8860.5 lb per main tire and 2126.5 per nose tire. Equation 10.2 shows the equation from Table 11.1 in Raymer was used to calculate the needed tire size, where X is either the diameter or width depending on the chosen coefficients (10). Equation 10.2 also shows the calculated diameter, D, and width, W, for the main and nose tires.

Equation 10.2 - Tire Size (Raymer T11.1)

$$X = AW_W^B$$

$$A_D = 1.63$$

$$B_D = 0.315$$

$$A_w = 0.1043$$

$$B_w = 0.480$$

$$D_m = 28.55\ in$$

$$W_m = 8.19\ in$$

$$D_n = 18.21\ in$$

$$W_n = 4.13\ in$$

Since the AVD will be stationed at military airstrips and aircraft carriers, a Type VIII tire with a pressure of 200 psi is chosen.

10.2 Length and Diameter of Struts

Strut length and diameter were calculated using equations 2.12 and 2.13 from Roskam Part IV(12). Equation 10.3 details the strut length calculation. Per recommendation in Raymer, nose stroke length will be the same as the main gear stroke (10). The main and nose gear strut diameters are calculated in Equation 10.4.

Equation 10.3 - Strut Length (Roskam Eq 2.12)

$$s_s = \left[\frac{0.5 \frac{W_L}{g} {w_t}^2}{n_s P_{m,l} N_g} - \eta_t s_t \right] \Big/ \eta_s + 1/12 = 1.8\ ft\ [21.7\ in]$$

$$W_L = 0.76 W_{TO} = 30{,}168\ lb$$

$$w_t = 22\ ft/sec$$

$$n_s = 2$$

$$P_{m,l} = \frac{W_L}{n_s} = 15{,}084$$

$$N_g = 3.0$$

$$\eta_t = 0.47$$

$$\eta_s = 0.8$$

Equation 10.4 - Strut Diameter (Roskam Eq. 2.13)

$$d_m = 0.041 + 0.0025\sqrt{P_{m,l}} = 0.35\ ft\ [4.2\ in]$$

$$d_n = 0.041 + 0.0025\sqrt{P_n} = 0.20\ ft\ [2.4\ in]$$

10.3 Preliminary Arrangement

The position of the main and nose landing gear was initially done graphically based on c.g. balance and take-off ground clearance constraints. Figure 10-1 below illustrates the positioning constraints placed on the AVD landing gear.

- 1 - Aircraft c.g
- 2 - Main landing gear
- 3 - Nose landing gear.
- A - 15 deg from vertical line from the c.g. used to set the forward limit for the main landing gear.
- B - 15 deg from horizontal line from the aft end of the tail boom used to set the aft limit for the main landing gear.
- C - Actual aft contact point of the main landing gear showing 6.5 deg of margin.
- D - 15 deg from horizontal line from the lowest part on the inverted V-Tail portion of the proposed X-Tail. This line is currently at the aft contact point of the main landing gear, and thus shows the max size of an inverted V-Tail.

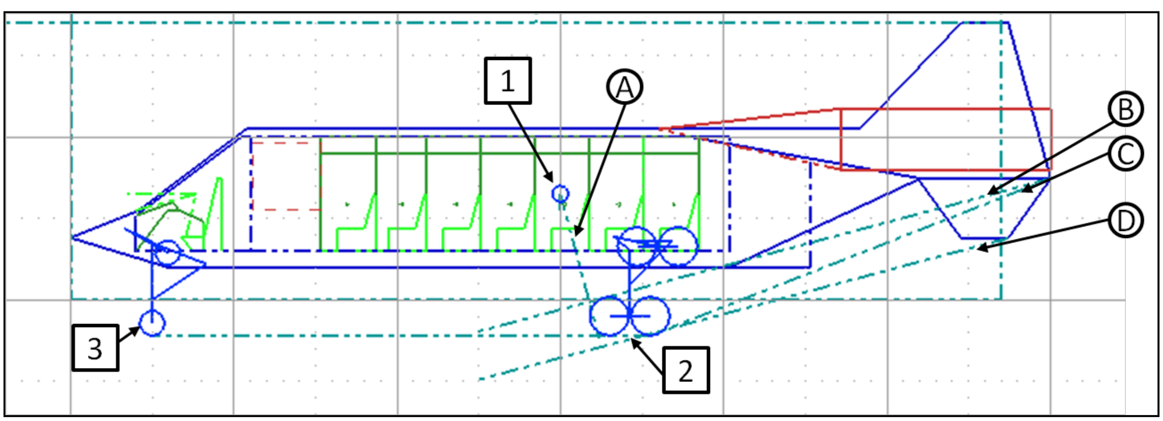

Figure 10-1 - Landing Gear Constraints

10.4 Retraction Feasibility

Figure 10-2 shows a side view of the proposed main landing gear.

- 1 - Aircraft c.g.
- 2 - Main landing gear extended.
- 2a - Main landing gear retracted.

The extended landing gear is depicted at its fully extended length (i.e. with space for the strut to compress without interference with the fuselage). The retracted landing gear is stowed in the fuselage adjacent to the last two rows of seats. This will impact storage in those areas. The main landing gear uses a tandem wheel configuration for packaging. The strut configuration used is a hybrid between the systems used on the DC-3 and C-141(12).

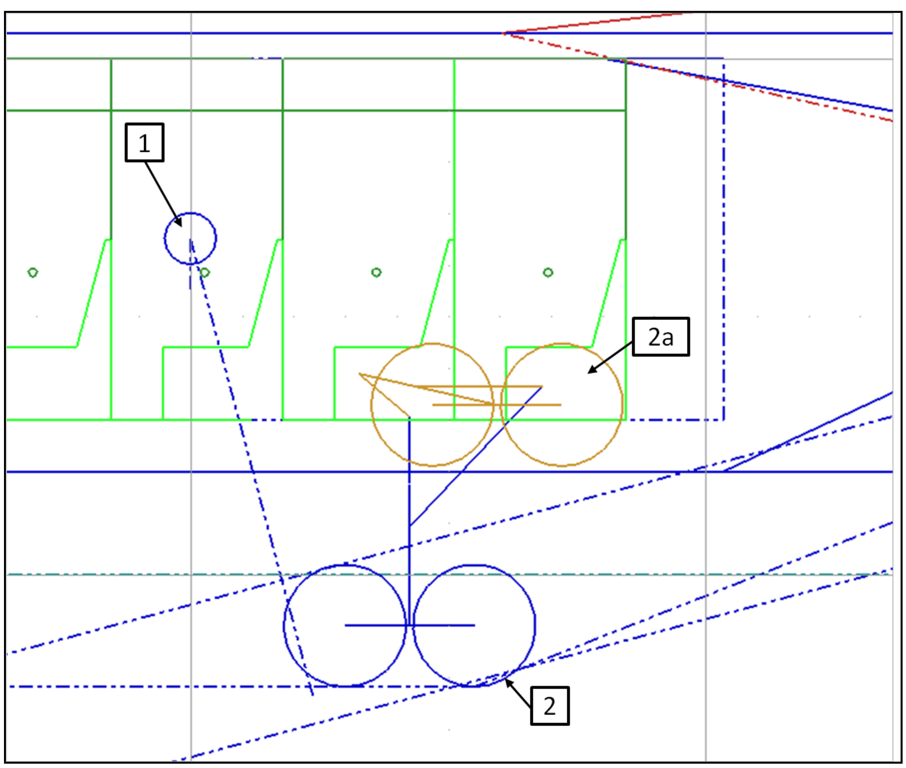

Figure 10-2 - Side View of Main Landing Gear

Figure 10-3 shows a side few of the proposed nose landing gear.

- 3 - Nose landing gear fully extended
- 3a - Nose landing gear retracted.

The dual wheel found on the nose landing gear will be stowed in the nose of the aircraft, aft of any critical electronic packages (e.g. radar dome, spherical antennae). Do to the required stroke length and limited volume for packaging, a hinged main strut was utilized on the nose landing gear.

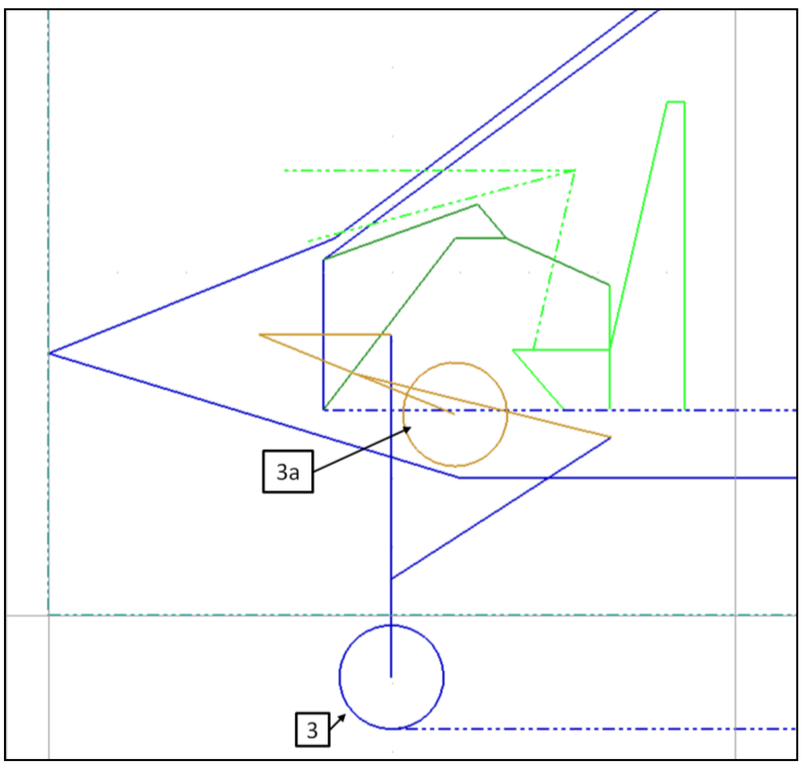

Figure 10-3 - Side View of Nose Landing Gear

Figure 10-4 shows a forward view of the landing gear.

- 2 - Fully extended main landing gear
- 2a - Retracted main landing gear
- 3 - Fully extended nose landing gear
- 3a - Retracted nose landing gear

The main landing gear utilizes space previously dedicated to equipment storage towards the aft of the aircraft.

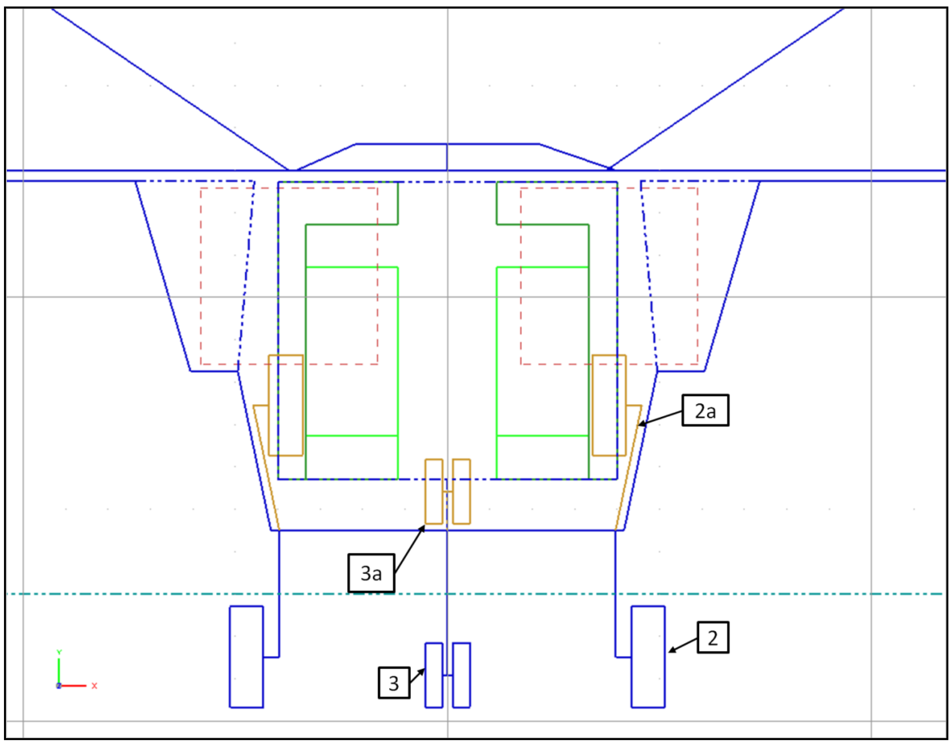

Figure 10-4 - Forward View of Landing Gear

10.5 Discussion

The preliminary landing gear parameters have been developed for the AVD. The selected parameters meet the design requirements as identified in this section. The landing gear packaging should be reevaluated once other subsystems (e.g. avionics) have been sized and positioned. This has potential to a significant impact on the aircraft station of nose landing gear.

11 Drag Polar Estimation

This section summarizes drag polar estimates for the AVD.

11.1 Airplane Zero Lift Drag

The wetted area and zero-lift drag coefficient for the AVD was calculated using the Class II methods in the geometry module in the AAA program. The parasite area was calculated using Equation 11.1, based on the total wetted area of 3532 ft^2 and a skin friction coefficient of 0.0030. Table 11-1 shows the calculated values in the subsonic and transonic regimes.

Table 11-1 - Aircraft Wetted Area and Drag

Component	Wetted Area [ft^2]	M=0.2		M=0.94	
		C_{D0}	$C_{D,L}$	C_{D0}	$C_{D,L}$
Wing	985	0.0037	0.0026	0.0164	0.3237
Fuselage	2063	0.0053	0.2021	0.0171	0.0238
V-Tail	484	0.0708	0.0251	0.0713	0.0001
Total	*3532*	*0.0798*	*0.2298*	*0.1048*	*0.3476*

Equation 11.1 - Parasite Area

$$\log_{10} f = a + b \log_{10} S_{wet} = 10.6\, ft^2$$

11.2 Low Speed Drag Increments

This section covers low speed drag calculations including takeoff and landing with and without landing gear.

11.2.1 High-Lift Device Drag Increments for Takeoff and Landing

Additional drag is seen while utilizing high lift devices for take-off and landing. Due to a lack of trim data Class I drag coefficients were used. Because aggressive methods are being used to attain high lift for takeoff and landing, drag coefficients for flaps were based on estimated geometry and Class II methods. The Class II values were then used to set the Class I ΔC_{D0} values. Table 11-2 has Class II values for C_{D0} and C_D calculated using AAA for the anticipated flap deflection during take-off and flap/slat deflection during landing. Table 11-3 has the corresponding Class I drag polar values.

Table 11-2 - Class II Drag Coefficients

Component	C_{D0}	C_D
Take-Off		
Trailing Edge Flap (40 deg)	0.0756	0.0801
Landing		
Trailing Edge Flap (60 deg)	0.117	0.1327
slats (est.)	0.01	0.02

Table 11-3 - Class I Takeoff and Landing Drag Polars (gear up)

	$\Delta C_{D0,L\_up}$	C_{D0,L_up}	B_{DP,L_up}	$C_{D0,clean}$
Takeoff	0.06	0.0744	0.1173	0.0144
Landing	0.11	0.1244	0.1254	0.0144

11.2.2 Landing Gear Drag

Drag is also induced from the extended landing gear. The Class II landing gear drag coefficient in Table 11-4 was calculated using AAA based on the geometry identified in section 9. The takeoff and landing drag with landing gear down is found in Table 11-5.

Table 11-4 - Class II Landing Gear Drag Coefficient

Component	CD
Landing Gear Extended	0.0152

Table 11-5 - Takeoff and Landing Drag Polars (gear down)

	$\Delta C_{D0,L\_dwn}$	CD0L_dwn	BDPL_dwn
Takeoff	0.075	0.0894	0.1173
Landing	0.115	0.1294	0.1254

11.3 Area Ruling

Wave drag is a large contributor to total drag in supersonic flight. Cross section area is needed to calculate wave drag as seen in Equation 11.2 where E_{WD} is the wave-drag efficiency factor. The ideal change in cross sectional area to minimize wave drag can be predicted by the Sears-Haack method(12). Figure 11-1 shows a cross-section area plot of the AVD at M=1 versus the ideal Sears-Haack plot. Equation 11.3 was used to produce the Sears-Haack curve, where r is the radius of the equivalent body of revolution (12).

Equation 11.2 - Drag Area (Roskam 12.46)

$$\left(D/q\right)_{S-H} = \frac{9\pi}{2}\left(\frac{A_{max}}{l}\right)^2$$

$$\left(D/q\right)_{wave} = E_{WD}\left[1 - 0.389(M - 1.2)^{0.57}\left(1 - \frac{\pi \Lambda_{LE}{}^{0.77}}{100}\right)\right]\left(D/q\right)_{S-H}$$

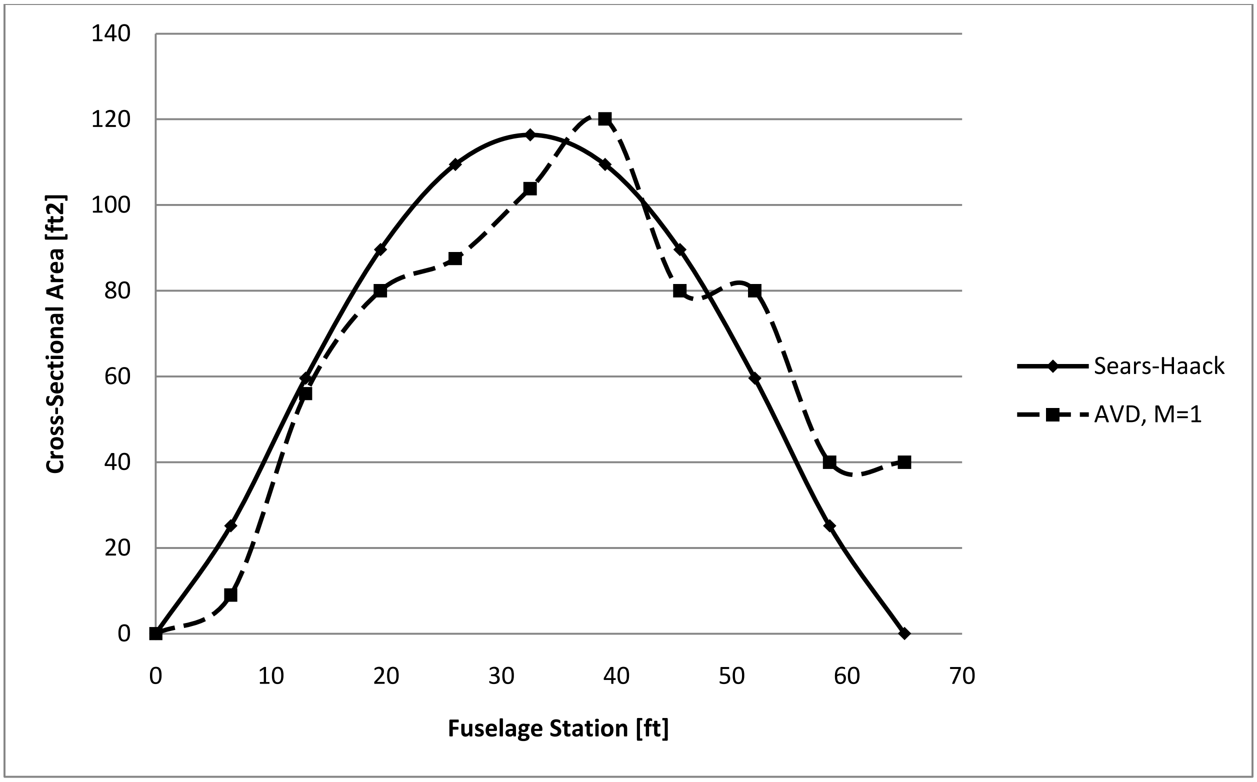

Figure 11-1 - Cross Section Area Distribution

Equation 11.3 Sears-Haack Area Distribution (Roskam 12.43)

$$\frac{r}{r_{max}} = \left[1 - \left(\frac{x}{l/2}\right)^2\right]^{0.75}$$

The cross sectional area used to calculate wave drag is a function of the mach angle, μ. Mach angle was approximated by asin(1/M). Mach angles for the supercruise condition, M=1.36, and max speed, M=1.67, are shown in Figure 11-2. The corresponding max areas are found in Figure 11-3. Since the fuselage will incorporate angles to help meet the low observability requirement, a rectangular cross-section was used to approximate the fuselage area.

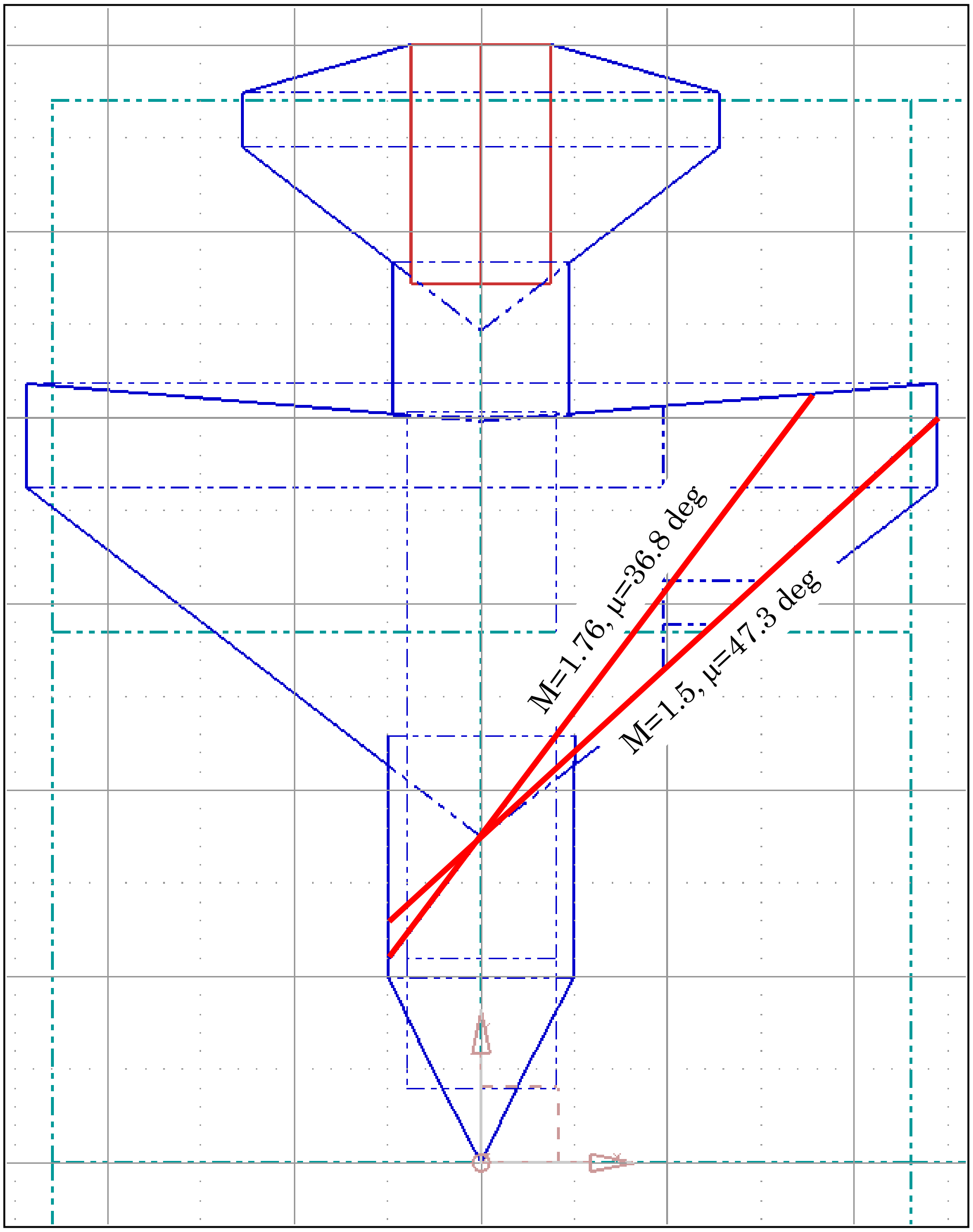

Figure 11-2 - Mach Angle Plans

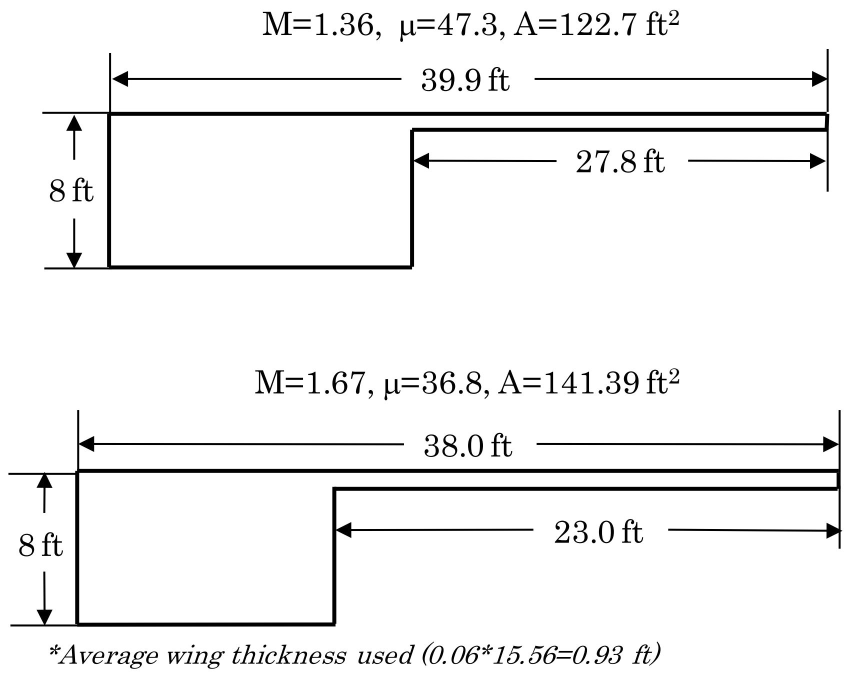

Figure 11-3 - Max Cross Section Area

Table 11-6 shows the calculated wave drag area, $(D/q)_{wave}$, for M=1.0, M=1.36, and M=1.67.

Table 11-6 - Wave Drag Area

$(D/q)_{wave}$ [ft²]	M	μ [deg]	A_{max} [ft2]	$(D/q)_{S-H}$ [ft2]
45.30	1.00	90.00	116.35	-
93.97	1.36	47.33	122.70	50.38
117.14	1.67	36.78	141.39	66.89

11.4 Airplane Drag Polars

Class I drag polars were calculated using AAA. Equation 11.4 is the parabolic drag polar equation used by the program. The Class I takeoff and landing values are located in Table 11-7 and Figure 11-4.

Equation 11.4 - Drag Polar

$$C_D = C_{D0,clean} + \Delta C_{D0} + B_{DP} C_L^2$$

$$B_{DP} = \frac{1}{\pi AR_w e}$$

Table 11-7 - Takeoff and Landing Drag Polars

Parameter	Value	Parameter	Value
FlightAlt	0	DeltaCDo	0.1
DeltaTemperature	35	PlotCLMin	0
FlightSpeedKTS	140	PlotCLMax	2
TakeoffWeight	37933.68	Qbar	62.16156
WingArea	680	CDoTakeoffGearDown	0.089368
WingAR	3.5	BofDPTakeoffGearDown	0.117349
ARegCoeffofParasiteArea	-2.5229	CDoTakeoffGearUp	0.074368
BRegCoeffofParasiteArea	1	BofDPTakeoffGearUp	0.117349
CRegCoeffofWettedArea	0.1628	CDoClean	0.018368
DRegCoeffofWettedArea	0.7316	BofDPClean	0.106995
OswaldFactorTakeoff	0.775	CDoLandingGearUp	0.114368
OswaldFactorClean	0.85	BofDPLandingGearUp	0.125442
OswaldFactorLanding	0.725	CDoLandingGearDown	0.129368
OswaldFactorEngineOut	0.8	BofDPLandingGearDown	0.125442
OswaldFactor	0.905519	CDoEngineOut	0.114368
DeltaCDoTakeoffGearDown	0.075	BofDPEngineOut	0.113682
DeltaCDoTakeoffGearUp	0.06	CDo	0.114368
DeltaCDoClean	0.004	BofDP	0.100435
DeltaCDoLandingGearUp	0.1	CLAirplane	0.897417
DeltaCDoLandingGearDown	0.115	CDAirplane	0.195254
DeltaCDoEngineOut	0.1	CLoverCDAirplane	4.596144

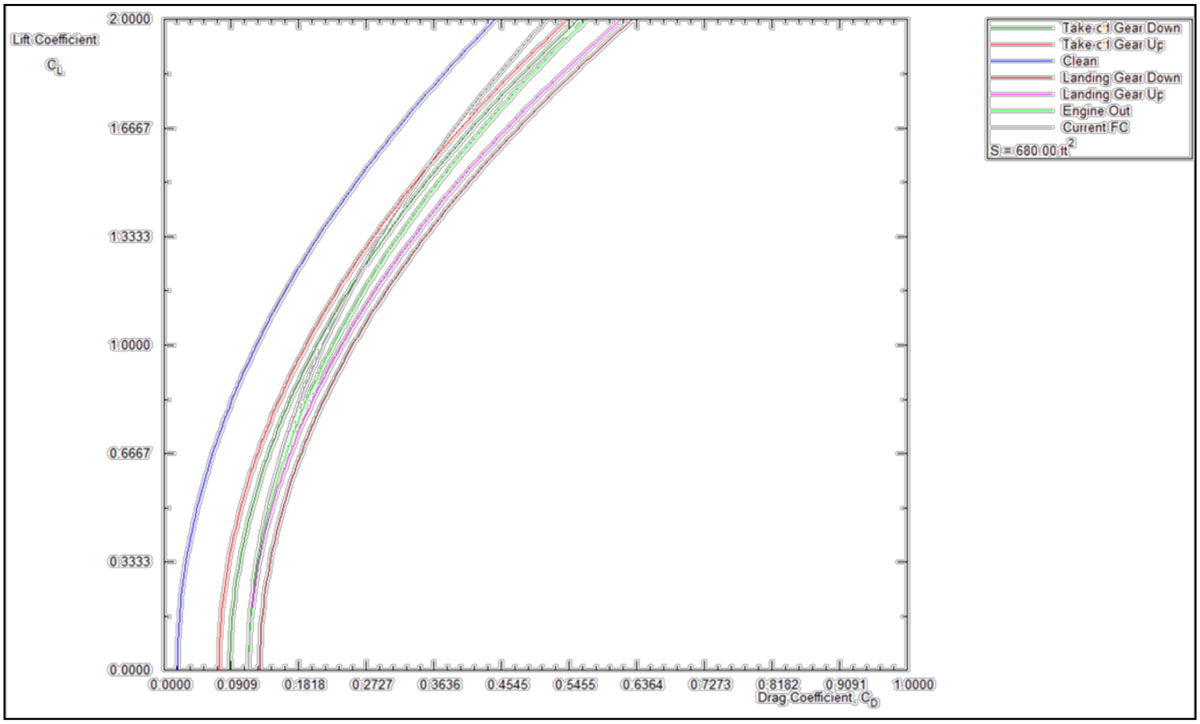

Figure 11-4 - Takeoff and Landing Drag Polar

Table 11-8 and Figure 11-5 shows the Class I drag polars for the cruise condition (M=0.94 @ 50 kft). Figure 11-5 also shows that the cruise L/D is closer to 12.6 versus the 12 estimated in section 4. Class II methods should be utilized before any adjustments in mass fuel fractions are made.

Table 11-8 - Cruise Drag Polar (M=0.98)

Parameters	Value
CDzeroClean	0.014368
CDo	0.014368
BofDP	0.107454

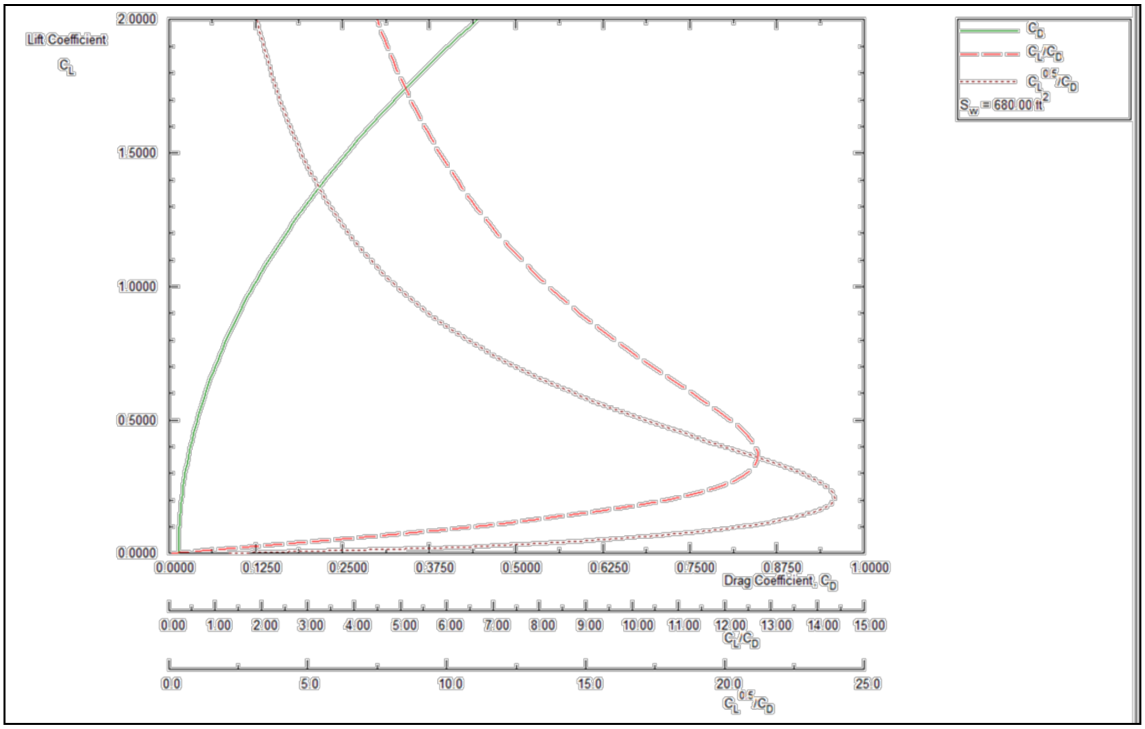

Figure 11-5 - Cruise Drag Polars

11.5 Discussion

Due to the high flap deflections needed for take-off and landing higher than typical ΔC_D values were utilized in the Class I method used. Once trim data is available the Class II analysis can be used to calculate a more accurate estimate. Supercruise and max speed drag polars were not calculated due to the limited drag calculations available in AAA. Drag polars should be calculated for supersonic flight conditions prior to detailed design.

12 Low Observables

The analysis needed to make detailed design decisions are outside of the scope of this report. Additional analysis of the detailed missions is required to determine observability requirements. Such information is classified, and such is outside of the scope of this project. This section will discuss the basic principles that will be utilized.

Low observability is crucial to the covert missions performed by the Special Forces units that will utilize the AVD. Several of the comparison aircraft mentioned in section 2 utilize low observable technology, including the F-22, F-35C, B-1B, and B2. Techniques such as radar absorbing materials, surface shaping, and augmented engine exhaust will be used to minimize the radar return of the AVD.

The sweep angles of the leading and trailing edges of the wing and tail are identical to minimize radar signature. Surfaces can also be angled to minimize the radar signature in a given direction. During flight electromagnetic currents build up on the skin when illuminated by radar. These currents naturally flow to a share edge and return a signal to the radar (10). Conductive material may be utilized to move this charge to the top of the aircraft for dispersion away from enemy radar.

Once an RCS profile has been chosen and corresponding geometry developed, aerodynamic data will need to be recalculated and aircraft performance reevaluated. The conservative estimates used in the selection of the initial aerodynamic values should minimize downstream impacts by geometry adjustments.

13 ENVIRONMENTAL

The AVD is a military aircraft and is therefore exempt from many regulations that guide commercial vehicles including emissions and noise requirements. The civil codes may be used as guidelines where appropriate.

The JT8D engines selected for the AVD are also used in commercial applications. As such their efficiency and emissions have been improved over the life of the engine family. The JT8D-7 selected for the AVD has a dry sfc of 0.585 and a cruise sfc of 0.796. Shaping in order to minimize sonic booms and general aircraft noise will be investigated as part of the stealth design.

14 Economic

The analysis of the economic feasibility of a military aircraft program is a critical. This was highlighted recently with the cancelation of the F-22 Raptor program. Despite going into production performing at or above requirements, the aircraft was seen as too expensive. This section covers the economic market as it applies to the AVD.

14.1 Market Analysis

The speech given by Secretary of Defense Robert Gates in April of 2009 highlighted the country's need for Special Forces-optimized transports. All of the aircraft currently used to transport Special Forces units do so as a secondary function. The shortcomings of existing vehicles make the need for an aircraft such as the AVD is clear. The AVD will be a specialized aircraft that will provide unparalleled capability to the Special Forces units within the United States armed forces.

14.2 Technical and Economic Feasibility

Due to the relatively low number of anticipated production units, minimizing production costs will be a major driver. Part of mitigating cost risks will be to leverage commercial off the shelf (COTS) products where possible. The program will also utilize specialized equipment designed for other military aircraft.

A few systems are anticipated to be high cost. An all carbon composite structure is recommended for the fuselage in order to reduce weight. This process is inherently expensive, but the program plans on utilizing modern techniques, such as those being used by HondaJet, to minimize production layout and development costs (9). Low observable design and materials will also be a costly effort. This system will leverage the company's previous experience in designing low observable vehicles and existing manufacturing process and vendors for production.

Although the AVD will utilize advanced technologies, none of them will be "new." This will decrease technical risk involved with moving forward into production. The proposed design is estimated to have performance capabilities that offset customer cost concerns. In the end the vehicle will not be cheap, but similar to the B2 the critical missions that it will facilitate will be worth the cost of maintaining the fleet.

15 DRAWINGS

This section contains drawings and illustrations of the AVD as defined by this report. Figure 15-1 is a dimensioned illustration of the AVD.

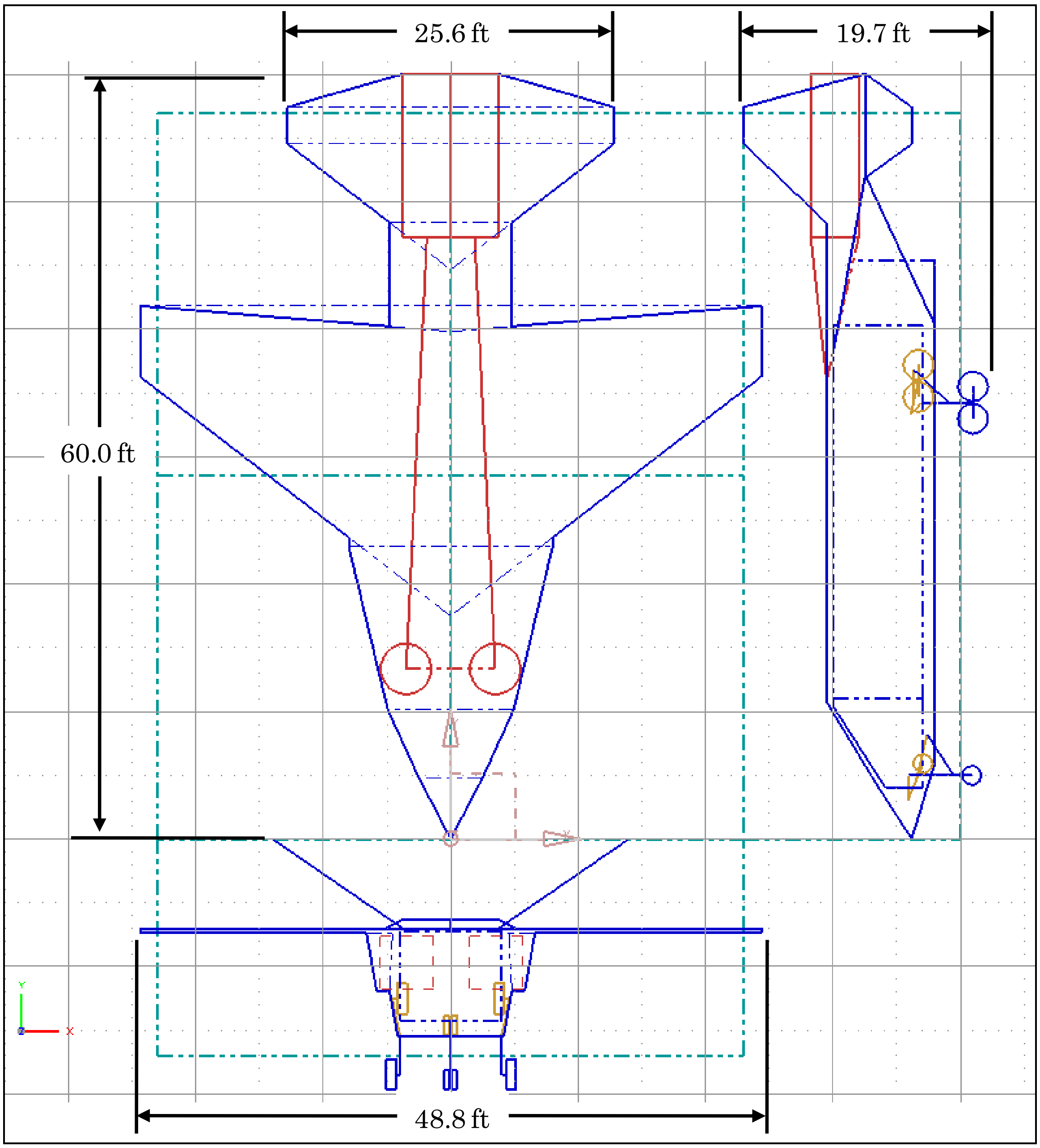

Figure 15-1 - Dimensioned AVD Trigraph

Figure 15-2 illustrates major components of the AVD.

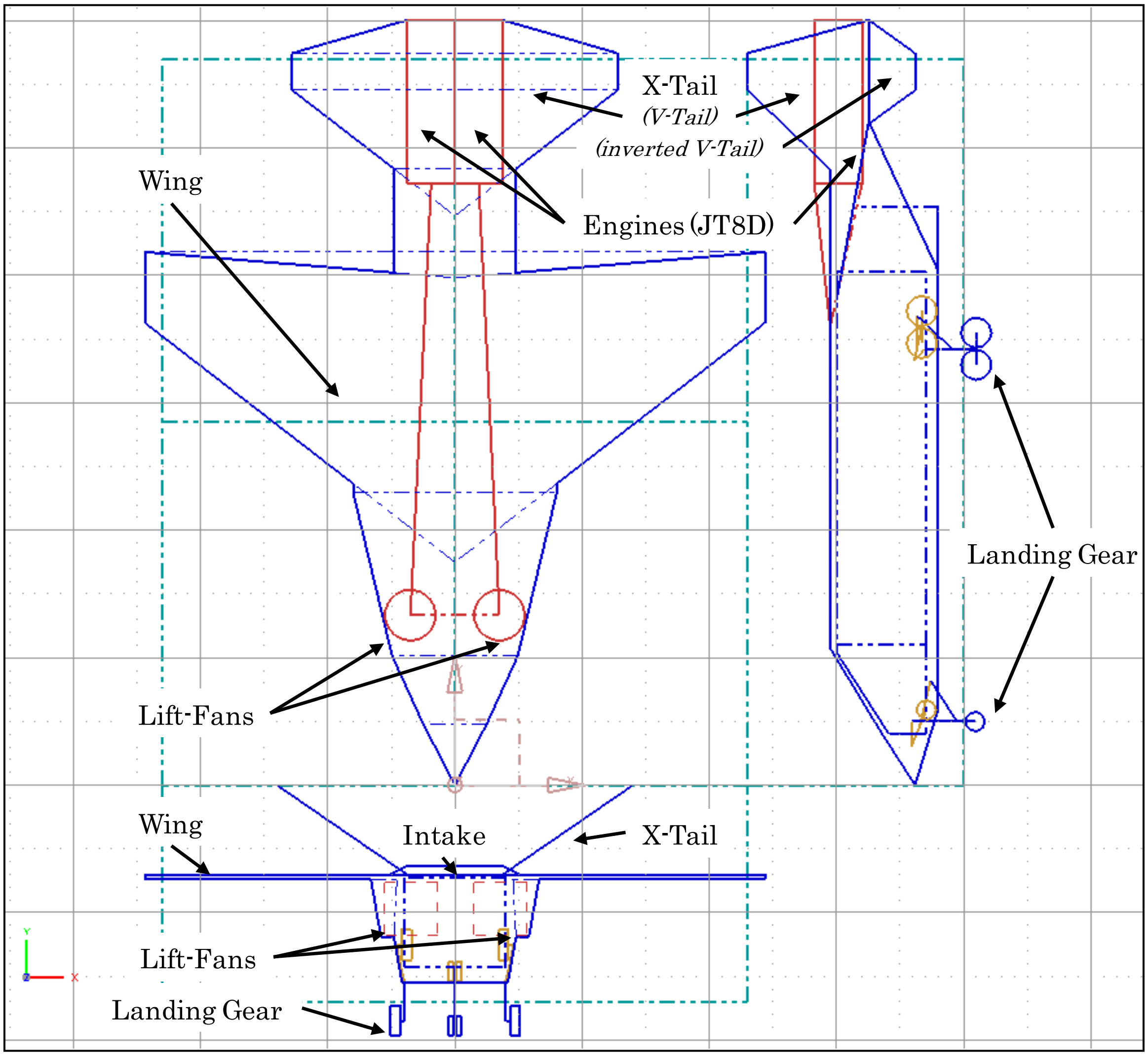

Figure 15-2 - AVD Trigraph with Components

Figure 15-3 shows the interior of the AVD.

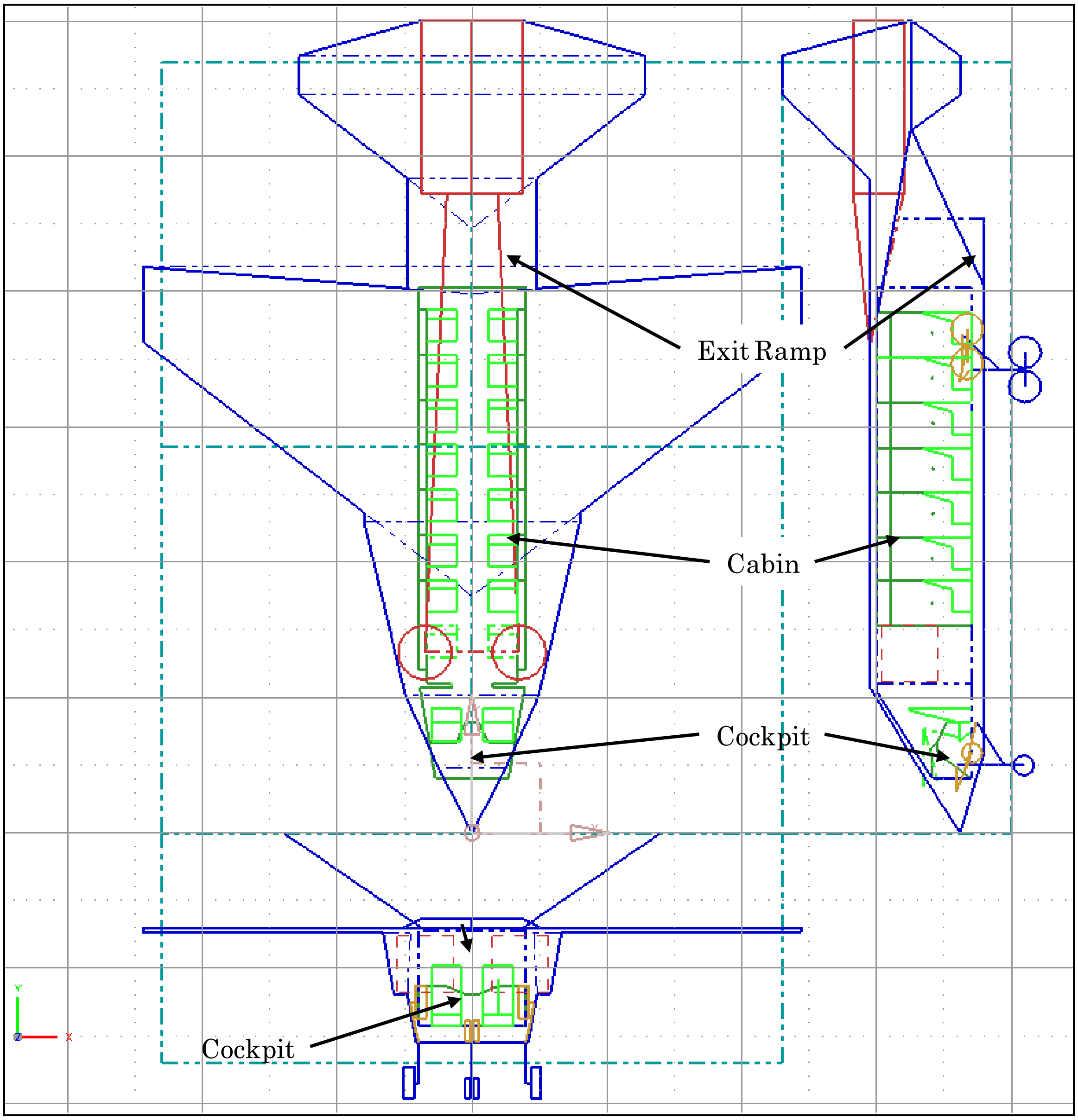

Figure 15-3 - AVD Trigraph with Interior

Figure 15-4 through Figure 15-6 are illustrations of the AVD produced with the Visual Sketch Pad (VSP) tool and Adobe Photoshop.

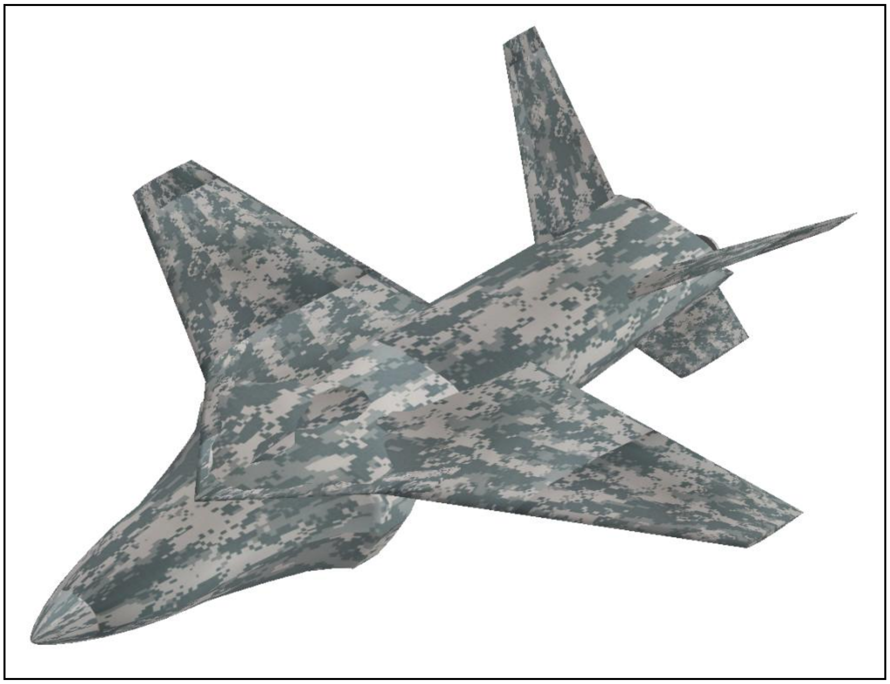

Figure 15-4 - AVD Rendered with VSP

Figure 15-5 - AVD Aerial Deployment

Figure 15-6 - AVD Carrier Vertical Landing

Figure 15-7 - Warfighter Deployment

Figure 15-8 - AVD Over Sea

16 DISCUSSION

Based on the preliminary analysis outlined in this report, the AVD offers enhanced capability over the closest alternative, the MV-22 Osprey. The AVD is capable of traveling at speeds three times that of the Osprey. This results in transit times that are three times faster, giving additional options to commanders and extra edge to Special Forces units. The range of the AVD is also over twice that of the Osprey. This increased range results in the ability to support missions much further from the units' base of operations. The added stealth feature also helps to ensure that the war-fighters make it in and out undetected.

17 Conclusion/Recommended Future Work

This report has detailed the preliminary design and analysis for the Advanced VTOL Dropship. Class I and II methods were utilized for configuration design, component sizing, and performance analysis. The analysis shows that the mission requirements are attainable. Additional preliminary analysis is required before detailed design. Areas of preliminary work include:

- Stability and Control Analysis
- Noise Level Estimation
- Avionics Selection
- Design Iteration

This analysis will provide adequate definition for proposal efforts and to start detailed design. Critical areas that are foreseen to be drivers in the detailed design phase are:

- Low Observables
- High Lift Devices
- Equipment Packaging

18 REFERENCES

1. Joint High Speed Vessel - JHSV. *Navy.mil.* [Online] October 28, 2009. [Cited: November 23, 2009.] http://www.navy.mil/navydata/fact_display.asp?cid=4200&tid=1400&ct=4.

2. US Army Factfiles: Chinook. *Army.mil.* [Online] [Cited: November 23, 2009.] http://www.army.mil/factfiles/equipment/aircraft/chinook.html.

3. CV-22 Osprey tilt-rotor aircraft: Aircraft profile. *Aviation Spectator.* [Online] [Cited: November 23, 2009.] http://www.aviationspectator.com/resources/aircraft-profiles/cv-22-osprey-tilt-rotor-aircraft-aircraft-profile.

4. SOF Future Aircraft . *Federation of AMerican Scientists.* [Online] 2008. [Cited: November 23, 2009.] http://www.fas.org/programs/ssp/man/uswpns/air/csar_sof/mcx.html.

5. **Hickman, Dwayne.** *Conceptural Design of an Advanced VTOL Dropship.* San Jose, CA : San Jose State University, 2009.

6. Various. *Wikipedia.* [Online] http://en.wikipedia.org.

7. V-22 OSPREY. *Naval Historical Center.* [Online] November 20, 2000. [Cited: December 4, 2009.] http://www.history.navy.mil/planes/v-22.html.

8. Rockwell International B-1A Construction. *National Museum of the US Air Force.* [Online] [Cited: December 4, 2009.] http://www.nationalmuseum.af.mil/factsheets/factsheet.asp?fsID=2752.

9. B-1B Lancer. *AF.mil.* [Online] May 2009. [Cited: December 4, 2009.] http://www.af.mil/information/factsheets/factsheet.asp?fsID=81.

10. F-35. *Lockheed Martin.com.* [Online] [Cited: December 4, 2009.] http://www.lockheedmartin.com/data/assets/aeronautics/products/f35/f35b_stovl_3view.jpg.

11. F-22 Raptor. *Wikipedia.* [Online] [Cited: December 4, 2009.] http://en.wikipedia.org/wiki/F-22_Raptor.

12. AV-8B Harrier II. *Wikipedia.* [Online] [Cited: December 4, 2009.] http://en.wikipedia.org/wiki/AV-8B_Harrier_II.

13. B-2 Spirit. *Wikipedia.* [Online] [Cited: December 4, 2009.] http://en.wikipedia.org/wiki/B2_Spirit.

14. *Aerion Coporation.* [Online] 2007. [Cited: November 23, 2009.] http://www.aerioncorp.com/home.

15. JT8D. *Pratt & Whitney.* [Online] [Cited: November 23, 2009.] http://www.pw.utc.com/vgn-ext-templating/v/index.jsp?vgnextoid=93cd34890cb06110VgnVCM1000004601000aRCRD.

16. **Meier, Nathan.** Civil Turbojet/Turbofan Specifications. *jet-engine.net.* [Online] 2005. [Cited: November 23, 2009.] http://www.jet-engine.net/civtfspec.html.

17. *HondaJet.* [Online] 2009. [Cited: November 23, 2009.] http://hondajet.honda.com/default.aspx?bhcp=1.

18. **Raymer, Daniel P.** *Aircraft Design: A Conceptual Approach.* Reston, VA : American Institute of Aeronautics and Astronautics, 1999.

19. **Roskam, Jan.** *Airplane Design I-VIII.* Lawrence, Kansas : DAR Corporation, 2004.

Appendix 1 - JT8D-7 Engine Data

Model		Application(s)	Thrust (dry) [lbf]	Thrust (wet) [lbf]	SFC (dry) [lb/lbf hr]	SFC (wet) [lb/lbf hr]	Airflow (static) [lb/s]	OPR (static)	FPR (static)	BPR (static)	Thrust (cruise) [lbf]	SFC (cruise) [lb/lbf hr]
Pratt Whitney	JT8D-7	727-100/-100C/-100QC/-100F/-200/-200F, 737-100/-200A/-200CA, DC-9-15/-15F(RC)/-31, Caravelle 10B1R/10B3/11R	14,000	-	0.585	-	315	15.8	1.93	1.07	4,270	0.796

Cruise Speed [M]	Cruise Altitude [ft]	TIT [K]	Number Spools	Fan Stgs	LPC Stgs	HPC Stgs	HPT Stgs	IPT Stgs	LPT Stgs	Fan Diameter [in]	Length [in]	Width/ Diameter [in]	Dry Weight [lb]
0.80	30,000		2	2	4B	7	1	-	3	42.5	123.5	42.5	3,096

(9)

APPENDIX 2 - SUMMARY OF PERFORMANCE CONSTRAINTS

This appendix contains screenshots from AAA of the performance values utilized for the design.

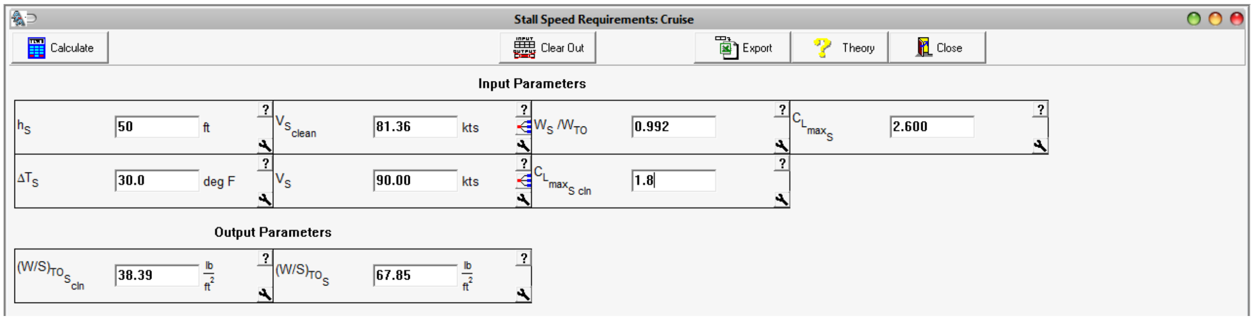

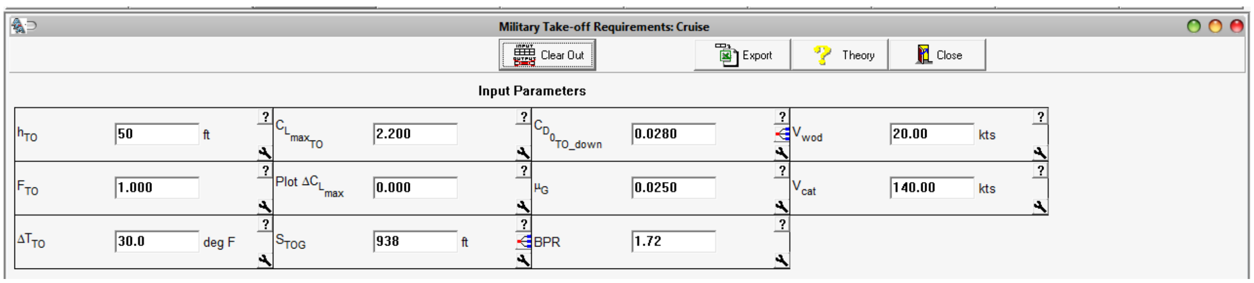

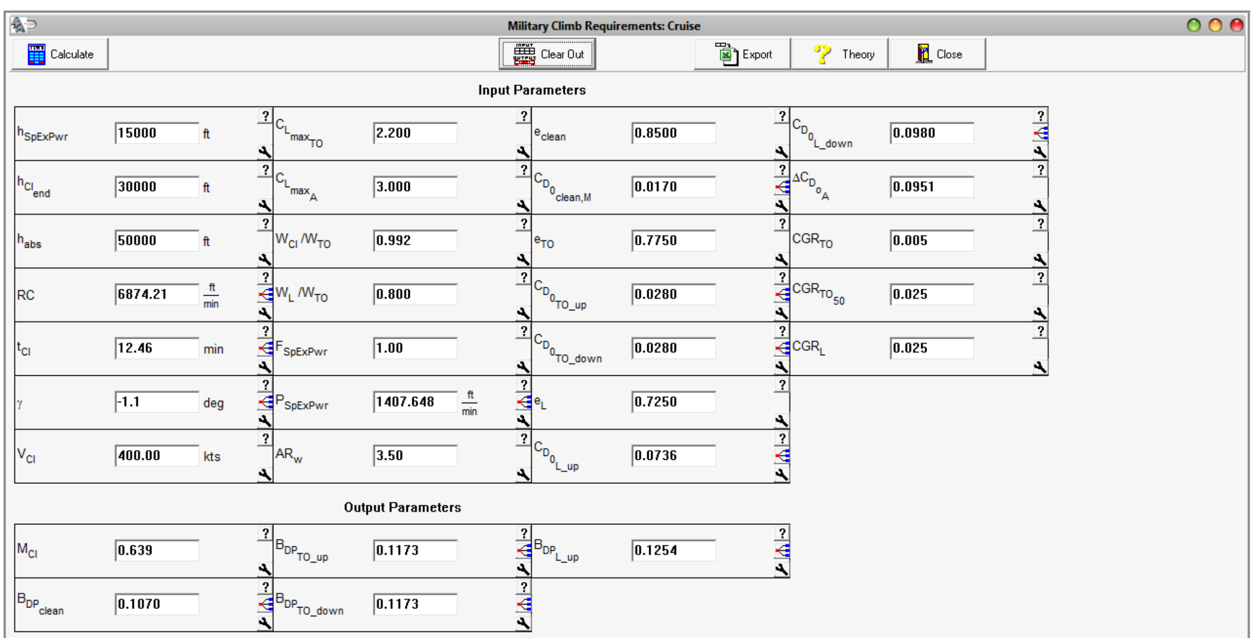

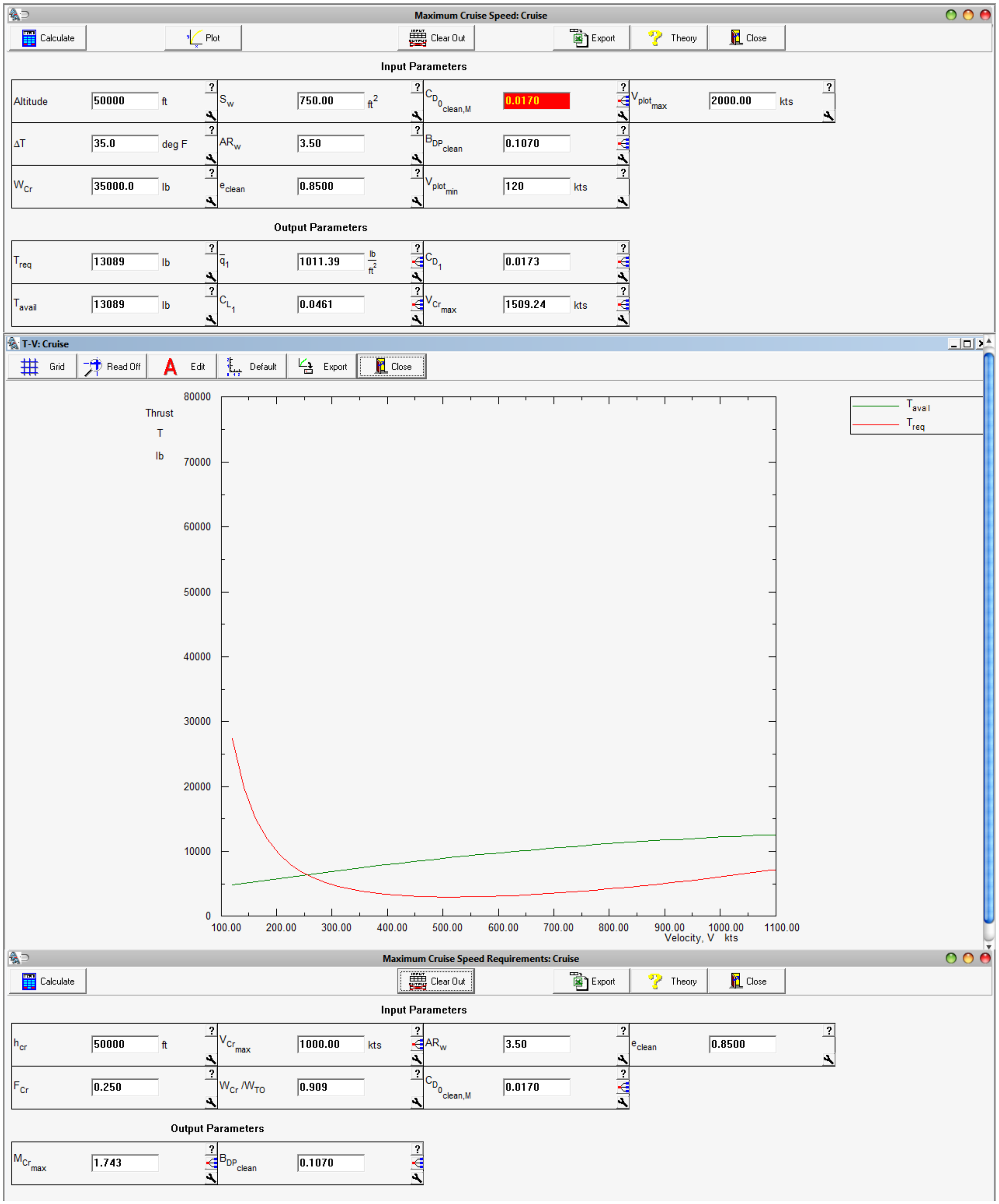
Maximum Cruise Speed: Cruise
Calculate
Plot
Clear Out
Export
Theory
Close
Input Parameters
Altitude 50000 ft
Sw 750.00 ft2
CD0 clean,M 0.0170
Vplot max 2000.00 kts
ΔT 35.0 deg F
ARw 3.50
BDP clean 0.1070
WCr 35000.0 lb
e clean 0.8500
Vplot min 120 kts
Output Parameters
Treq 13089 lb
q1 1011.39 lb/ft2
CD1 0.0173
Tavail 13089 lb
CL1 0.0461
VCr max 1509.24 kts
T-V: Cruise
Grid
Read Off
Edit
Default
Export
Close
Thrust T lb
80000
70000
60000
50000
40000
30000
20000
10000
0
100.00
200.00
300.00
400.00
500.00
600.00
700.00
800.00
900.00
1000.00
1100.00
Velocity, V kts
Tavail
Treq
Maximum Cruise Speed Requirements: Cruise
Calculate
Clear Out
Export
Theory
Close
Input Parameters
hcr 50000 ft
VCr max 1000.00 kts
ARw 3.50
e clean 0.8500
FCr 0.250
WCr /WTO 0.909
CD0 clean,M 0.0170
Output Parameters
MCr max 1.743
BDP clean 0.1070

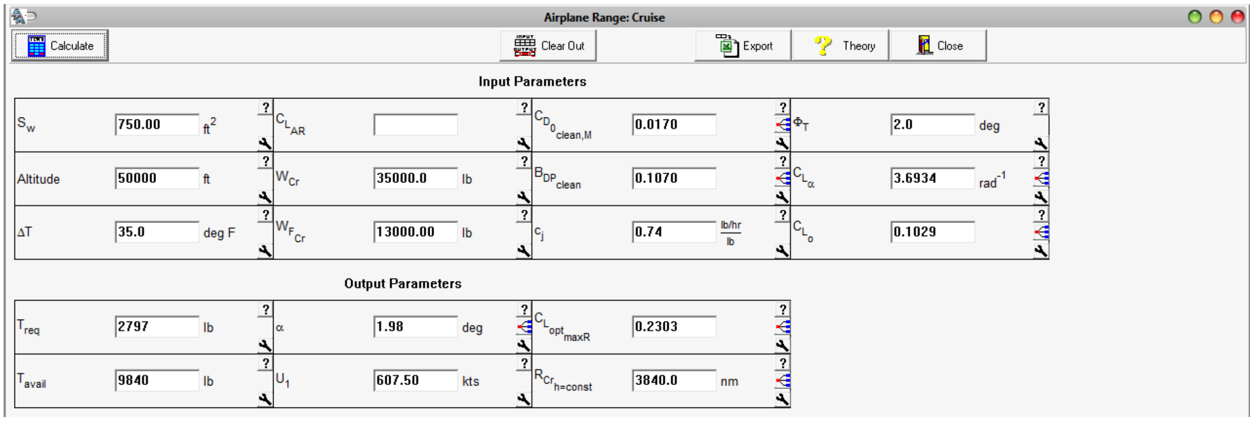
Airplane Range: Cruise
Calculate
Clear Out
Export
Theory
Close
Input Parameters
S_w 750.00 ft^2
C_L_AR
C_D_0_clean,M 0.0170
Φ_T 2.0 deg
Altitude 50000 ft
W_Cr 35000.0 lb
B_DP_clean 0.1070
C_L_α 3.6934 rad^-1
ΔT 35.0 deg F
W_F_Cr 13000.00 lb
c_j 0.74 lb/hr / lb
C_L_o 0.1029
Output Parameters
T_req 2797 lb
α 1.98 deg
C_L_opt_maxR 0.2303
T_avail 9840 lb
U_1 607.50 kts
R_Cr_h=const 3840.0 nm

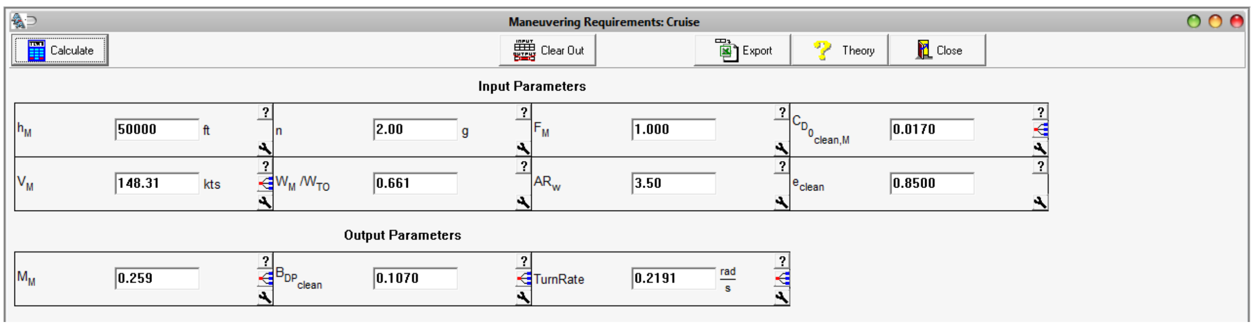
Maneuvering Requirements: Cruise
Calculate
Clear Out
Export
Theory
Close
Input Parameters
h_M 50000 ft
n 2.00 g
F_M 1.000
C_D_0_clean,M 0.0170
V_M 148.31 kts
W_M /W_TO 0.661
AR_w 3.50
e_clean 0.8500
Output Parameters
M_M 0.259
B_DP_clean 0.1070
TurnRate 0.2191 rad / s

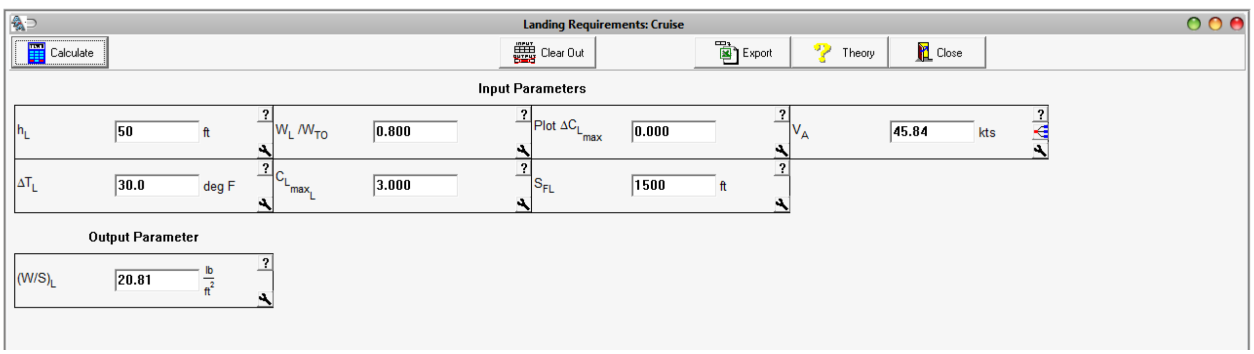
Landing Requirements: Cruise
Calculate
Clear Out
Export
Theory
Close
Input Parameters
h_L 50 ft
W_L /W_TO 0.800
Plot ΔC_L_max 0.000
V_A 45.84 kts
ΔT_L 30.0 deg F
C_L_max_L 3.000
S_FL 1500 ft
Output Parameter
(W/S)_L 20.81 lb / ft^2